UiT
THE ARCTIC
UNIVERSITY
OF NORWAY

Faculty of Science and Technology
Department of Geosciences

Sedimentation in Lake Nordlaguna – a closed basin on Jan Mayen

Marianne Christoffersen
GEO-3900 Master's thesis in geology, May 2018

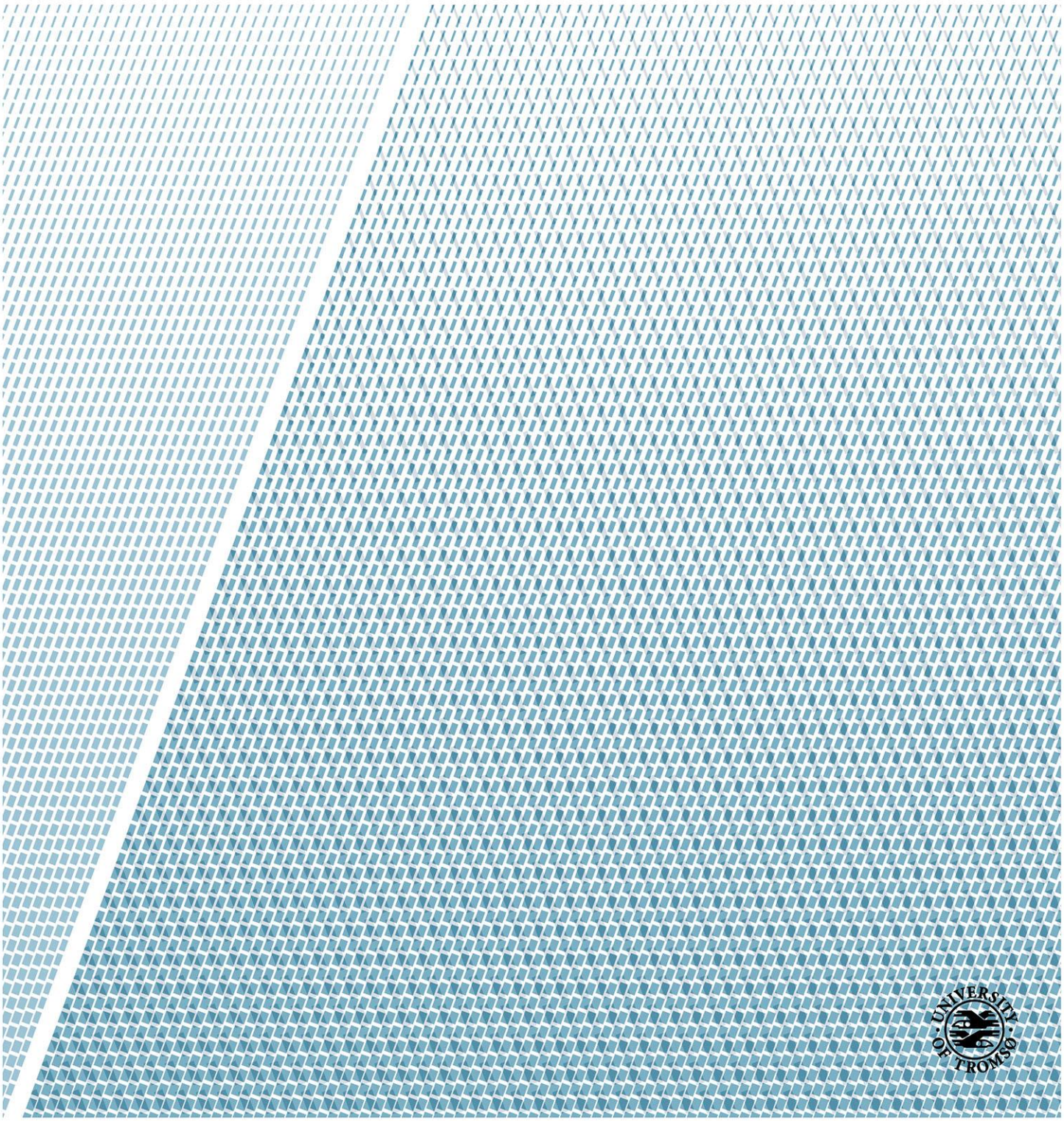

Abstract

This thesis focuses on the lake Nordlaguna on Jan Mayen. Nordlaguna is closed basin separated from the ocean by a barrier and surrounded by steep mountains and valleys. The lake has the potential to be a paleoclimatic archive and provide information about the unknown sea-level history of the island. When lake sediments are used in paleoclimatic studies, it is useful to acquire knowledge about the modern sedimentary processes of the lake in order to trace changes in the sedimentary record, as well as obtaining a reliable chronology. The overall aim of the thesis is to gain knowledge about the sedimentation in the lake and to evaluate the potential of using two sediment cores from the lake, NL2 and NL1B, to study past environmental conditions. A geological map of the sediment distribution and geomorphology of the study area was produced by combining field investigations of the terrestrial environment with bathymetry and Side Scanning Sonar data from the lake. Field observations, lithological logging, and roundness- and grain-size analyses from the terrestrial environment were used to gain knowledge of the importance of the sedimentary sources. Two sediment cores from the lake were used to connect the modern sedimentary processes with the sediment record.

Five main sedimentary sources were found: temporal and seasonal fluvial activity, deposition by wash-over events on the barrier, mass movement processes from the slopes that extend into the lake, wind-blown sediments, and pyroclastic fallout. The distribution of the sediments are controlled by the proximity to the source as well as processes within the lake, such as the transport of sediments in suspension or underflows, wave- and current-activity, lake-level fluctuations and subaqueous slides.

The dating of core NL2 revealed an irregular pattern that may be a result of deposition of old terrestrial material or redistribution of the sediments. In core NL2, the absence of organic material provided an inadequate chronology. This suggests that the chronology of the cores can be considered unreliable, and may complicate their use in studies of past environmental conditions. Although the chronology is poor, variations in the sedimentary records that may be traced to changes in local environmental conditions were observed. Variations in thickness of laminated silt, that were interpreted as annually deposited varves, can be caused by glacier fluctuations that are recorded from the island, and a significant increase in the amount of wash-over sediments suggests increased coastal erosion due to decreasing sea-ice extent.

Acknowledgement

I would like to thank all the people who helped and supported me during my studies. First, I want to thank my supervisors, Astrid Lysså, Eiliv Larsen and Anders Schomacker, for excellent counselling and support in the field, on the laboratory and during the writing process. I am grateful for all the knowledge and advice you have shared with me, and for getting the opportunity to write my master thesis about Jan Mayen and conduct fieldwork at this unique location.

Thanks to Trine Merete Dahl, Ingvild Hald and Karina Monsen at UiT for lab-related help, Lina Gislefoss at NGU for GIS-related help and Martin Ludvigsen at NTNU for providing and helping me with the subaqueous data. Furthermore, I would like to thank Ingrid for correcting my English.

Finally, a big thank-you to my family and friends for supporting and motivating me at all times. Special thanks to Christoffer for being the most patient and positive person that I know.

Marianne Christoffersen

Tromsø, May 2018

Table of Contents

List of Figures

List of Tables

1. Introduction

This master thesis was carried out at the Department of Geosciences at the University of Tromsø – The Arctic University of Norway between August 2017 to May 2018. In this chapter, the aims and objectives are presented, as well as a theoretical background that provides the framework of the thesis.

1.1 Aims and objectives

The main aim of this thesis is to understand the sedimentary processes in the lake Nordlaguna on Jan Mayen and its adjacent land area, as well as evaluating the potential of using two sediment cores to study past environmental conditions. It is a part of the scientific project 'Climate and glacier variations since the Last Glacier Maximum in Jan Mayen (ClimJam)' by the Geological Survey of Norway (NGU), which is financed by the Research Council of Norway. The lake Nordlaguna has the potential to be a paleoclimatic archive and provide information about the unknown sea level history of the island. When a lake is used to study paleoclimatic conditions, it is useful to acquire knowledge about the modern sedimentary processes of the lake, as this can be used to interpret the stratigraphic pattern of the sediment record and tracing changes in climatic conditions (Retelle & Child, 1996). The use of lake sediments in paleoclimatic studies requires that they can be sufficiently dated (Bradley, 2014).

The objectives of this thesis are to:

- Gain knowledge about the sedimentary sources and processes within the lake that control the sedimentation and sediment distribution in the lake Nordlaguna
- Connect the modern sedimentary processes to the sedimentary record of the lake
- Evaluate the potential of using two sediment cores from the lake to study past environmental conditions
- Use the knowledge of the modern sedimentary processes to trace changes in deposition in the sediment record that can be linked to changes in the environmental conditions

1.2 Theoretical background

1.2.1 Lakes, coastal lagoons and estuaries

Lakes, coastal lagoons and estuaries are all bodies of water that are accumulated in depressions in the landscape (Boyd et al., 1992). However, there are some significant differences in location, processes and sources of water and sediments. A fundamental difference is that a true lake does not have any exchange with the open ocean, in contrast to coastal lagoons and estuaries, which are located in coastal settings and receive water from the ocean (Nichols, 2009).

Lakes

A lake is a depression in the landscape where water is accumulated (Nichols, 2009). Water is transported to a lake by precipitation, groundwater or streams and rivers (Wetzel, 2001). A depression that hosts a lake may form as a result of a variety of processes, such as tectonic rifting, in a volcanic crater, by glacial erosion, damming by vegetation or sediments etc. (Eugster & Hardie, 1978; Wetzel, 2001).

Coastal lagoons

A coastal lagoon is a shallow body of water in a coastal setting that is connected to the ocean. It is separated from the ocean by a barrier that encloses or semi-encloses the lagoon (Boyd et al., 1992). The connection to the ocean is by either one or more channels or by water seeping through the barrier. Waves from the ocean can overtop the barrier during storm, and deposit wash-over sediments from the barrier in the lagoon (Dalrymple et al., 1992).

Estuaries

An estuary is a shallow body of water in a coastal setting where seawater is mixed with freshwater from streams or rivers. The supply of water and sediments to the estuary are from both marine and fluvial sources (Dalrymple et al., 1992).

1.2.2 Open and closed lakes

A lake can be classified as hydrologically open or hydrologically closed, based on the rate of inflow and outflow. A lake is hydrologically open when there is a balance between the inflow and outflow of water. Such lakes are overfilled, and the water level is more or less constant. The water in open lakes is usually fresh (low salinity) (Einsele, 2013). Sediments in suspension can be transported out from the lake by outlet streams (Rafferty, 2011).

In hydrologically closed lakes, there are no outflow of water, but the rate of evaporation and/or internal drainage into groundwater exceeds the rate of inflow. This controls the water level, and the lake does not overfill (Einsele, 2013). The water level in such lakes may be fluctuating, which can influence the accumulation area and rework the nearshore sediments (Einsele & Hinderer, 1997). The water is often brackish (intermediate salinity) or saline (high salinity) (Wetzel, 2001). Hydrologically closed lakes are

of particular interest for paleoclimatic reconstructions, as all sediments supplied to the lake is deposited within the basin (Rafferty, 2011).

1.2.3 Mechanisms and controls of sedimentation in a lake

Sediments in a lake may be derived from a variety of sources, and the importance of the sources are individual for different lakes (Sly, 1978). The formation of lake sediments is mainly controlled by climatic conditions (Carrol & Bohacs, 1999; Wetzel, 2001) as well as the properties of the drainage area (Zolitschka et al., 2015). Lake sediments can origin from the sources within its drainage area or from external sources (Leeder, 2011).

Sources from within the drainage area

As river input is a common source of water and sediment to most lakes, sediments of fluvial origin are often found in the sedimentary record (Wetzel, 2001). The amount of fluvial sediments that are transported to a lake is controlled by the climate, drainage area and the supply of sediments (Leeder, 2011). A delta is often developed where the river enters a lake, as the sediments that are transported as bedload are deposited when the velocity of the river decreases as it enters the lake water (Rafferty, 2011).

If steep subaerial slopes surround a lake, gravity driven processes can be directly transported downslope and deposited in the lake (Dearing, 1991; Van Daele et al., 2015). This is a common source of sediments in lakes in mountainous areas (Bøe et al., 2004).

External sources

Wind-derived sediments are a common source of lake sediments (Leeder, 2011). In Arctic lakes, aeolian sediments are a common deposit in the sedimentary record, and are recognized as isolated grains and layers of coarse sand that are deposited on the winter ice and settled on the lake floor during spring or summer (Retelle 1986; Lamoureux & Gilbert, 2004).

Volcanic ash deposits may be found in lakes in volcanic settings (Thompson et al., 1986), but such particles can be transported and deposited far away from its source, and are also found in areas where there is no volcanic activity (Lowe & Turney, 1997; Wastegård et al., 1998). Such deposits can be used as a stratigraphic marker in the sediment record (Turney et al., 2006; Blockley et al., 2007), and to reconstruct past atmospheric circulation, as the transportation route is controlled by the wind (Eaton, 1963).

1.2.4 Sediment distribution

The sediments that are supplied to a lake are not evenly distributed throughout the lake floor, and the distribution of sediments on the lake floor can have great local variations (Einsele & Hinderer, 1997). A fundamental control on the distribution of sediments is the proximity to the source (Leeder, 2011). As

a consequence of this, the central parts of the basin usually consist of fine sand and mud, which can be transported further away from the source, while coarser material is deposited close to the lake margins (Rafferty, 2011).

In climatic settings where winds are strong, waves and currents can form in a lake and be an important part of the distribution of sediments, as they can erode and redistribute the lake sediments (Larsen & MacDonald, 1993). However, as the sizes of lakes are limited, the waves are unable to develop to the same size as in the open ocean (Einsele, 2013), and will therefore only affect down to 10-20 m water depths, while the deeper parts are unaffected by waves or current activity (Nichols, 2009). Reworking of the sediments at the margins of a lake can create beach deposits, similar to beaches found on marine coastlines (Reid & Frostick, 1985).

The hydrological properties of a lake can control the sediment distribution. If a lake is stratified, the properties of the layers can transport sediments as underflows or in suspension (Fig. 1). High-density mixtures of water and sediments can be transported as a turbulent underflow in the hypolimnion (cold and dense lower layer of water masses), and will then be deposited as a turbidite (Nichols, 2009). The turbidity currents can transport material across a relatively flat lake floor, and thereby deposit coarse grained material on the deepest part of the lake, possibly at great distances from the source (Collinson et al., 2006). Low-density mixtures of water and sediments can be transported as suspended material in the epilimnion (warm and less dense upper layer of water masses). A plume of sediments can then develop in the lake, before it falls out of suspension and the particles are deposited on the lake floor (Fig. 1). This allows the fluvial sediments to be distributed throughout the lake (Nichols, 2009).

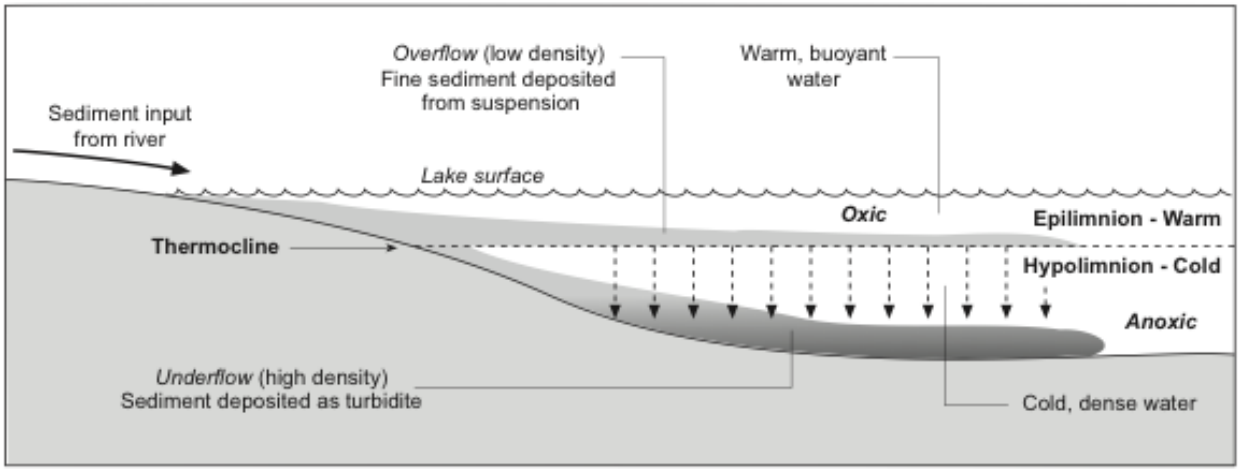

Fig. 1 The sediment distribution within a lake can be controlled by the lake stratification. High-density mixtures of water and sediments can be transported as underflows in the hypolimnion, while low-density mixtures of water and sediments can be transported in suspension in the epilimnion (Nichols, 2009)

Mass movement deposits in a lake can be initiated by slope failures within the subaqueous slopes, and redistribute the lake sediments (Schnellman et al., 2005; Wilhelm et al., 2015). Slope failures can be triggered by deposition of high loads of sediments, snow avalanches, fluctuating water levels, rockfalls, earthquakes or by fluid escape (Van Daele et al., 2015; Wilhelm et al., 2015). Such redistributed sediments can be transported to the deep parts of the lake, by a process called sediment focusing (Lehman, 1975). The lake morphology can be used to predict where sediments are focused, as the subaqueous flows are directed by the slopes (Blais & Kalff, 1995).

1.2.5 Characteristics of Arctic lake sedimentation

In general, Arctic lakes have a lower sedimentation rate than lakes in temperate regions, as the hydrological season is shorter and the winter ice covers the lake from sedimentation (Wolfe et al., 2004). These seasonal variations in climatic conditions can deposit varved sediments, which is a common deposit in the sediment record in Arctic lakes, and consists of annually deposited couplets of silt and clay. The silt is deposited during spring and summer, when snowmelt- and fluvial activity is high. The clay is deposited from suspension when the winter ice is covering the lake (Lowe & Walker, 2015). Varved sediments can be useful in paleoclimatic reconstructions, as one couplet of silt and clay represents one year of deposition (Zolitschka et al., 2015), and can potentially provide high-resolution records of past climate (Bradley, 2014). The use of varves in paleoclimatic studies is only possible when these finely laminated deposits are preserved, which requires a minimal mixing of sediments (Larsen & MacDonald, 1993).

2. Setting

2.1 Jan Mayen

Jan Mayen is a volcanic island that is located 456 km east of Greenland and 966 west of Norway, at 71°N, 8°30'W (Fig. 2). The island is 54 km long with a total area of 373 km^2, and the width is ranging from 15.8 to 2.5 km. It is the northernmost island at the Mid-Atlantic Ridge, and hosting the northernmost subaerial active volcano in the world. Jan Mayen is positioned at the northern edge of the microcontinent Jan Mayen Ridge (Fig. 2), which was created in the early Tertiary period, during the opening of the Atlantic Ocean (Mjelde et al., 2008). Right north of Jan Mayen is the Jan Mayen Fracture Zone, an active transform fault with WNW-direction. This has caused a 200 km displacement of two ridges at the Mid-Atlantic Ridge, Kolbeinsey Ridge in south and Mohns Ridge in north (Sylvester, 1975) (Fig. 2).

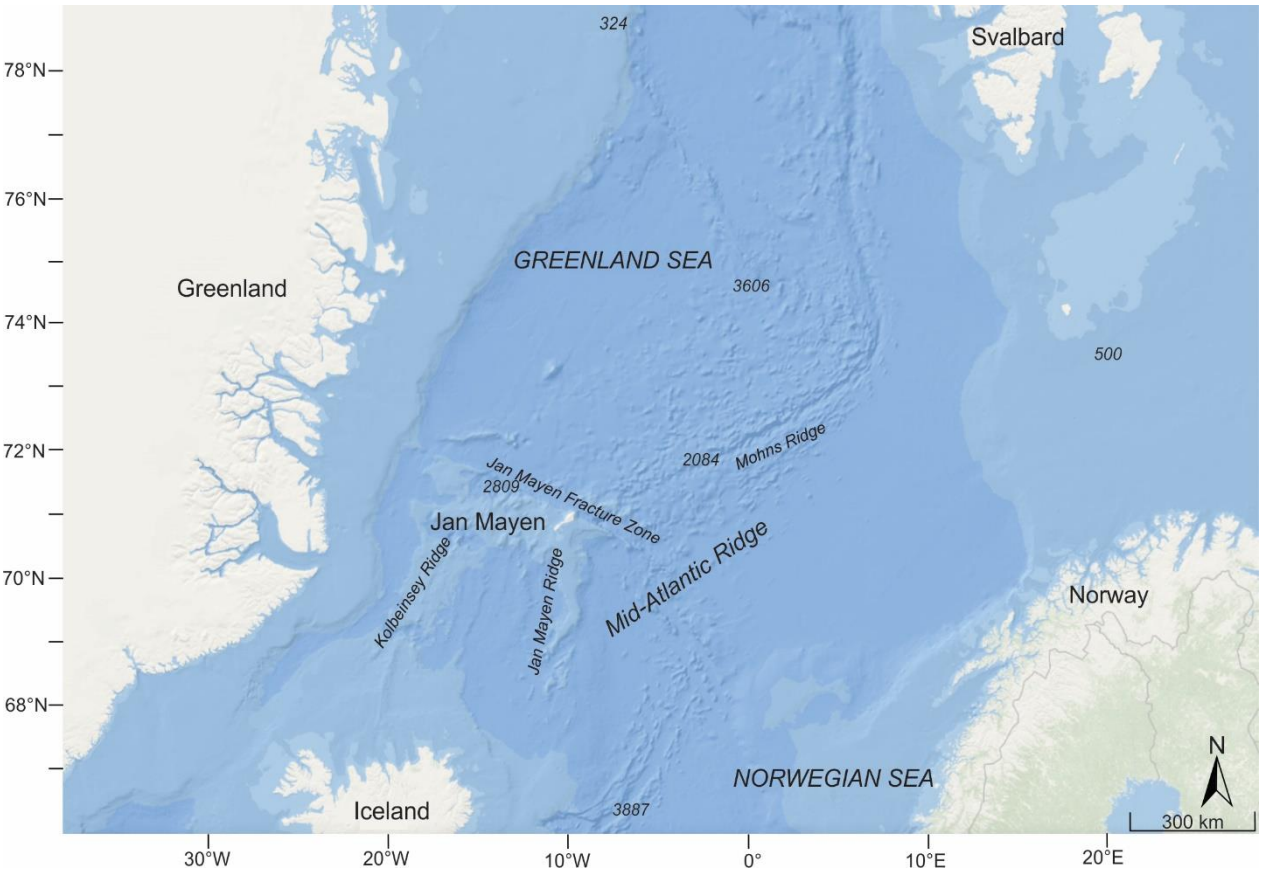

Fig. 2 Jan Mayen is located at the Mid-Atlantic Ridge, at the microcontinent Jan Mayen Ridge, between Kolbensey ridge in south and Mohns ridge in north

Jan Mayen is divided into three parts with distinctly different landscapes. Sør-Jan is the southern part of the island, Nord-Jan is the northern part, while Midt-Jan is the middle part and the connection between south and north (Fig. 3).

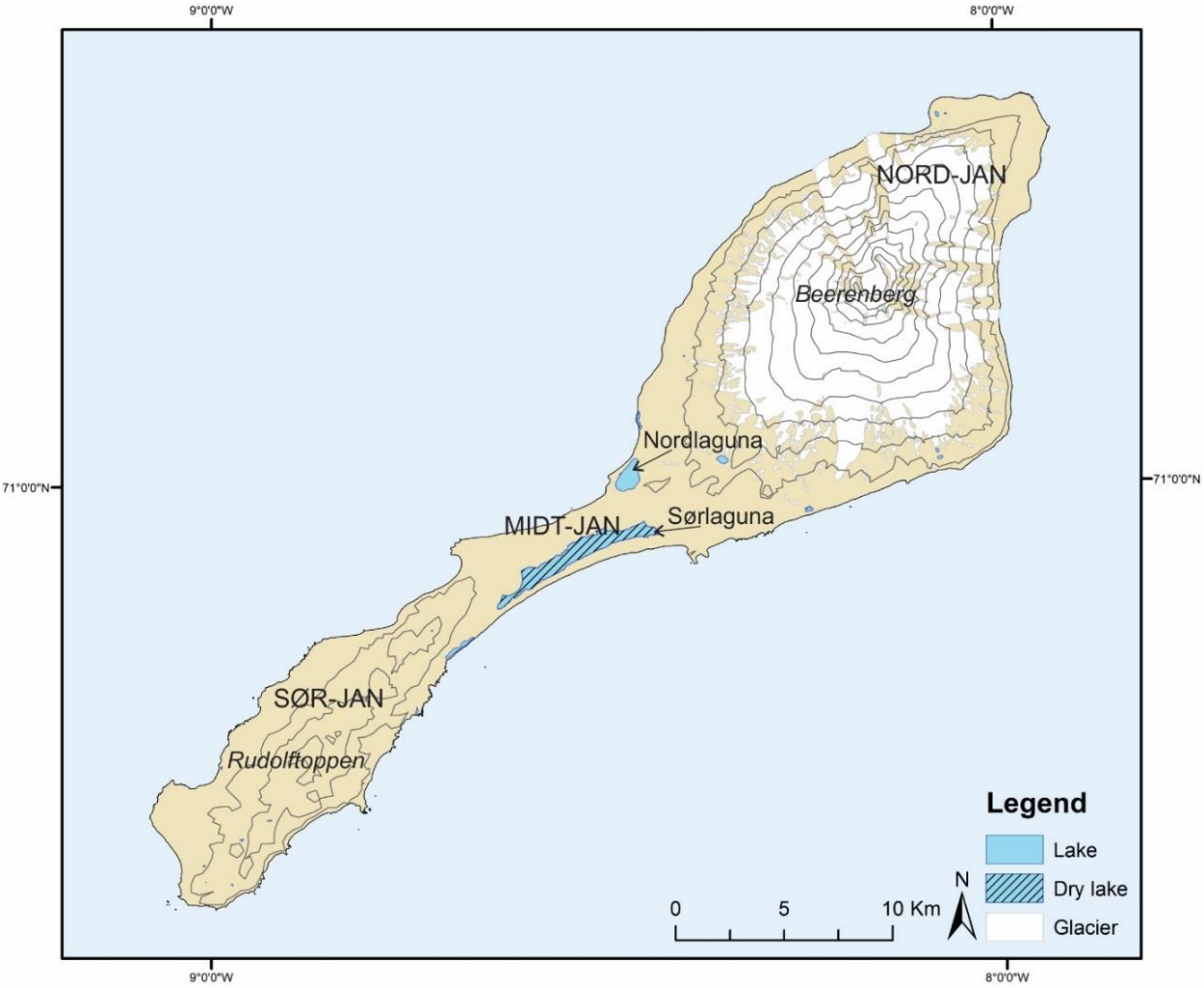

Fig. 3 Jan Mayen is divided in three parts,Nord-Jan in north, Sør-Jan in south and Midt-Jan in the middle. The volcano Beerenberg (2277 m a.s.l.) is the highest mountain at Nord-Jan, and Rudolftoppen (760 m a.s.l.) is the highest mountain at Sør-Jan. Nordlaguna is the largest permanent lake at the island, while Sørlaguna is a shallow lake that dries out during summer. Contour interval 200 m

Nord-Jan is dominated by the active volcano Beerenberg (2277 m a.s.l.) (Fig. 4). The summit is covered by an ice cap with 20 outlet glaciers down the slopes, some extending down to sea level. The glaciers cover an area that is approximately one third of the total area of the island (Hagen et al., 1993; Orheim, 1993).

Fig. 4 Nord-Jan is the location of the active volcano Beerenberg (2277 m a.s.l.)

Midt-Jan is the narrow connection between Nord- and Sør-Jan (Fig. 3). This is where the two largest water bodies on the island are located, Nordlaguna at the western side and Sørlaguna at the eastern side. Nordlaguna is almost 40 m deep, and the largest permanent lake on the island, while Sørlaguna is shallow and usually dries out during summer (Skreslet, 1969). Sør-Jan is long and narrow with several peaks. The highest peak is Rudolftoppen (769 m a.s.l.) (Fig. 5). There are no glaciers and no active volcanism at this part of Jan Mayen today, but there are remains of volcanic activity from northeast-trending fissures, single craters, lava fields, domes, tuff cones etc. (Imsland, 1978).

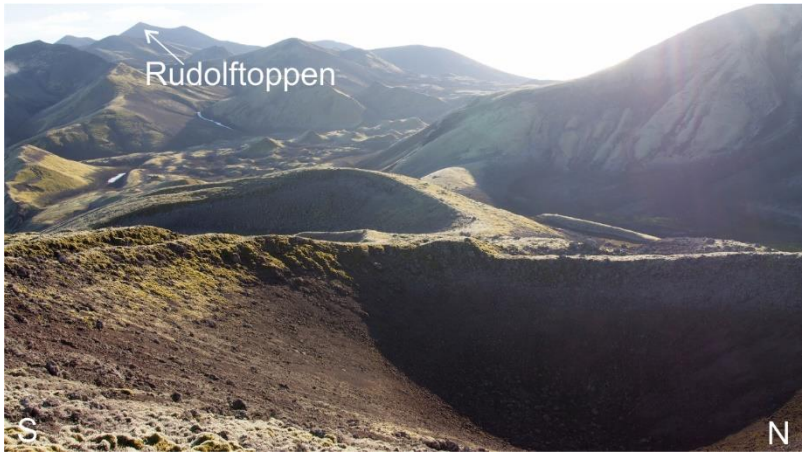

Fig. 5 Typical landscape at Sør-Jan. The highest peak at Sør-Jan, Rudolftoppen (769 m a.s.l.) is seen in the background

Since the rediscovery of Jan Mayen in the 17th century, four eruptions have been observed: in 1732, 1818, 1979 and 1985 (Gabrielsen et al., 1997). Sylvester (1975) suggested that an eruption has occurred between 1650 and 1882, based on historical maps providing evidence of changes to the coastline. Imsland (1978) estimates that there has been at least 75 eruptions during Holocene, with an average of 100-133 years between each eruption. However, the historically recorded eruptions gives an indication of one or two per century (Gjerløw et al., 2015).

2.1.1 Climate and oceanography

The information about the climate at Jan Mayen below is collected from Gabrielsen et al. (1997). The climate on Jan Mayen can be defined as Arctic-marine. Meteorological observations since 1922 shows that the summers are cool with an average temperature of 4.9°C during the warmest month (August), while the winters are mild and has an average temperature of -6.1°C during the coldest months (February-March). The winds are often strong, especially during wintertime. 22 % of the days in January had a maximum wind strength of 6 or more on the Beaufort scale (strong breeze), but the percentage is almost half of this in June. The average yearly precipitation is approximately 700 mm. These measurements are from the location of the present meteorological station, but the wind and precipitation can have great local variations due to the topography of the island. The humidity is high, and there is an average of 3-7 days without fog during a year.

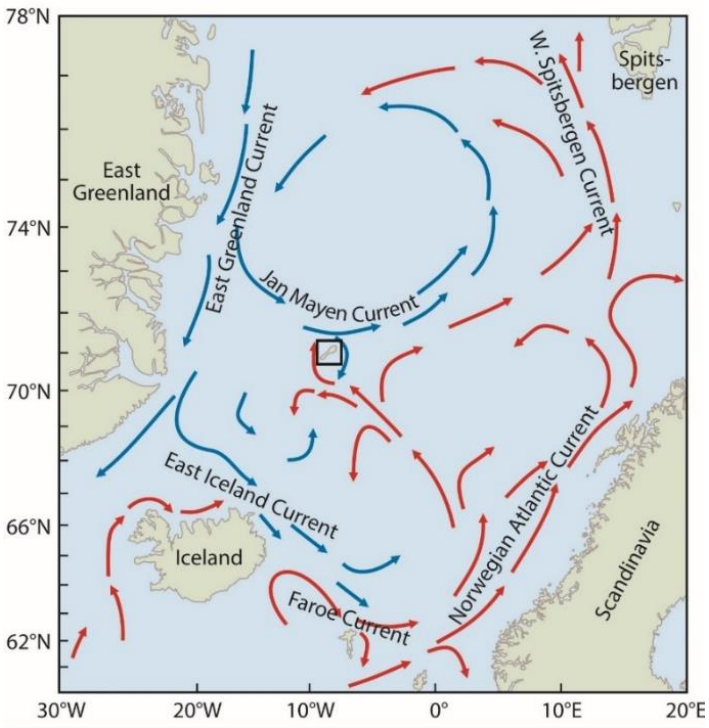

Fig. 6 Ocean currents in the Norwegian-Greenland Ssea. Jan Mayen is located between the warm Atlantic current (red arrows) and the cold east Greenland current (blue arrows) (modified from Gabrielsen et al. (1997))

The island is located between the two ocean currents in the Norwegian-Greenland Sea, the warm Atlantic Current and the cold East Greenland Current (Fig. 6) (Bourke et al., 1992).

Throughout the years, variations in sea ice conditions at Jan Mayen has been observed. During the first polar year in 1882-83, an Austrian-Hungarian expedition team stayed on the island through the winter. According to their observations, the sea ice surrounded the island until July (Barr, 2015). From 1920 to the end of 1930s, there was little or no sea ice around Jan Mayen (Iversen, 1936). The sea ice extent increased after this period, and until the end of 1990, Jan Mayen was usually surrounded by sea ice from November to May (Steffensen, 1982). However, the sea ice in the Arctic is decreasing (Stroeve et al.,

2007), and since the end of 1990s, the sea ice has not reached the island (pers. comm. staff at the station, 2016).

Large amounts of driftwood is accumulated on the beaches of Jan Mayen. This originates from Siberia and northwest Russia, and is transported to Jan Mayen by the East Greenland Current (Johansen, 1998). In order to be transported such long distances without sinking, the wood needs to be transported by the sea ice (Häggblom, 1982). As the sea ice has not reached Jan Mayen since the end of 1990s, there is no driftwood transported to the island today

2.1.2 Bedrock geology

The oldest subaerial rocks on Jan Mayen have an age of 460.9±55.8 ka. (Cromwell et al., 2013). The island is composed of potassic alkaline volcanic rocks with a composition ranging from ankaramites to trachytes (Imsland, 1978). The bedrock geology is divided into five stratigraphic units based on their relative age, and compiled by W. Dallmann/The Norwegian Polar Institute (Gabrielsen et al., 1997) (Fig. 7). The following information about the stratigraphic units is from Imsland (1978). All units, except the basements rocks, are seen in the geological map in Fig. 7.

"Hidden" formation

The basement rocks of Jan Mayen extend up to the present sea level, and the knowledge of this formation is from xenoliths and small exposures in cliffs close to sea level. The composition of the rocks range from ankaramites to trachytes.

Havhestberget formation

This formation is found all over Jan Mayen. It is above the basement rocks, and mostly occurs below the other stratigraphic units. The base of this formation is only seen at small outcrops at sea level on Sør- and Midt-Jan, where rocks from the hidden formation are exposed. The unit consists of hyaloclastite, which is a volcanic rock that is formed submarine or subglacial (Jakobsson & Gudmumdsson, 2008), as well as lava and tuff. The rocks are, with one exception, ankaramitic and basaltic tuffs and breccias.

Nordvestkapp formation

A large proportion of the rocks on Jan Mayen belong to this formation, which is found all over the island. The formation overlies the Havhestberget formation. It is suggested that prior to the formation of this unit, Jan Mayen consisted of many small islands, and that subaerial eruptions on these islands gradually connected them. The formation mainly consists of effusive subaerial rocks, ankaramitic- and basaltic lavas. Intermediate lavas and hyaloclastites are also found in this formation.

Inndalen formation

This formation is found on the surface almost all over the island, and is the youngest rocks on Jan Mayen, which are believed to form postglacially. It usually overlies the Nordvestkapp formation, but is also found on the Havhestberget formation. Due to its young age, the surface of the formation has not been as exposed to weathering processes as the other formations, and the surface structures of the lava flows are often well preserved. The rocks in this formation are basic lavas, scoria craters and scoria cover, trachytic domes and two hyaloclastite occurrences.

Unconsolidated deposits

This unit includes material formed by weathering and erosion, such as beach sediments, moraines, screes, outwash deposits and blocky ground. These deposits are found throughout the island.

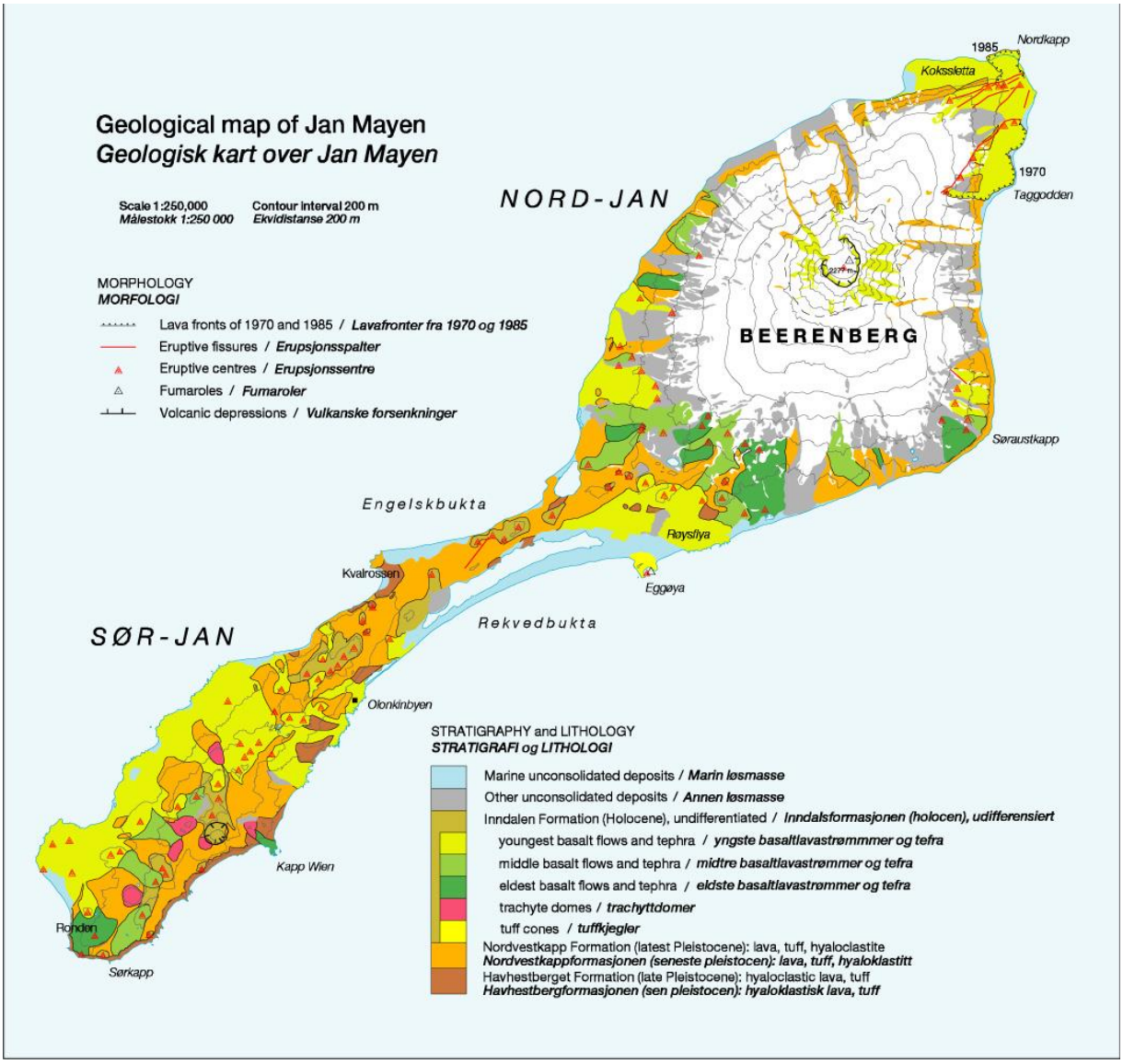

Fig. 7 Geological map of Jan Mayen by W. Dallmann/The Norwegian Polar Institute (Gabrielsen et al., 1997)

2.1.3 Glacial geology

There are few studies of the glacial history of Jan Mayen**.** Fitch (1964) and Fitch et al. (1965) described two tillites from Jan Mayen, at the eastern and northern side of Nord-Jan. Since no other tillites are found higher in the stratigraphy, these were interpreted by Fitch (1964) to be from the last glacial maximum, or alternatively from younger dryas. Imsland (1978) denies this and claims that the island has been without major glaciers during Pleistocene, as the island would be too small for large glaciers to form. However, recent studies demonstrate that the entire island was covered by a large glacier during the last glaciation (Lysså et al., in prep, Lysså pers. comm. 2018).

According to Anda et al. (1985), the glaciers on Jan Mayen are likely to have two major advances during Holocene, around 2500 years BP and a maximum extent at AD 1850. Sporadic observations of glaciers since 1632 have shown several periods of fluctuations of the glacier fronts, as summarized by Orheim (1993): maps and descriptions of Sørbreen by expeditions in 1632 and 1817-18 shows that the glacier front did not reach sea level at that time. In 1861 and 1878, however, observations show an extension of the glacier front to sea level. This period is the maximum of the Little Ice Age at Jan Mayen. In 1882-83, it was observed that the glacier front had retreated from the sea, and it has continued its retreat ever since. Aerial photographs from 1949 shows that the glaciers had a minimum extent around this time (Orheim, 1993; Hulth et al., 2010**)**. Around 1960, Sørbreen started a new period of advance (Lamb et al., 1962; Kinsman & Sheard, 1963), but has since then retreated, and was in 2010 close to the 1949-position (Hulth et al., 2010).

A quaternary geological map of Jan Mayen is published by K. Høgvard/The Norwegian Polar Institute (Gabrielsen et al., 1997) (Fig. 8).

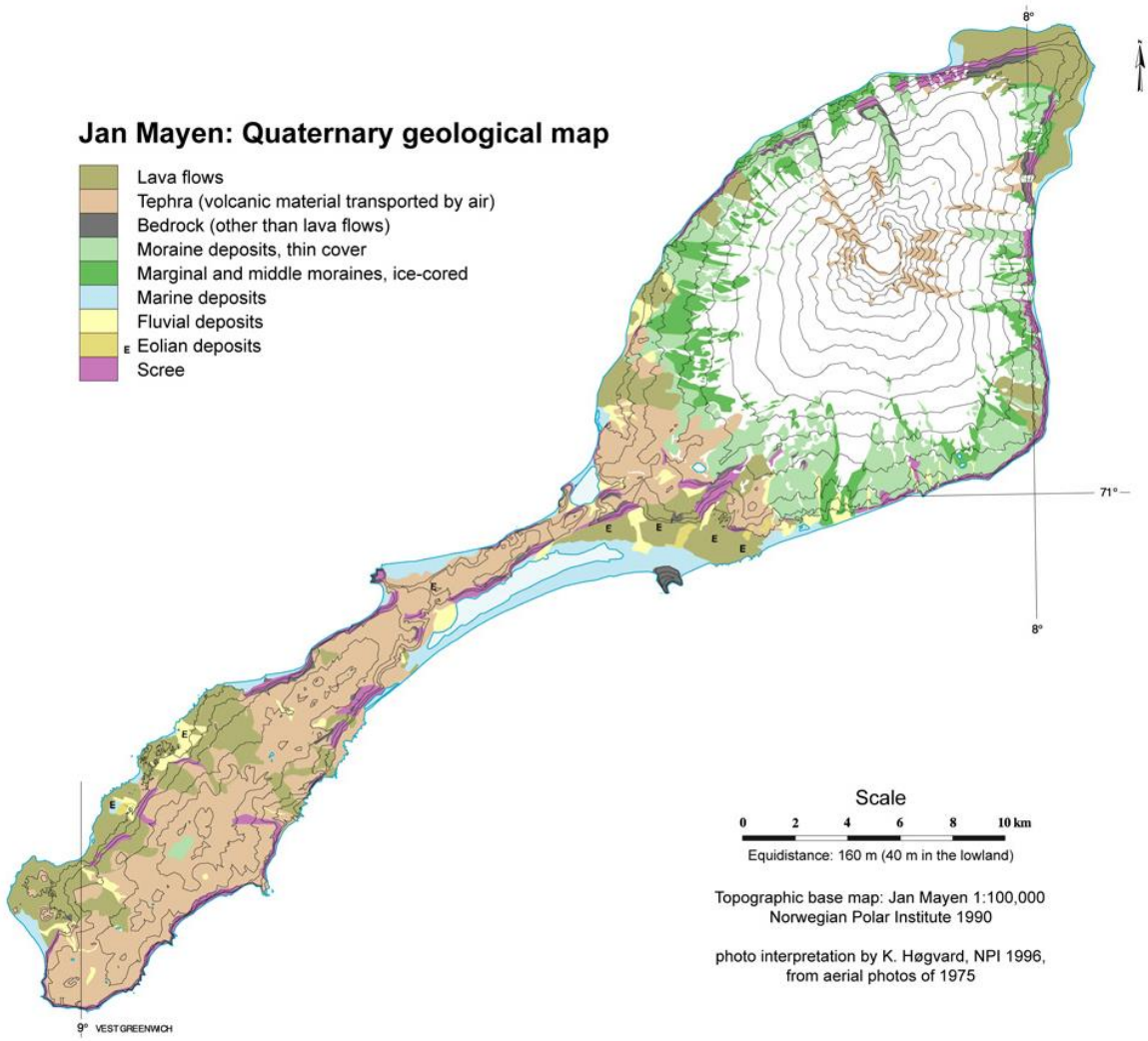

Fig. 8 Quaternary geological map of Jan Mayen by K. Høgvard/Norwegian Polar Institute (Gabrielsen et al., 1997)

2.2 Study area: Nordlaguna and the adjacent land area

The study area for this thesis is the lake Nordlaguna and the adjacent land area (Fig. 9). The lake is located on the western side of Jan Mayen, at the foot of Beerenberg (Fig. 3). It is located approximately 2 m a.s.l., and has no outlets to the ocean.

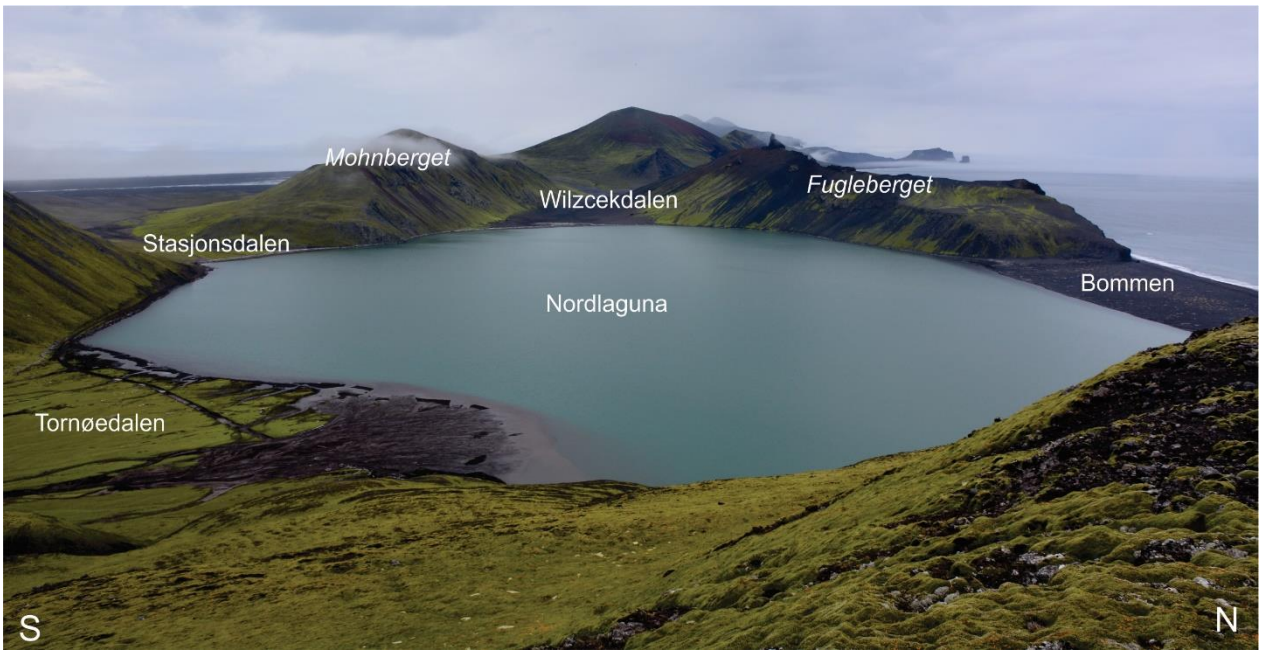

Fig. 9 Nordlaguna seen from east. See Fig. 10 for overview map with place names (photo: A. Lysså)

The lake is separated from the ocean by a 1 km long barrier, Bommen (Fig. 10). The American base from the Second World War, Atlantic City, was located at the northeastern side of the barrier, and was destroyed during a storm in 1954 (Barr, 2015). Only a few remnants of the buildings are found today, as well as a hut from the hunting period in early 1900s.

Four mountains with steep slopes surround the lake, Hochstetterkrateret (138 m a.s.l.) in the north, Wildberget (300 m a.s.l.) in the east, Mohnberget (180 m a.s.l.) in the south and Fugleberget (136 m a.s.l.) in the west (Fig. 10). Three valleys separate the mountains, Tornøedalen, Stasjonsdalen and Wilzcekdalen (Fig. 10). Channel systems are found in all valleys, but there are no permanent rivers entering the lake.

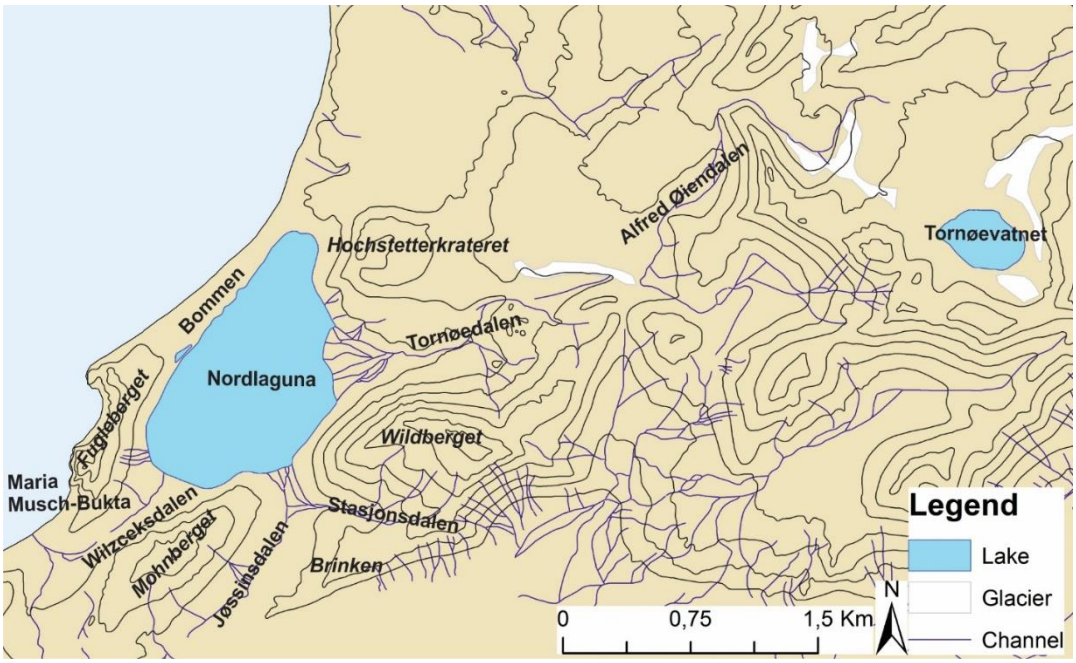

Fig. 10 Overview of the subaerial environment around Nordlaguna. The lake is surrounded by valleys and steep slopes, and is separated from the ocean by a barrier. Contour interval 40 m

Nordlaguna is located approximately 2 m a.s.l. It is 1 km long and 1.5 wide. The subaqueous slopes are steep, and the bottom is flat with a maximum depth of 35.5 m (Fig. 11). A population of Arctic char exists in the lake, evidencing earlier connection with the ocean (Skreslet, 1969). It is suggested that they were separated from the ocean approximately 1500-4000 years ago, based on a suggestion that Nordlaguna was isolated when Bommen became subaerial during land rise (Skreslet, 1973). However, recent studies shows that the lake likely had an outlet via Wilzcekdalen that became blocked during an explosive eruption in Maria Musch-Bukta some 600-800 years ago (Larsen pers. comm. 2018).

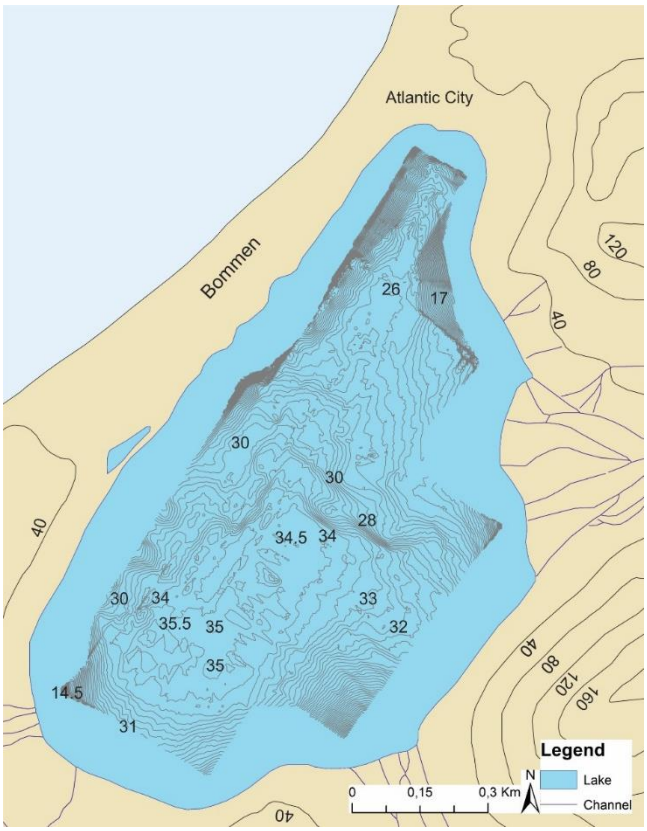

Fig. 11 Nordlaguna is steep sided with a flat bottom and a maximum depth of 35.5 m. Terrestrial contour interval 40 m, bathymetric interval 0.5 m

3. Material and methods

All the material and methods that were used in this thesis are described below. The work is divided into two sections, where the material and methods used for creating the geological map are presented in section 3.1, the field- and labwork is described in sections 3.2 and 3.3 respectively.

3.1 Geological mapping

A geological map showing the distribution of sediments and geomorphology of the terrestrial and subaqueous environment at the study area was created based on field observations and interpretation of high-resolution satellite images. The software and materials that were used are presented below.

Satellite images

Two satellite images of the study area from Kongsberg Satellite Services (KSAT) were provided through the 'ClimJam' project. The images are four band Pancromatic with 0.5 m ground sample distance.

Digital elevation model (DEM)

A digital elevation model (DEM) was used as a background on the geological map in order to visualize the terrestrial topography. The model was downloaded as mosaic files from the ArcticDEM project by the Polar Geospatial Center, where they are distributed as 50 x 50 km sub-tiles with 5 m resolution.

Software

ArcMap version 10.3 was used to analyze the satellite images and create the geological map. The coordinate system used is WGS84/UTM 29N. Shapefiles were created as polygons, polylines or dots to best represent the features that were mapped. The symbols that are used are based on the standards for Quaternary geological mapping used by the Geological Survey of Norway (NGU).

Corel Draw x8 (64-bit) was used to finalize the maps, draw the lithological logs and modify figures. Excel 2013 was used to display graphs and plots from the roundness-, shape- and grain-size analyses.

Sea Scan Review version 5.1.0 was used to display the data from Side Scanning Sonar (SSS). The SSS-images are viewed as a profile that can be controlled forward or backward, with the "Navigation Plotter" window allowing control of the route (Fig. 12). A marker tool is used to create points of interest, which are imported to ArcMap and used to map the lake.

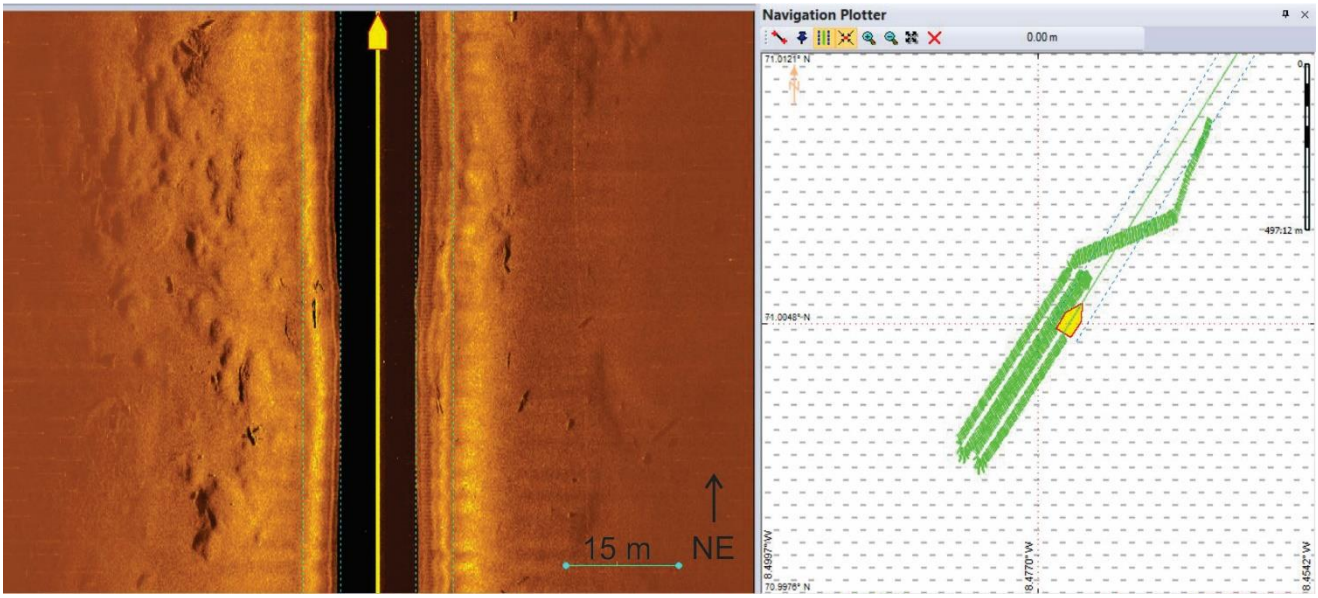

Fig. 12 Example of SSS-profile in Sea Scan Review. The SSS-profile is at left in the image, while the Navigation Plotter window is at right

3.2 Fieldwork

Field investigations

Field investigations were carried out from 11th to 15th of August 2016. The base during fieldwork was the old meteorological station at Jan Mayen, which is located close to the lake. During fieldwork, observations of the terrestrial environment were done and images were taken, which were used when the geological map was created. The surface of the barrier was leveled with approximately 1 m precision. Maximum Particle Size (MPS) was measured at the longest axis of the ten largest clasts within a radius of either 5 or 2 m. Three samples for roundness- and shape analysis and 28 samples for grain-size analysis were collected and lithological logging of three sections were conducted.

Lithological logging

Three sections were described during fieldwork to record the horizontal variations in stratigraphy. Sections from pits approximately one meter deep were cleaned, and lithological logs of the sections were created. The symbols used in the lithological logs are based on Nichols (2009).

Collecting the sediment cores

Two sediment cores (NL1B and NL2) were obtained from the lake in April 2016 in the ClimJam project. These were collected from winter ice (Fig. 13) by using a Nesje-corer, as described in Nesje (1992). SSS-data was used to find locations suitable for coring.

Fig. 13 Collecting of sediment cores from winter ice at Nordlaguna (photo: E. Larsen)

Side-Scanning Sonar (SSS)

SSS-data from the lake was collected by Martin Ludvigsen in August 2015. This was done by mounting a SSS to a Remotely Operated Vehicle (ROV) (Fig. 14), which were driving in a pre-programmed route. The SSS transmits fan-shaped pulses of acoustic energy along the lake floor, to achieve a wide vertical image (Klein, 2002).

Fig. 14 Remotely Operated Vehicle (ROV) with Side Scanning Sonar (SSS) (photo: E. Larsen)

3.3 Labwork

Grain-size analysis

During fieldwork, 28 samples for grain-size analyses were collected from the terrestrial environment around Nordlaguna, and processed in the laboratory at the Department of Geosciences at the University of Tromsø – The Arctic University of Norway. The samples were dried at 40 °C for approximately 24 hours. Sieves were then stacked according to the grain-size classification from the Udden-Wentworth scale (Fig. 15), from 63 µm to 8 mm with a bottom pan to collect the grains <63 µm. One by one, the samples were tipped on top of the stacked sieves and placed in a shaker for 5-10 minutes. The sediments from each sieve were then poured into pre-weighed plastic bags, and the amount of each fraction was weighed. The results are presented as cumulative curves.

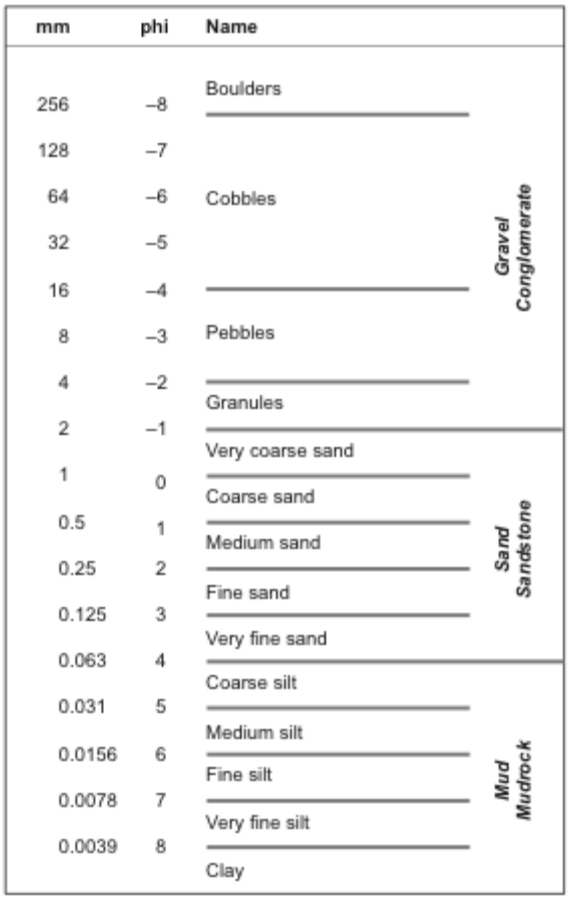

Fig. 15 The Udden-Wentworth scale for classifying grain sizes (Nichols, 2009)

Roundness and shape analysis

Three samples for roundness and shape analysis were collected during fieldwork. The standards by Benn & Balantyne (1994) were used, where 100 clasts with long axis between 35 and 125 mm were collected

for each sample. The clasts that were above or below the maximum and minimum sizes were excluded from the analyses.

Clast shape analyses was conducted by: 1) measuring the a- (long), b- (intermediate) and c- (short) axis of the clast with a caliper 2) calculating the c:a and b:a ratios as well as the disc-rod index ((a-b)/(a-c)) (Benn, 2014). The results were then plotted in a triangle diagram with the three end members blocks, slabs and elongates (Fig. 16).

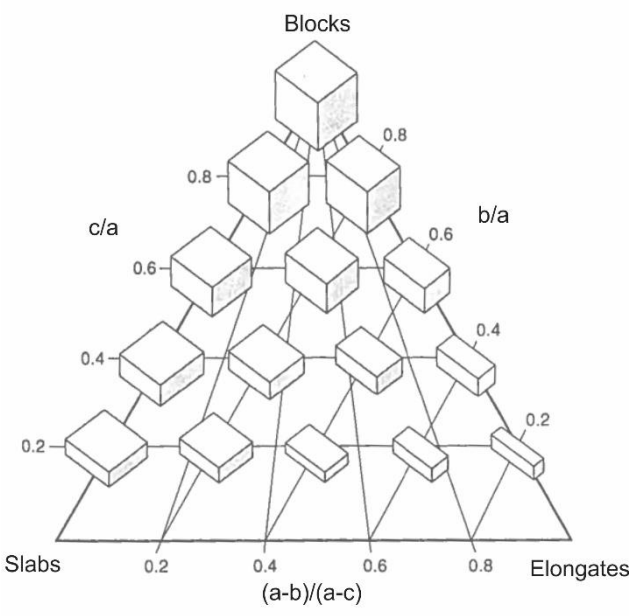

Fig. 16 Clast shape triangle diagram with blocks, slabs and elongated as end members (modified from Benn (2014))

The roundness analysis were carried out by comparing the clasts to the comparison chart in Fig. 17 (Pettijohn et al., 1987) as well as the classification criteria defined by Benn & Ballantyne (1994) (Table 1). The results are presented as a column chart.

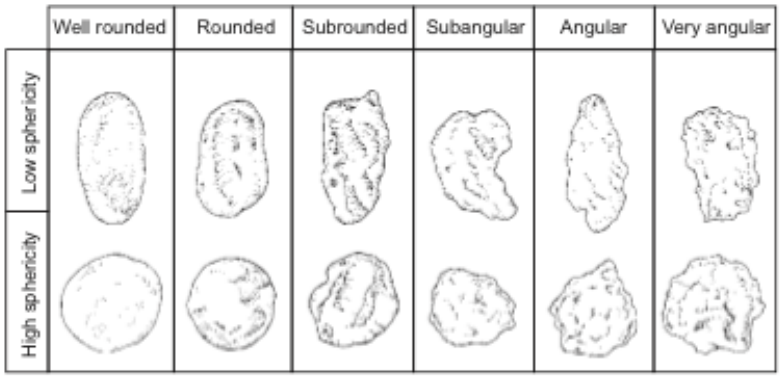

Fig. 17 Comparison chart for roundness analysis (Pettijohn et al., 1987)

Table 1 Roundness classification as defined by Benn & Ballantyne (1994)

Classification	**Description**
Very angular (VA)	Edges and faces unworn, sharp edges
Angular (A)	Edges and faces unworn
Sub angular (SA)	Edges worn, faces unworn
Sub rounded (SR)	Edges and faces unworn, but distinguishable
Rounded (R)	Edges and faces unworn and barely distinguishable
Well rounded (WR)	No edges or faces distinguishable

Processing the sediment cores

The two sediment cores used in this thesis were processed in the laboratory at NGU in Trondheim. All the data from the cores, except the lithological logging, are collected by others and placed at my disposal. This includes ^{14}C-dating, grain-size analyses, measurements of physical properties of the fractional porosity, density and magnetic susceptibility, x-ray images as well as high-resolution images of the core surface. The lithological logging were done by cleaning the core surfaces, and record the sedimentological properties. The symbols that are used are based on Nichols (2009).

The ^{14}C dating of the cores were obtained by Accelerator Mass Spectrometry (AMS) at the Radiocarbon Dating Laboratory in Lund. The material that was dated is of terrestrial origin. The ^{14}C-ages were calibrated with Calib (version 7.0.4), which uses the Intcal13 database.

Samples for grain-size analysis were collected from the cores. A Coulter laser particle size analyzer was used on fractions <500 µm, while fractions >500 µm were measured gravimetric. Gravimetric measurements were done by sieving the sample through sieves with sizes according to the Udden-Wentworth scale (Fig. 15), up to 2 mm. The results of the grain-size analysis are presented as a cumulative curve.

4. Results

The results of the investigations are presented in this chapter. The investigations includes fieldwork at the subaerial environment of the study area, laboratory work and interpretations of data collected by others.

Section 4.1 is a presentation of the results of the geological mapping of the study area, and the main depositional elements are described. In section 4.2, the study area is divided into five sub-areas that are presented individually: Bommen, Tornøedalen, Stasjonsdalen, Wilzcekdalen and the subaerial slopes around the lake. Detailed maps of the sub-areas are presented and described in the sections, as well as the results of the field- and labwork. Section 4.3 is a presentation of the data from Nordlaguna, which includes a map of the sediment distribution in the lake as well as two sediment cores.

4.1 Sediment distribution and geomorphology of the study area

The superficial and geomorphologic deposits in the study area is shown in the overview map in Fig. 18. Legend for the subaerial elements of all maps is presented in Fig. 19, and legend for the subaqueous elements are presented in Fig. 20.

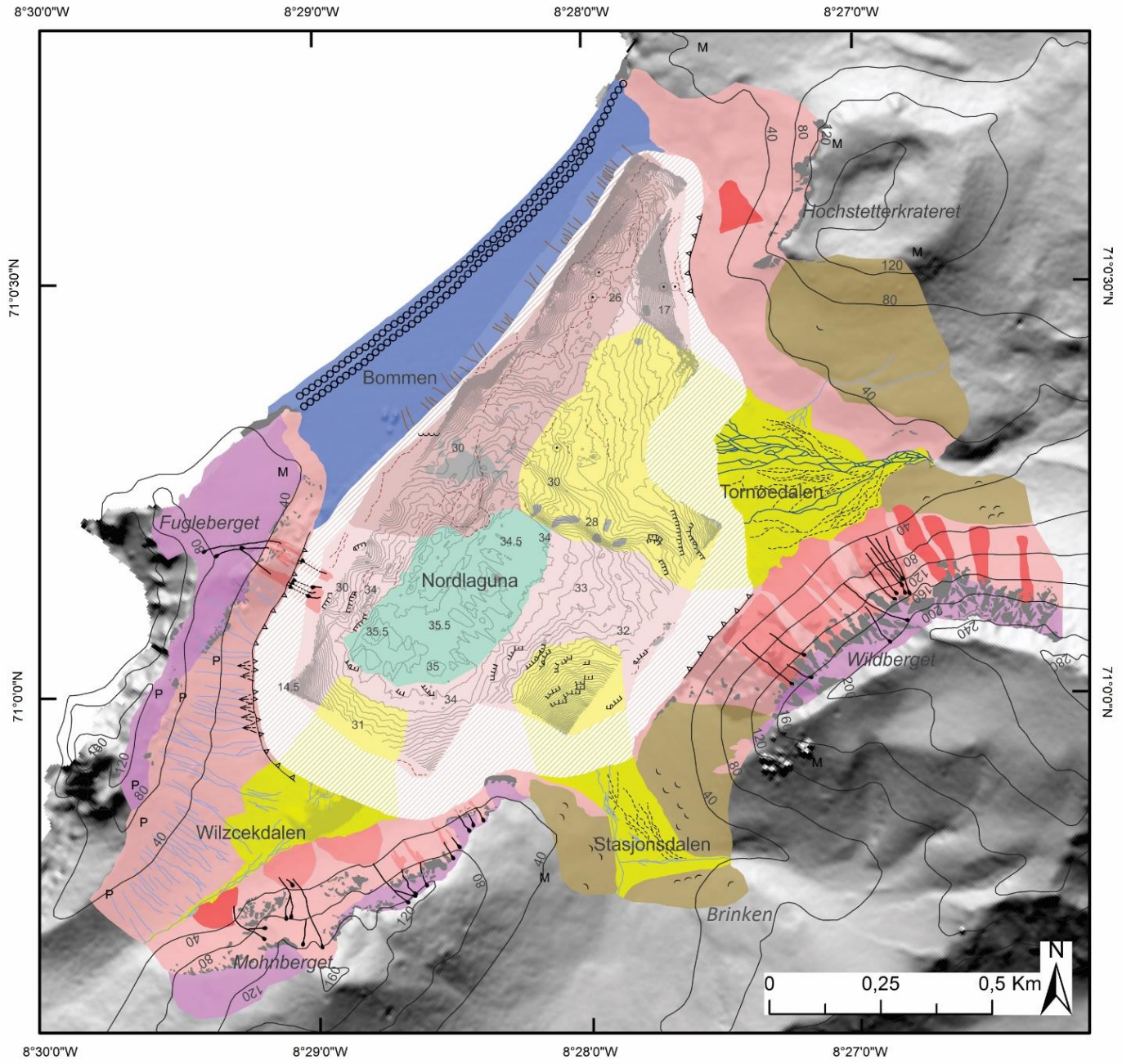

Fig. 18 Geological map of the study area with the main deposits and geomorphological elements in Nordlaguna and the subaerial environment around the lake. Terrestrial contour interval 40 m, bathymetric interval 0.5 m

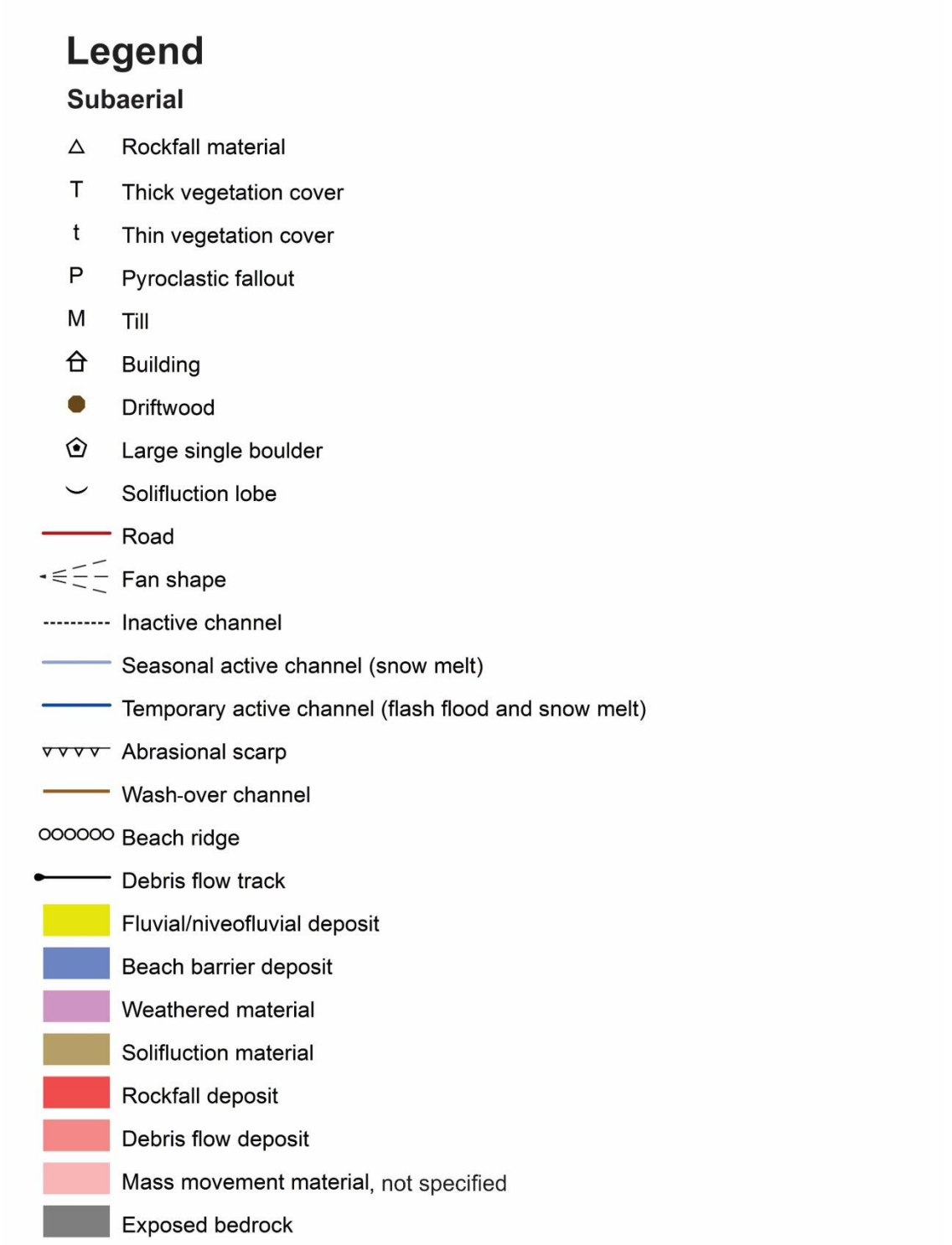

Fig. 19 Legend for the elements at the subaerial environment around Nordlaguna. The legend is for the maps in Fig. 18, Fig. 27, Fig. 79, Fig. 97, Fig. 106 and Fig. 116

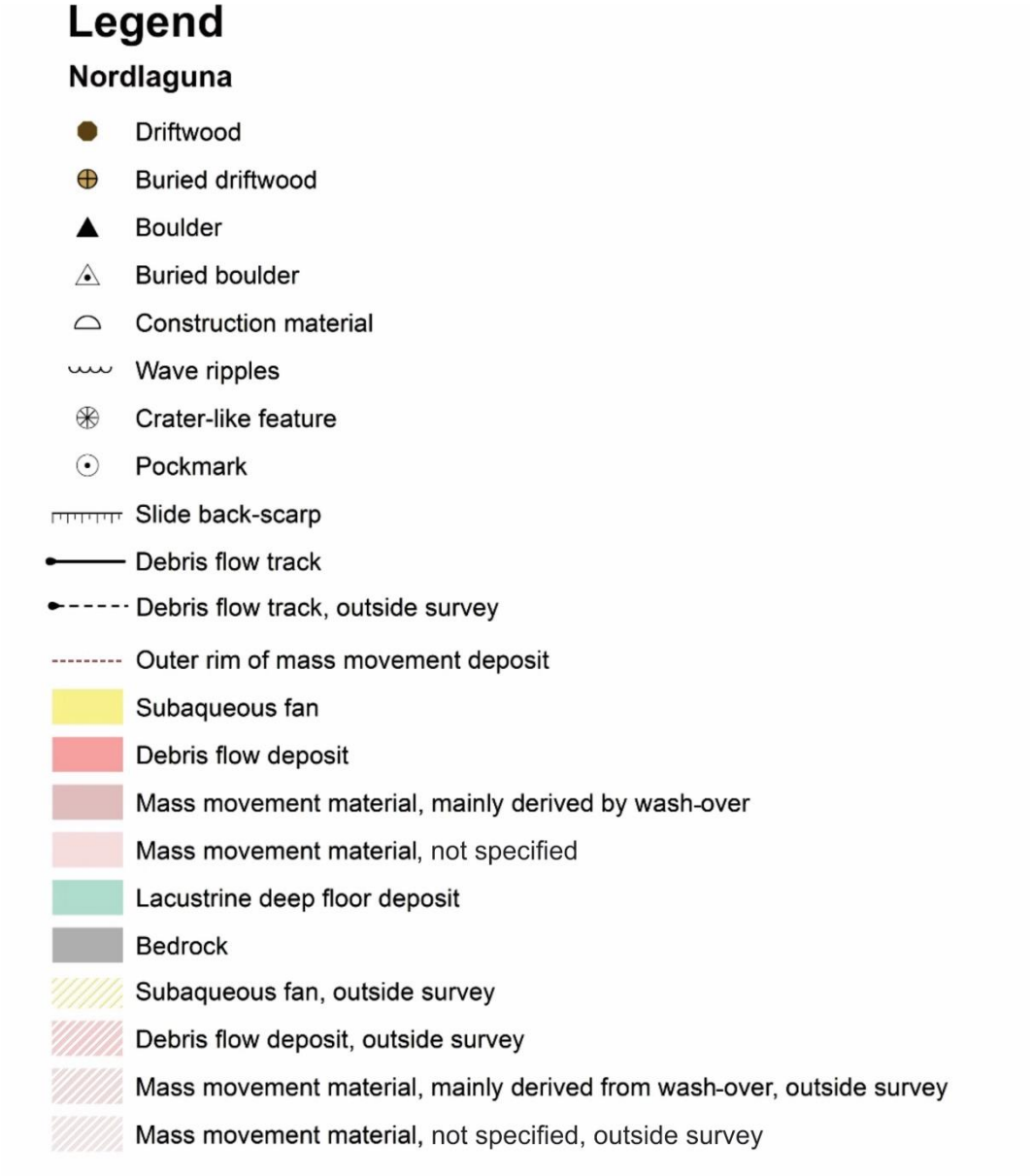

Fig. 20 Legend for the elements at the subaqueous environment in Nordlaguna. The legend is for the maps in Fig. 18, Fig. 27 and Fig. 116

4.1.1 Map description

This section is a brief description of the main depositional elements in the map and their associated morphological features.

Fluvial/niveofluvial deposits

The valley floors in Tornøedalen, Stasjonsdalen and Wilzcekdalen are mapped as fluvial/niveofluvial deposits (Fig. 18). Braided channel systems that are not permanently active are found on the valley floors, indicating that the deposition is dominated by fluvial activity. The terms fluvial and niveofluvial are used to classify the deposits since the deposition is estimated to be derived from temporal fluvial activity throughout the year and seasonal niveofluvial activity during snowmelt season. The subaqueous slopes from the three valleys are mapped as subaqueous fan deposits.

Beach deposit

Beach deposits are found at the surface on the barrier between Nordlaguna and the ocean (Fig. 18). The surface of the deposit consists of a variety of grain sizes, as well as driftwood and vegetation. The barrier is asymmetric in profile, with the ocean-ward side being steeper than the lake-ward side. There are active beach processes on the ocean-ward side of the barrier, and two main beach ridges are developed. Small beach ridges are also observed. The lake-ward side consists of wash-over channels that are created when waves overtop the barrier during storms. Material from the barrier is then transported into the lake. In the lake, the deposition on the subaqueous slope down from Bommen is thus estimated to be mass movement material that are mainly derived from wash-over deposition. This can be illustrated by the large amount of construction material that is found on the subaqueous slope at the northeast-side of the barrier (Fig. 21), which is interpreted to origin from the Atlantic City that was destroyed during a storm in 1954 (Barr, 2015).

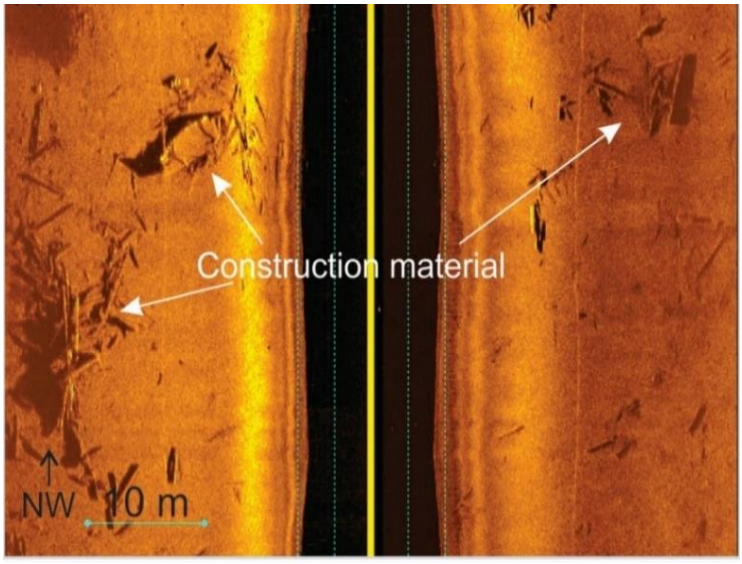

Fig. 21 Large amounts of construction material is found on the subaqueous slope down from Bommen. The material is assumed to be the remains of the American base during the second world war, Atlantic City, which was located on the northeastern side of the barrier, and was destroyed during a storm in 1954 (Barr, 2015)

Solifluction material

Solifluction material is mapped on the north-facing slope down from Wildberget to Tornøedalen, Wildberget, Brinken and Mohnberget in Stasjonsdalen and the slope down from Hochstetterkrateret in Tornøedalen (Fig. 18). The slopes are quite gentle, and is dominated by vegetation rather than loose debris. The vegetation is both thick and thin, and debris is visible on the surface. Lobate shapes can be seen on the slope (Fig. 22). These are interpreted to be solifluction lobes, and is here used as an indicator to recognize solifluction material.

Fig. 22 Solifluction material on the slope down from Mohnberget to the valley floor in Stasjonsdalen. Arrows pointing at examples of solifluction lobes

Weathered material

Loose debris is resting on top of the bedrock at Mohnberget, Wildberget and Fugleberget. This is mapped as weathered material (Fig. 18), since the debris are resting on top of the bedrock and are not likely to be deposited by gravity-driven processes. Pyroclastic fallout has been observed on top of Fugleberget (Lysså and Larsen, pers. comm. 2018), and can therefore be the origin of the debris on top of the slopes, but this requires further field investigations to be established.

Mass movement material, not specified

The steep slopes around Nordlaguna consists of loose debris that undergoes different gravity-driven deposits. The dominating process can not always be specified, and the materials on the slopes are therefore mapped as not specified mass movement material (Fig. 18). The subaqueous slopes in Nordlaguna that are located below the slopes with unspecified mass movement materials are mapped with the same criteria.

Debris flow deposit

On the slopes down from Wildberget in Tornøedalen, Mohnberget in Wilzcekdalen and Fugleberget between Bommen and Wilzcekdalen, debris flow deposits are found (Fig. 18). The deposits have a lobate front, and can often be connected to a debris flow track. Debris flow deposits are also observed on the subaqueous slope below Fugleberget, between Bommen and Wilzcekdalen. The deposits have eroded into the sediments, and debris flow tracks are found on the slope above (Fig. 23).

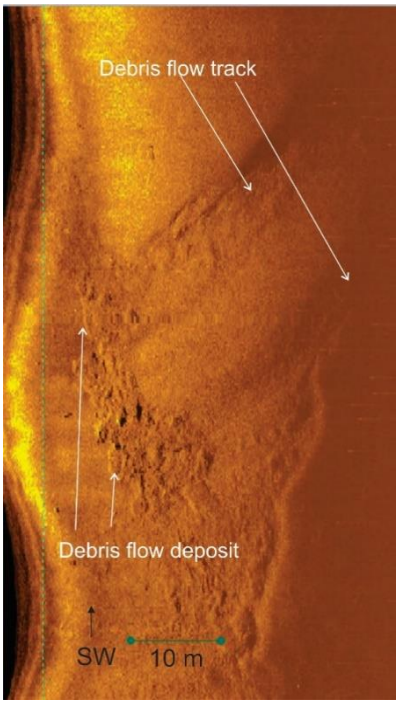

Fig. 23 Debris flow deposit and debris flow tracks on the subaqueous slope down from Fugleberget between Bommen and Wilzcekdalen

Rockfall deposit

Coarse debris are concentrated on the slope below the exposed bedrock at Wildberget in Tornøedalen, Hochstetterkrateret between Bommen and Tornøedalen, and Mohnberget in Wilzcekdalen (Fig. 18). The debris spreads out on the slope, and is deposited as either a thin (Fig. 24) or a thick cover.

Fig. 24 Thin cover of rockfall deposit on the slope down from Wildberget in Tornøedalen

On the valley floors below Wildberget in Tornøedalen and Mohnberget in Wilzcekdalen, boulders are scattered. Bouncing marks from the rockfall material can be seen in the vegetation on the slopes (Fig. 25).

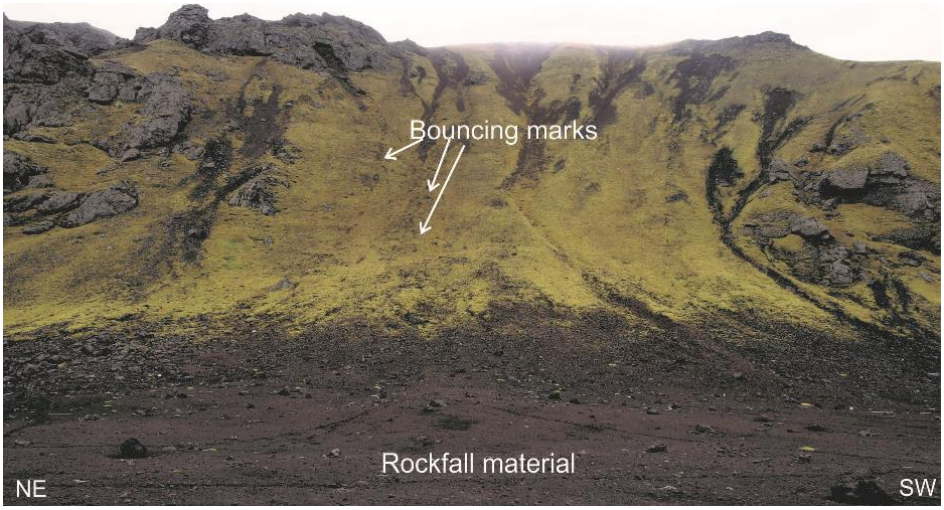

Fig. 25 Rockfall material is scattered on the valley floor in Wilzcekdalen, below the exposed bedrock at Mohnberget. Note the bouncing marks in the vegetation on the slope

Exposed bedrock

Exposed bedrock is found on all of the subaerial slopes around Nordlaguna, Hochstetterkrateret, Wildberget (Fig. 26A), Mohnberget (Fig. 26B) and Fugleberget.

Fig. 26 Examples of exposed bedrock on the subaerial slopes around Nordlaguna A) Wildberget in Tornøedalen B) Mohnberget in Wilzcekdalen (photo: E. Larsen)

4.2 Sedimentary sources

The results of the investigations of the subaerial environment at the study area - the sedimentary sources to the lake - are presented in this chapter. Detailed maps of the sub-areas, field observations and laboratory work is presented in the sections of the sub-areas Bommen (section 4.2.1), Tornøedalen (section 4.2.2), Stasjonsdalen (section 4.2.3), Wilzcekdalen (section 4.2.4) and the subaerial slopes (section 4.2.5).

4.2.1 Bommen

Bommen is the southwest-northeast oriented barrier that separates the lake from the ocean (Fig. 27). It is 1 km long, between 5.4 and 7.1 m high and between 135 and 253 m wide. Bommen is at its widest and highest on the southwest-end, while it becomes lower and narrower towards northeast. Remains of the buildings from the Atlantic City, the American base during World War 2, is located at the northeast-end of the barrier, and large amounts of driftwood cover the surface. Exposed bedrock is found at the seaward side on both ends of Bommen. Beach ridges and channels with levees are found at the lake-ward side (Fig. 28A). 39 channels between 15 m to 40 m long and up to 5 m wide were identified. The channels are more prominent on the northeastern-side of the barrier (Fig. 28B), and become less visible towards southwest. They are roughly oriented 90° to the lake shoreline. The channels are interpreted to be wash-over channels that are formed by waves when they overtop the barrier during storms, which is observed to occur on Bommen (Richter, 1946; Barr, 2015).

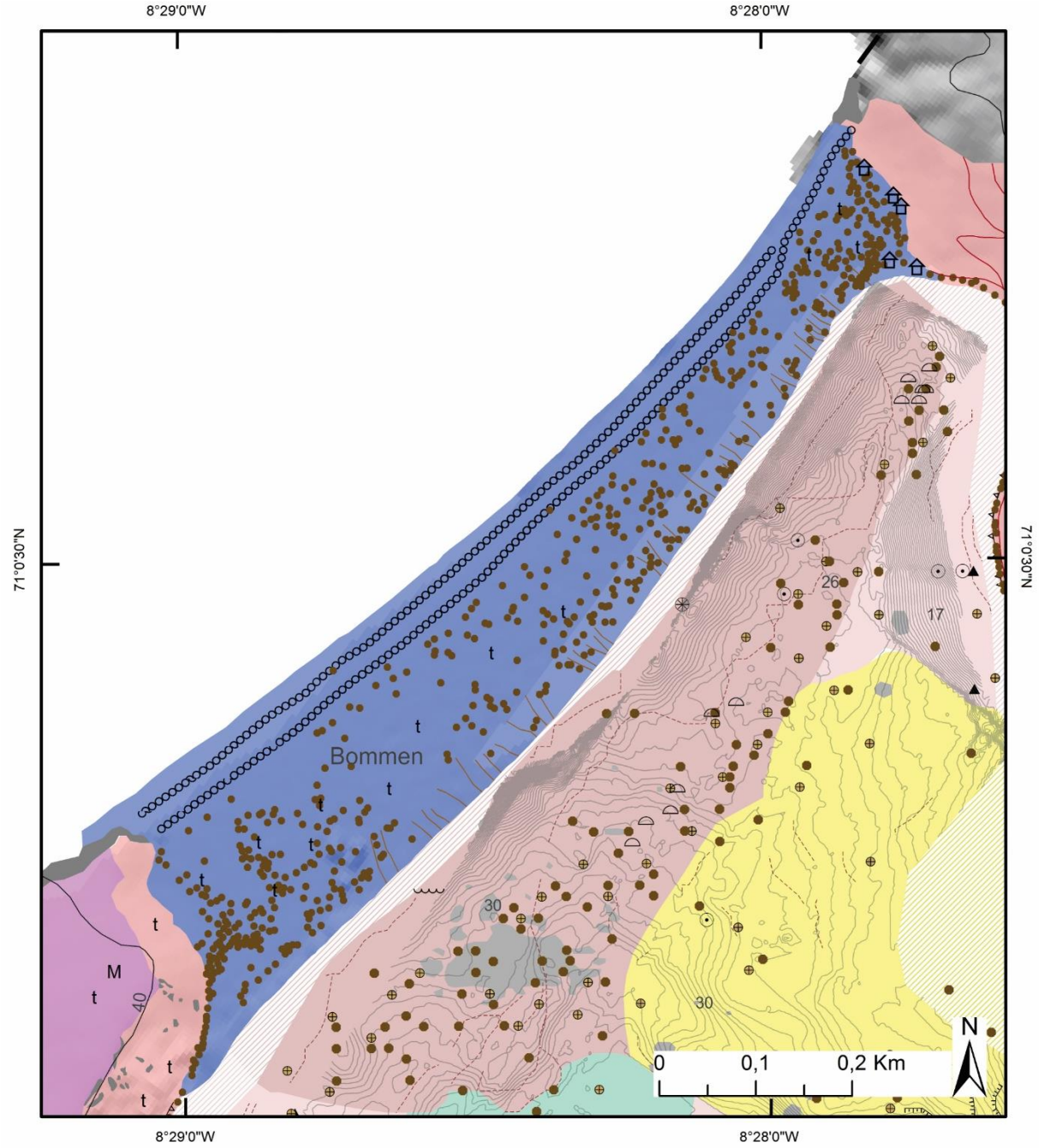

Fig. 27 Detailed geological map of Bommen. Terrestrial contour interval 40 m, bathymetric interval 0.5 m. Legend of elements at the subaerial environment is in Fig. 19, and legend of the elements at the subaqueous environment in Fig. 20

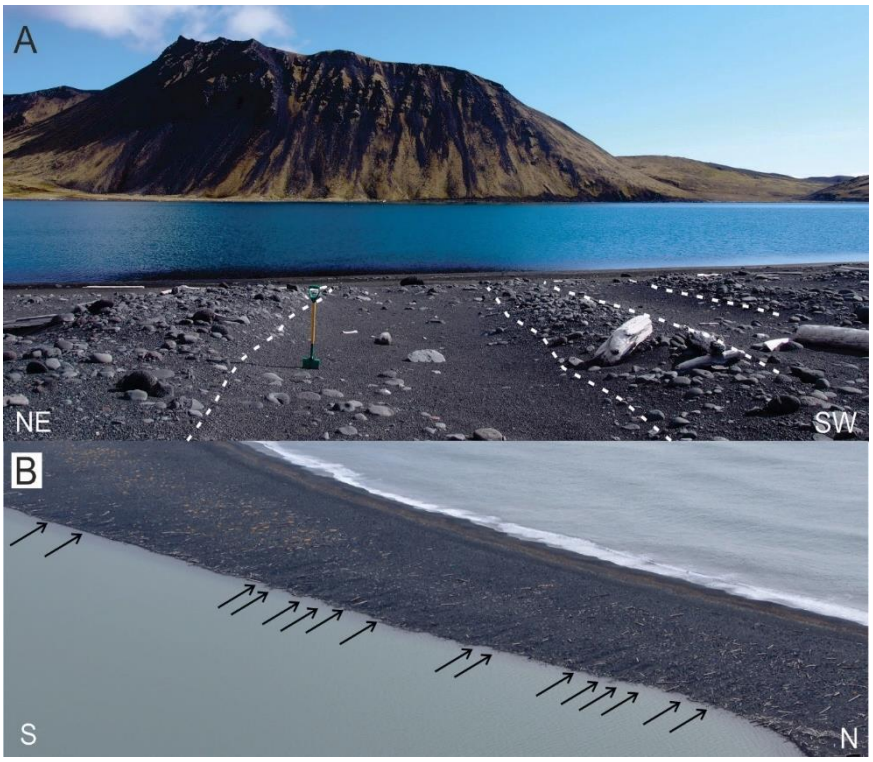

Fig. 28 Wash-over channels on the lake-ward side of the barrier A) Channels with levees at the NE-side of the barrier. The outline of the channels are marked with white B) Arrows pointing to examples of wash-over channels at the NE-side of the barrier seen from above (photo: E. Larsen)

During fieldwork, three profiles on the barrier were investigated (Fig. 29). The surface was leveled and samples were taken for roundness- and shape analyses as well as grain-size analyses. The profiles are divided into two parts, part A extends from the ocean to the peak of the profile, and part B extends from the peak of the profile to the lakeshore.

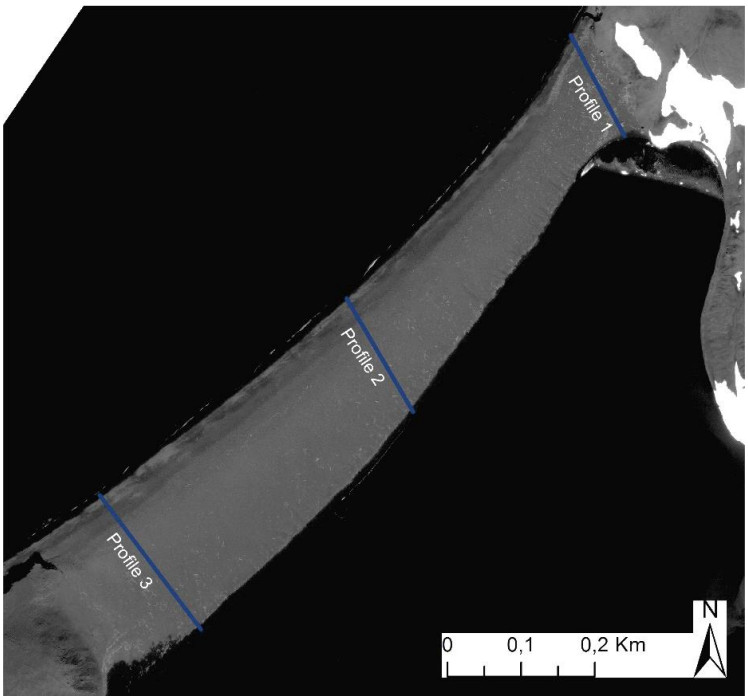

Fig. 29 Location of the three profiles that were investigated on the barrier. Profile 1 is located at the NE-part, profile 2 at the middle part and profile 3 at the SW-part (satellite image: KSAT)

Profile 1

The first profile that was investigated is located at the northeast-side of the barrier (Fig. 29). At this location, the barrier is 135 m wide and has a maximum height of 5.4 m (Fig. 30). Part A of the profile extends from 0-45 m from the ocean, and part B extends from 45-135 m from the ocean. Seven samples were collected along the profile (Fig. 31), one for roundness- and shape analysis (sample B1-1) and six for grain-size analyses (samples B1-2 – B1-7).

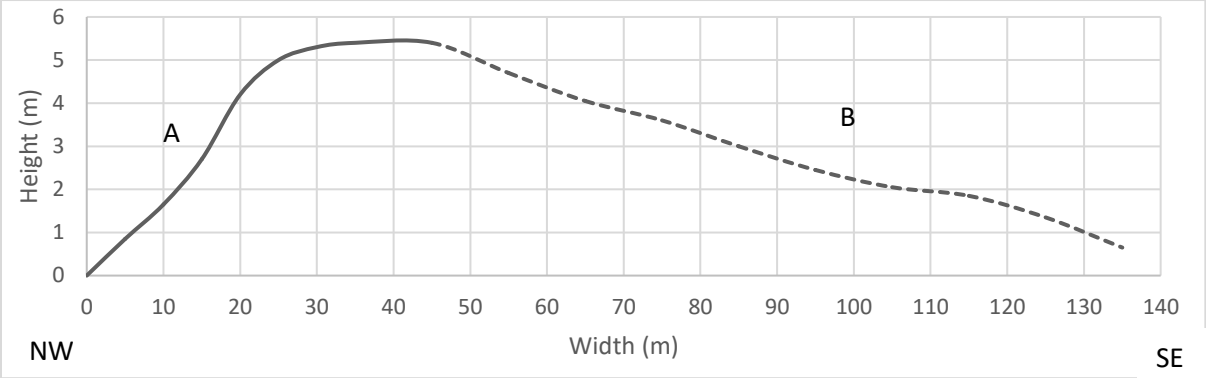

Fig. 30 Leveled surface of the barrier at profile 1. At this location, the barrier is 135 m wide and has a maximum height of 5.4 m a.s.l. Vertical scale is exaggerated

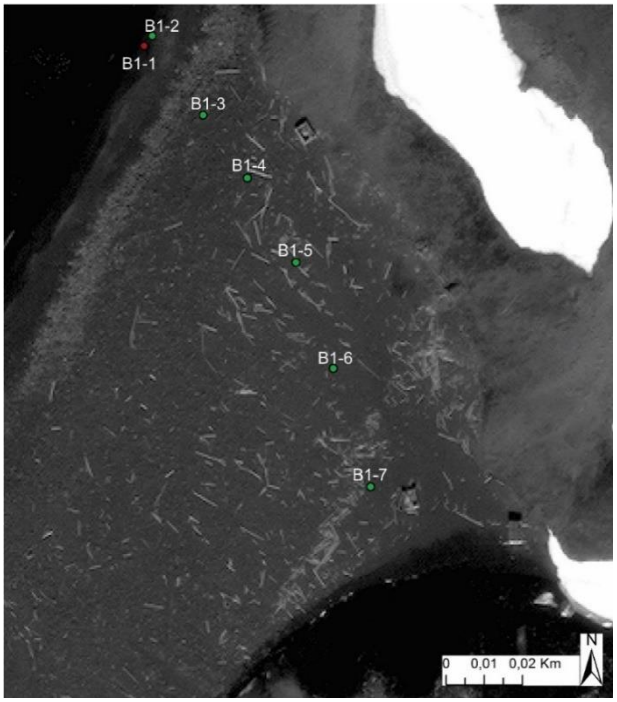

Fig. 31 Locations of samples for roundness- and shape analysis (sample B1-1, red dot) and grain-size analyses (samples B1-2 – B1-7, green dots) on profile 1 (see Fig. 12 for location). Note the large amount of driftwood at the surface (satellite image: KSAT)

Part A (0-45 m):

Waves break at the shoreline of profile 1, and enrichments of gravel are found (Fig. 32). Sand is deposited between the enrichments, and boulders up to 1.5 m long are scattered in the sand. Sample B1-1 for roundness- and shape analysis was collected from one of the enrichments of gravel. The clasts are mainly subrounded (44 %) and rounded (42 %), and small amounts of subangular (9 %) and well rounded (5 %) clasts (Fig. 33A). There are a variety of clast shapes, but there is a dominance of blocky and slightly elongated clasts (Fig. 33B). Sample B1-2 for grain-size analysis (Fig. 34) was collected from the sand between enrichments of gravel at the shoreline (Fig. 32). The sample consists of well sorted sand, and less than 3 % gravel.

Fig. 32 Waves break around enrichments of gravel at the shoreline of profile 1 at the barrier. Sample B1-1 for roundness- and shape analysis (Fig. 33) was collected from one such enrichment, and sample B1-2 (Fig. 34) is collected from the sand between two enrichments

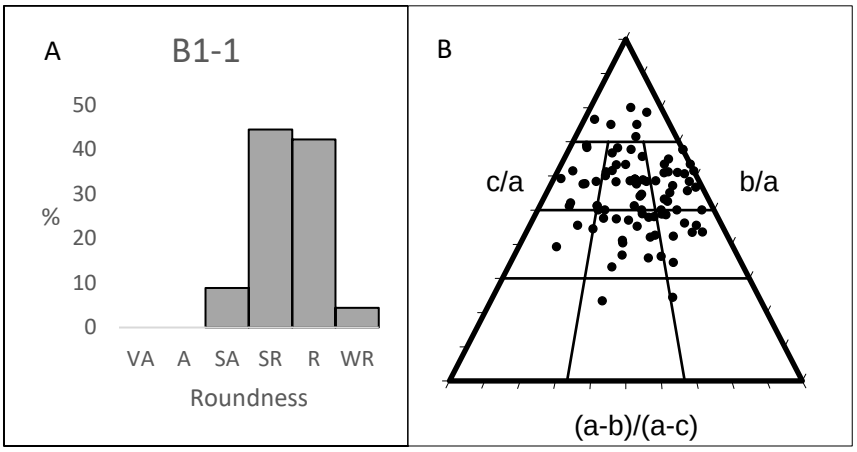

Fig. 33 Sample B1-1 (see Fig. 31 for location) A) Roundness analysis of sample B1-1. The majority of the clasts are subrounded and rounded B) Clast shape analysis of sample B1-1. The sample consists of a variety of shapes, but there is a dominance of blocky and slightly elongated clasts

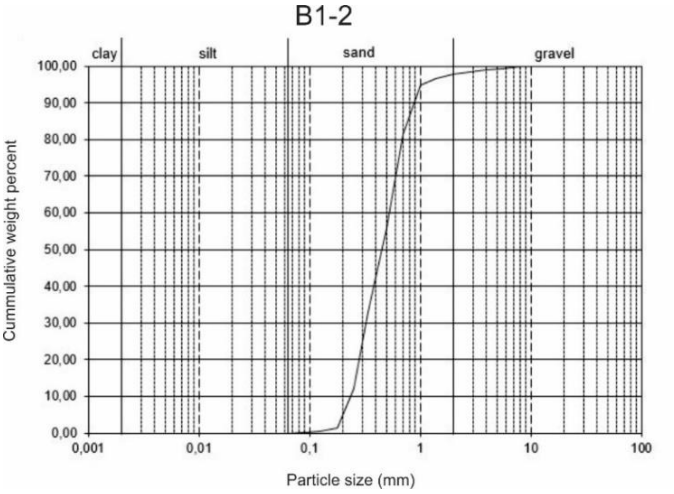

Fig. 34 Grain-size analysis of sample B1-2. The sample is collected from the sand between enrichments of gravel at the shoreline (see Fig. 31 for location). It consists of well sorted sand, and less than 3 % gravel

15 m from the ocean, there is an increase in the slope gradient to the top of the beach ridge at the profile (Fig. 30). The surface contains mainly boulders (Fig. 35). MPS was measured at the long axis of the 10 largest clasts within a radius of 5 m, which gave the following measurements (in cm): 92, 93, 98, 103, 105, 110, 124, 126, 129, 151. This gives an average of 100.5 cm.

Fig. 35 An increase in the slope gradient is seen 15 m from the ocean, and boulders cover the surface.

The peak of the beach ridge is 28 m from the ocean, where the surface flats out (Fig. 30). The amount of boulders is decreasing (Fig. 36). Sand is deposited between the boulders, and sample B1-3 for grain-size analysis (Fig. 37) was sampled at this location. The sample consists of well sorted sand, and less than 4 % gravel.

Fig. 36 The surface at the barrier flats out 28 m from the ocean. The surface contains a variety of grain sizes. Sample B1-3 for grain-size analyzing (Fig. 37) is collected from sand between the boulders

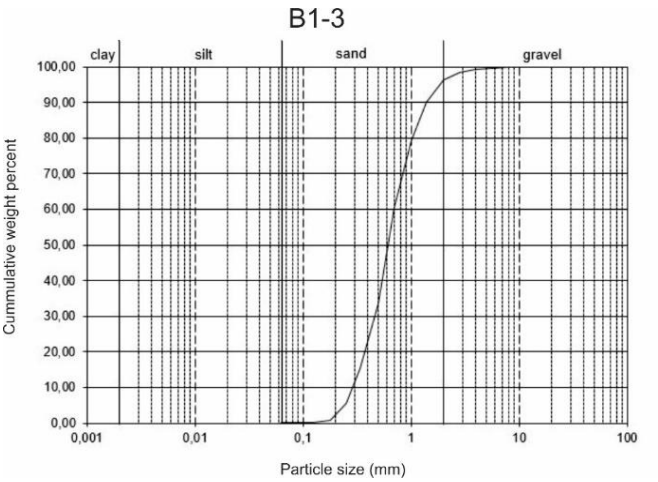

Fig. 37 Grain-size analysis of sample B1-3. The sample is collected from sand between boulders at the flat surface of the barrier (see Fig. 31 for location). It is dominated by sand, and consists of less than 4 % gravel

Towards the end of the flat surface, and the end of part A of profile 1, the size and amounts of boulders decrease, and the surface consists of a variety of grain sizes. Sample B1-4 (Fig. 38) was collected from the end of part A. It consists of mainly sand, and approximately 5 % gravel.

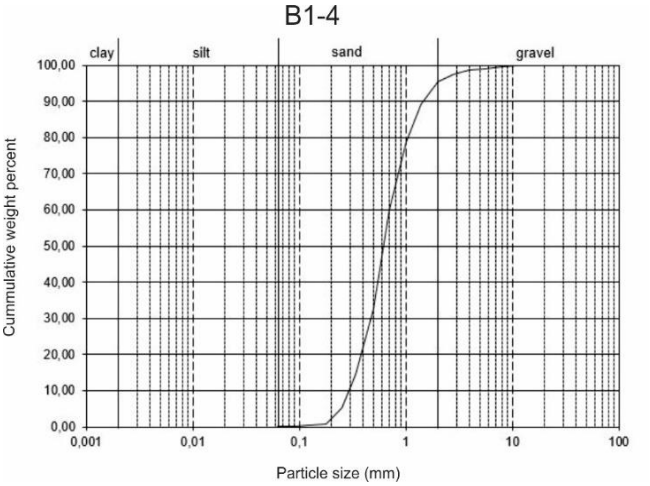

Fig. 38 Grain-size analysis of sample B1-4. The sample is collected from the end of part A at profile 1 (see Fig. 31 for location). The sample consists of mainly sand, and the amount of gravel is approximately 5 %

Part B (45-135 m):

The flat top of the barrier ends 45 m away from the ocean, where the gentle slope to the lake begins. The lake-ward slope has a gentler gradient than the ocean-ward slope (Fig. 30). Driftwood is scattered on the surface, and vegetation is growing (Fig. 39).

Fig. 39 The gentle slope to the lake consists of a variety of grain sizes as well as driftwood and vegetation

Asymmetric ripples are found at the surface on part B of profile 1. The ripples have a stoss- and lee side and more or less straight crests. They have a maximum height of 1 cm, and wavelength of 18 cm. The stoss side is dipping towards northwest. At the same location, the surface consists of concentrations of gravel, suggesting that the sand has been removed (Fig. 40). The two features described above are interpreted to be associated with aeolian activity, and is classified as wind ripples and lag-surface (Collinson et al., 2006).

Fig. 40 Example of lag-deposits at part B of profile 1. Gravel are concentrated at the surface, and the sand is removed

Samples B1-5 (Fig. 41), B1-6 (Fig. 42) and B1-7 (Fig. 43) for grain-size analyses were collected from the surface of the slope to Nordlaguna (see Fig. 31 for location). The samples are dominated by sand. The amounts of gravel in the samples decrease towards the lake, and contains 13 %, 5 % and <1 % respectively.

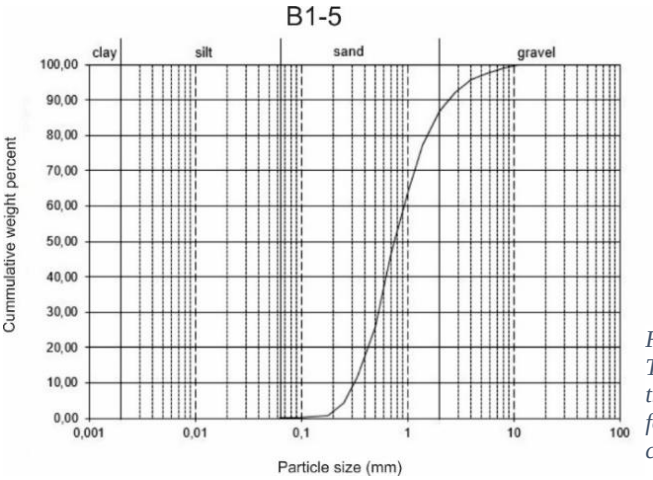

Fig. 41 Grain-size analysis of sample B1-5. The samples is collected from the surface of the slope to Nordlaguna (Part B, see Fig. 14 for location) It is dominated by sand and contains 13 % gravel

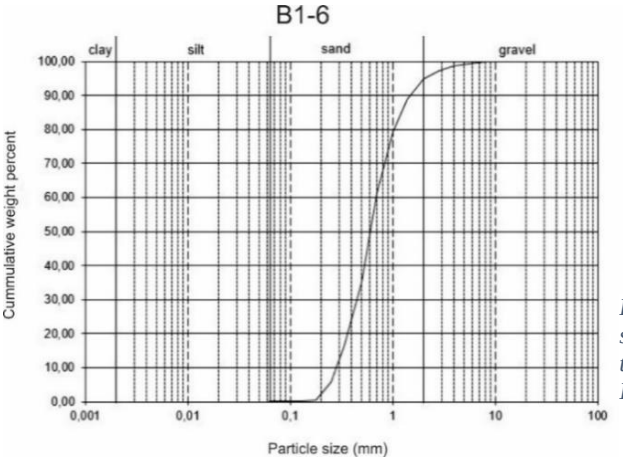

Fig. 42 Grain-size analysis of sample B1-6. The sample is collected from the surface of the slope to Nordlaguna (part B, see Fig. 14 for location). It is dominated by sand and contains 5 % gravel

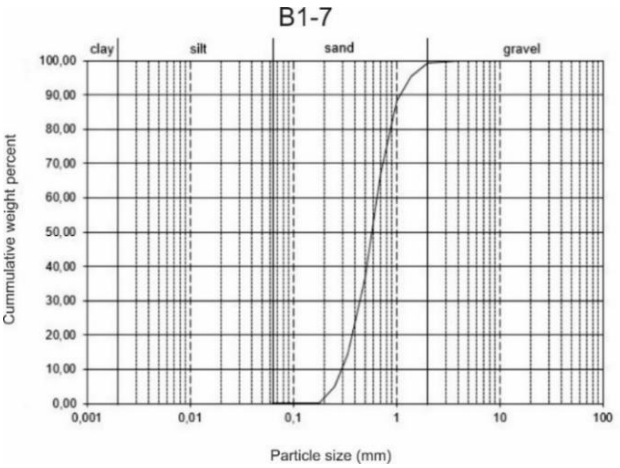

Fig. 43 Grain-size analysis of sample B1-7. The sample is collected from the surface of the slope to Nordlaguna (part B, see Fig. 14 for location). It consists of well sorted sand, and the amount of gravel is <1 %

Profile 2

Profile 2 is from the middle part of Bommen (Fig. 29). At this location, the barrier is 178 m wide and has a maximum height of 6.3 m (Fig. 44). Part A of the profile extends from 0-72 m from the ocean and part B extends from 72-178 m from the ocean. Nine samples were collected along the profile (Fig. 45), one for roundness- and shape analysis (sample B2-1) and eight for grain-size analyses (samples B2-2 – B2-9).

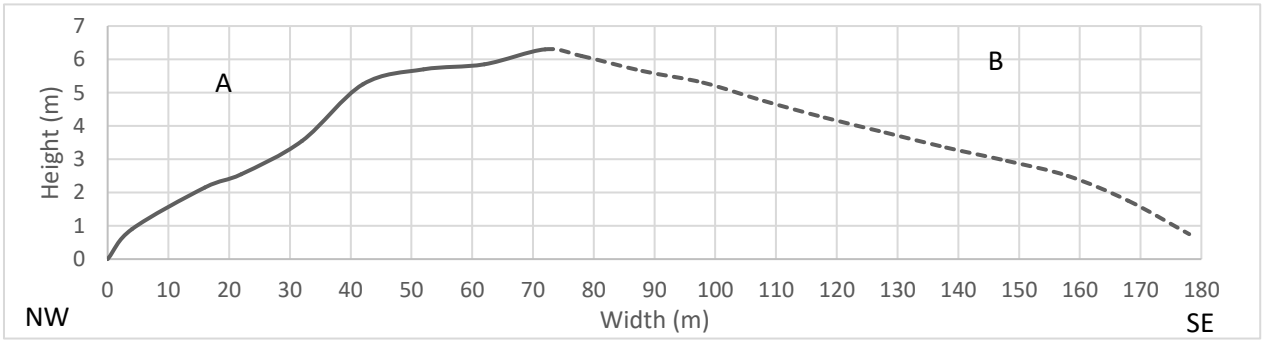

Fig. 44 Leveled surface of the barrier at profile 2. At this location, the barrier is 178 m wide and has a maximum height of 6.3 m a.s.l. Vertical scale is exaggerated

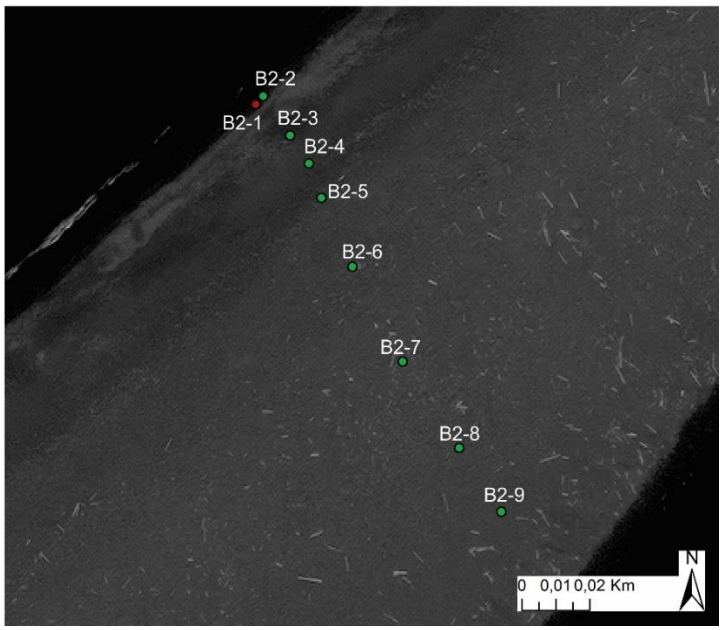

Fig. 45 Locations of samples for roundness- and shape analysis (sample B2-1, red dot) and grain-size analyses (samples B2-2 – B2-9, green dots) on profile 2 (see Fig. 16 for location) (satellite image: KSAT)

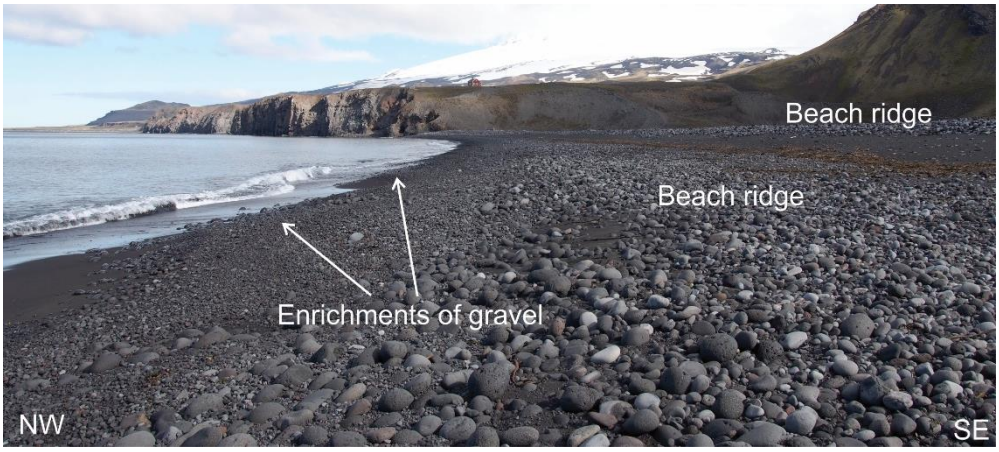

Fig. 46 Waves break around enrichments of gravel at the shoreline of profile 2. Sample B2-1 for roundness- and shape analysis (Fig. 47) was collected from one such enrichment. Sample B2-2 for grain-size analysis (Fig. 48) was collected from the sand between the enrichments. Two beach ridges are found on profile 2 at the barrier

Part A (0-72 m): Waves break at the shoreline of profile 2, and gravel is accumulated in enrichments (Fig. 46). Sand is deposited between the enrichments. Sample B2-1 for roundness- and shape analysis was collected from one of the enrichments of gravel (see Fig. 45 for location). The clasts are mainly rounded (57 %). 30 % are subrounded, 12 % are well rounded and 1 % is subangular (Fig. 47A). The shape analysis shows that the clasts are mainly blocky (Fig. 47B). Sample B2-2 (Fig. 48) for grain-size analysis was collected from the sand at the shoreline. The sand is poorly sorted and shows a bimodal curve, with high amounts of sand and 33 % gravel.

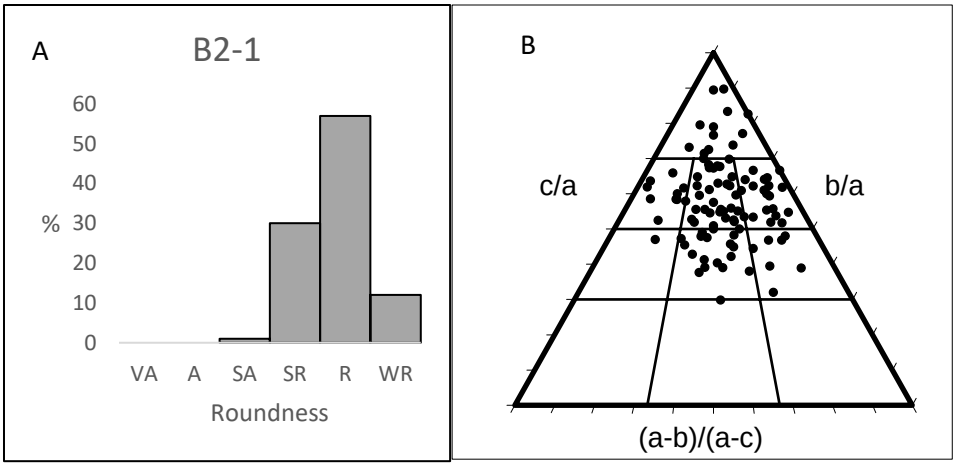

Fig. 47 Sample B2-1 (see Fig. 45 for location) A) Roundness analysis of sample B2-1. The sample is dominated by rounded clasts B) Clast shape analysis of sample B2-1. The clasts in the sample are sample are dominantly blocky

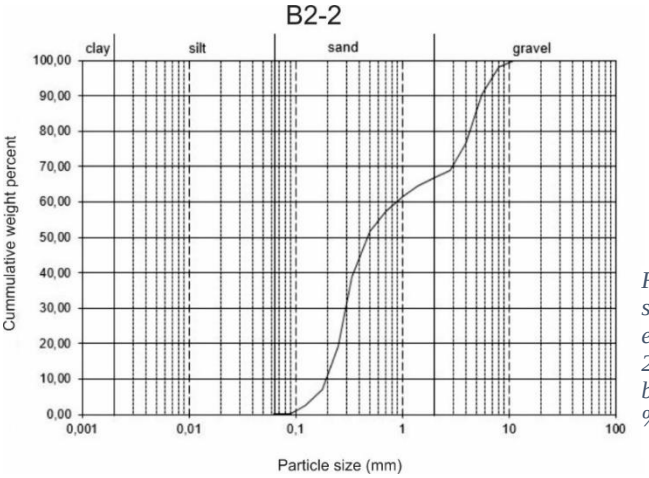

Fig. 48 Grain-size analysis of sample B2-2. The sample is collected from the sand between enrichments of gravel at the shoreline of profile 2 (see Fig. 45 for location). The analysis shows a bimodal curve, with high amounts of sand and 33 % gravel

A beach ridge is located 7 m from the ocean (Fig. 46). This is the shortest beach ridge (890 m long) that is mapped on the barrier (Fig. 27). The beach ridge is 6 m wide at this point, and consists mainly of gravel with a maximum length of 20 cm. Sample B2-3 (Fig. 49) is collected from the sandy surface just beyond the beach ridge, approximately 14 m from the ocean. The sample contains well sorted sand an <1 % gravel

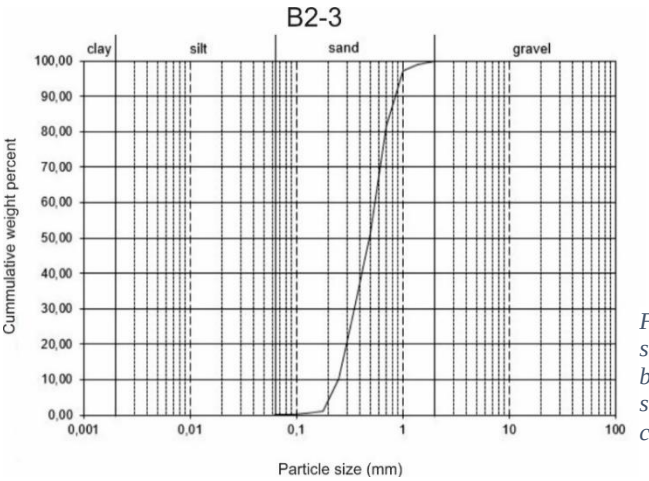

Fig. 49 Grain-size analysis of sample B2-3. The sample is collected from the surface beyond the beach ridge, approximately 14 m from the shoreline (see Fig. 45 for location). The sample consists of well sorted and <1 % gravel

A belt of seaweed is deposited on the sand approximately 19 m from the shoreline. Sample B2-4 (Fig. 50) is collected 24 m from the ocean. The sample shows well sorted sand that is slightly coarser than sample B2-3 (Fig. 49). The amount of gravel is <1 %.

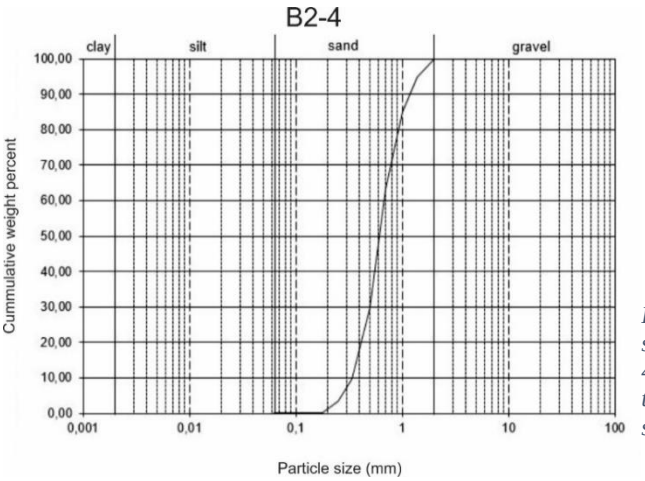

Fig. 50 Grain-size analysis of sample B2-4. The sample is collected 24 m from the ocean (see Fig. 45 for location), between the two beach ridges on the barrier. The sample consists of well sorted sand and <1 % gravel

31 m from the ocean, a beach ridge consisting of mainly boulders are found, which is the southwest-extension of the upper 1 km long beach ridge (Fig. 27) that is also found at profile 1. MPS was measured at the long axis of the 10 largest boulders within a radius of 5 m, which gave the following measurements (in cm): 32, 33, 34, 35, 37, 39, 41, 42, 44, 56. This gives an average of 39.3 cm. The surface beyond the upper beach ridge is flat, and gravel and boulders are scattered in the sandy surface (Fig. 51). Sample B1-5 for grain-size analysis (Fig. 52) was collected from the flat and sandy surface just beyond the upper beach ridge. The sample contains well sorted sand, and the amount of gravel is <1 %.

Fig. 51 Two beach ridges are found at profile 2 on the barrier, with a sandy surface between them. The lower ridge is the 890 m long beach ridge and the upper ridge is the 1 km long beach ridge mapped in Fig. 27. The upper ridge is also found at profile 1. The surface beyond the upper beach ridge is flat, and boulders and gravel are scattered in the sandy surface

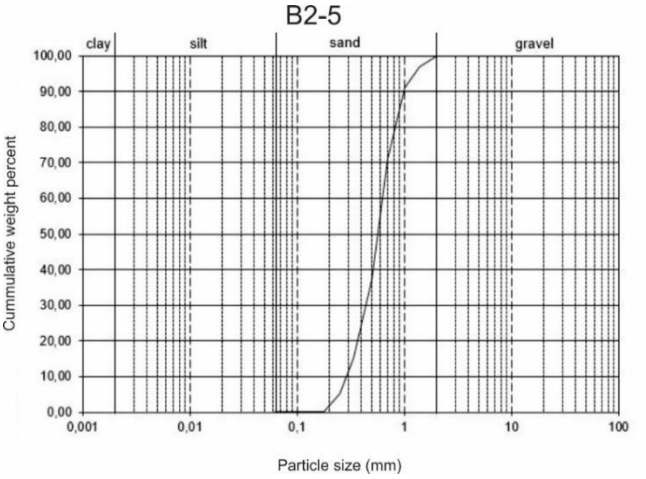

Fig. 52 Grain-size analysis of sample B2-5, which is collected from the sandy surface beyond the uppermost beach ridge (see Fig. 45 for location).. The sample is well sorted, and contain <1 % gravel

The flat surface continues until 63 m from the ocean, where a small third beach ridge begins and reaches its peak at 72 m from the ocean, marking the end of part A at the profile (Fig. 44). Driftwood are scattered on the surface, and vegetation is growing. Imbricated clasts are found on the flat surface. The long axis is dipping towards the ocean in southwest, suggesting that the current that created the imbrication was oriented from the ocean in northwest to Nordlaguna in southeast. Since waves from the ocean can overtop the barrier during storm, the imbrication is interpreted to be formed by this process.

Fig. 53 A) and B) shows examples of imbricated clasts at Bommen. The long axes of the clasts are dipping towards the ocean in northwest, indicating that the current that created the imbrication was oriented from the ocean towards the lake. This suggests that the clasts are imbricated by waves that has overtopped the barrier during storm

Asymmetric ripples with a sinuous-shaped crest are found in the sandy surface at the end of part A at the profile (Fig. 54). They have a maximum height of approximately 0.5 cm, and wavelength is approximately 7 cm. The stoss side of the ripples are dipping towards northwest. The ripples are interpreted to be created by aeolian activity, and are classified as wind ripples (Collinson et al., 2006). Sample B2-6 for grain-size analysis (Fig. 55) is collected from the sandy surface at the end of part A at the profile (Fig. 45). The sample shows a dominance of sand, and contains 5 % gravel.

Fig. 54 Example of wind-ripples in the sandy surface at the end of part A at the profile. The ripples has a slightly asymmetric profile, maximum height of approximately 0.5 cm and wavelength of approximately 7 cm

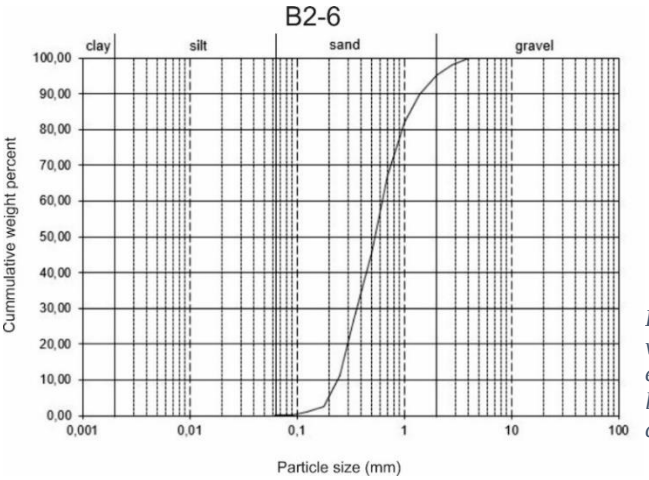

Fig. 55 Grain-size analysis of sample B2-6, which is collected from the sandy surface at the end of part A at the profile (see Fig. 45 for location). The sample is dominated by sand, and contains 5 % gravel

Part B (72-78 m):

At 72 m from the ocean, the barrier has reached its peak at a height of 6.3 m a.s.l. From this height, the slope to Nordlaguna begins (Fig. 44). The surface consists of boulders and gravel scattered in a sandy surface (Fig. 56). The amount of driftwood and vegetation increases towards the lake. Concentrations of gravel at the surface

Fig. 56 Part B of the profile is the slope to Nordlaunga. The surface consists of boulders and gravel scattered in a sandy surface, as well as driftwood and vegetation

(Fig. 57A) and asymmetric ripples with a stoss side dipping towards northwest is found on the slope (Fig. 57B). The ripples have a maximum height of 1.5 cm and wavelength 20 cm, and short and straight crests. Similar features are described at the surface of profile 1, and are interpreted to be wind ripples and lag-surface that is created by aeolian activity (Collinson et al., 2006).

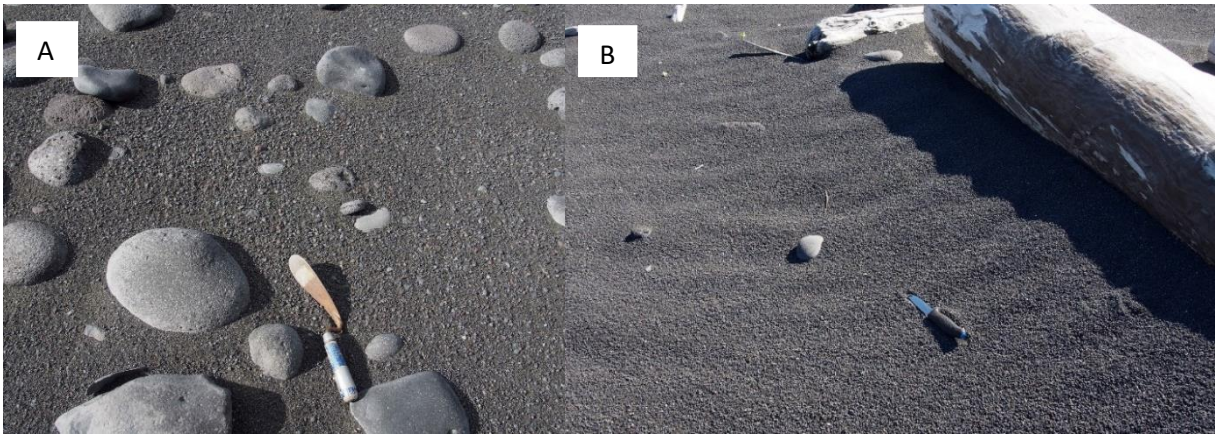

Fig. 57 Surface deposits characteristic of aeolian activity A) Concentration of gravel at the surface, suggesting that the sand has been removed B) Wind ripples in the sandy surface with stoss side dipping towards NW. The ripples has a maximum height of 1.5 cm and wavelength 20 cm

Wash-over channels are found at the end of part B at profile 2, close to the lakeshore (Fig. 58). The channels at this location is up to 25 m long and 3 m wide, and are roughly oriented normally to the lakeshore. The channels consists of medium sand with small boulders and gravel scattered on the surface. Levees consisting mainly of small gravel and small boulders are developed between the channels.

Fig. 58 Wash-over channels at the end of part B of profile 2, by the lakeshore. The channels are approximately 25 m long, 2.5 m wide and is roughly oriented normally to the lakeshore

Three samples for grain-size analyses B2-7 (Fig. 59), B2-8 (Fig. 60) and B2-9 (Fig. 61) were collected from the sandy surface on the slope to Nordlaguna. Sample B2-7 (Fig. 59) is well sorted, and contains <1 % gravel. Sample B2-8 (Fig. 60) is poorly sorted and shows a bimodal curve with high amounts of sand and 20 % gravel. Sample B2-9 (Fig. 61) is collected from the beginning of a wash-over channel, and is poorly sorted with 14 % gravel.

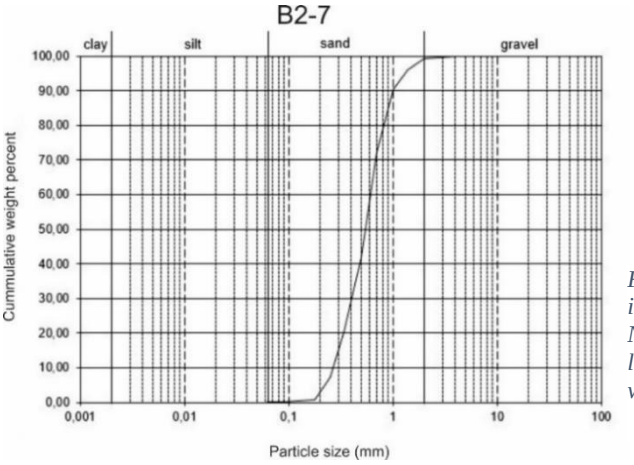

Fig. 59 Grain-size analysis of sample B2-7, which is collected from the sandy surface on the slope to Nordlaguna, at part B of the profile (see Fig. 45 for location). The sample consists of well sorted sand with <1 % gravel

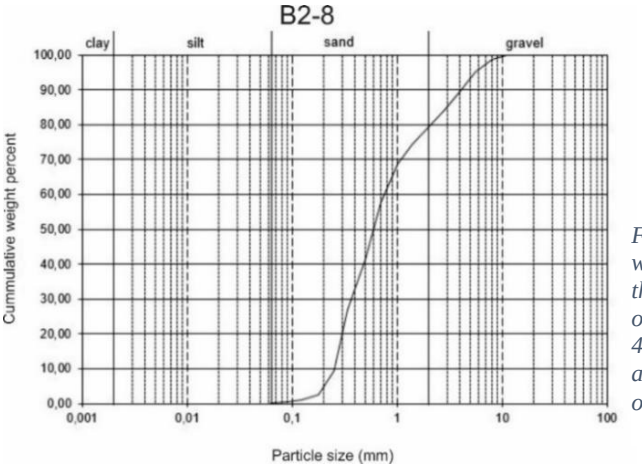

Fig. 60 Grain-size analysis of sample B2-8, which is collected from the sandy surface on the slope to Nordlaguna, close to the wash-over channels at part B of the profile see Fig. 45 for location). The sample is poorly sorted and shows a bimodal curve with high amounts of sand and 20 % gravel

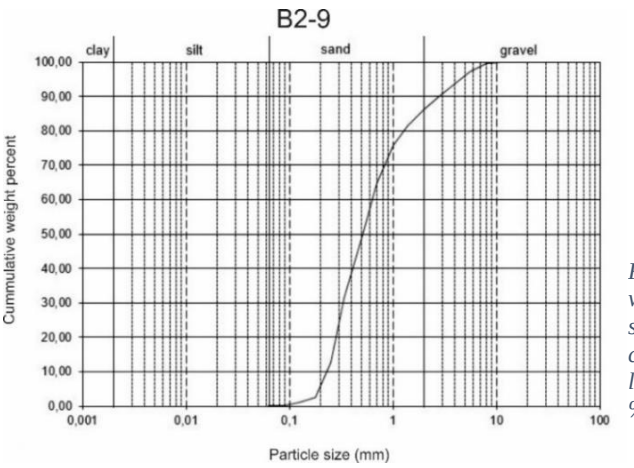

Fig. 61 Grain-size analysis of sample B2-9, which is collected from the sandy surface on the slope to Nordlaguna, close to the wash-over channels at part B of the profile (see Fig. 45 for location). The sample is poorly sorted, with 14 % gravel

Profile 3

Profile 2 is from the southwestern part of Bommen (Fig. 29). At this location, the barrier is 253 m wide and has a maximum height of 7.1 m a.s.l. (Fig. 62). Part A of the profile extends from 0-120 m from the ocean and part B extends from 120-253 m from the ocean. Nine samples were collected along the profile (Fig. 63), one for roundness- and shape analysis (sample B2-1) and eight for grain-size analyses (samples B2-2 – B2-9).

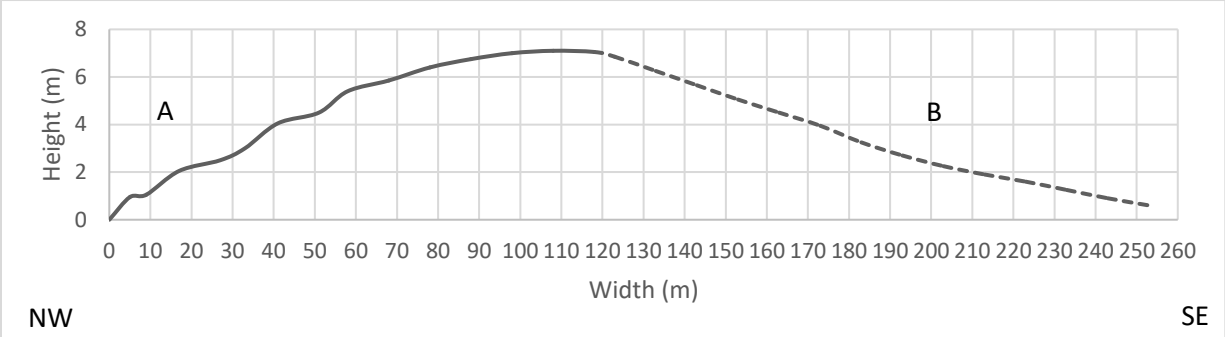

Fig. 62 Leveled surface of the barrier at profile 3. At this location, the barrier is 253 m wide and has a maximum height of 7.1 m a.s.l. Vertical scale is exaggerated

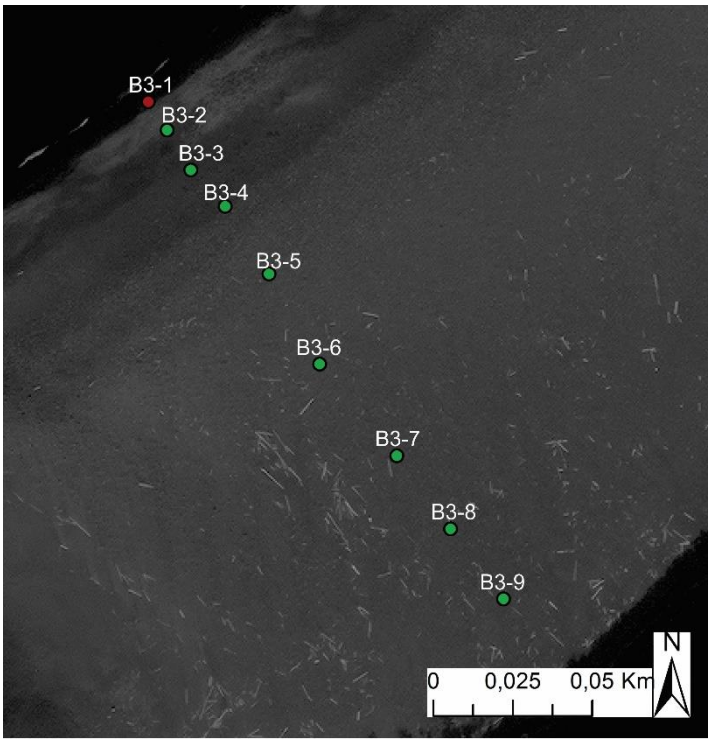

Fig. 63 Locations of samples for roundness- and shape analysis (sample B3-1, red dot) and grain-size analyses (samples B3-2 – B3-9, green dots) on profile 3 (see Fig. 16 for location) (satellite image: KSAT)

Part A (0-120 m):

The shoreline at profile 3 consists of gravel that the waves break around, creating enrichments (Fig. 64). Sample B3-1 for roundness- and shape analysis (Fig. 65) was collected from one of the enrichments. The clasts are mainly rounded (48 %) and subrounded (46 %). 4 % of the clasts are well rounded, and 2

% are subangular (Fig. 65A). The shape analysis shows that the clasts have a variety of shapes, mainly ranging between blocky and slightly elongated (Fig. 65B).

Fig. 64 Fig. 33 Waves break around enrichments of gravel at the shoreline of profile 3. Sample B3-1 for roundness- and shape analysis (Fig. 65) was collected from one such enrichment

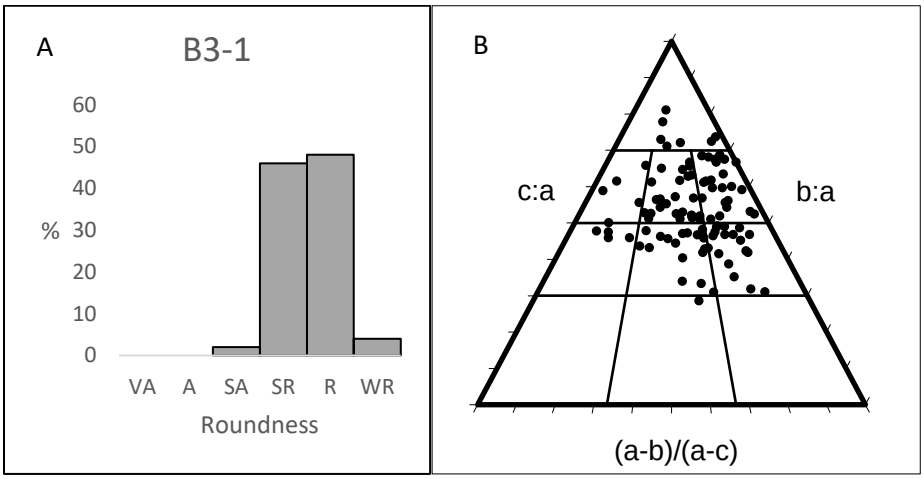

Fig. 65 Sample B3-1 (see Fig. 63 for location) A) Roundness analysis of sample B3-1. The clasts are mainly subrounded and rounded B) Clast shape analysis of sample B3-1. The clasts shows a variety of shapes, but there is a dominance of blocky and slightly elongated clasts

A beach ridge is found 6 m from the ocean (Fig. 66). This ridge extends towards northeast, and is connected to the lower beach ridge described from profile 2, which is the 890 m long ridge that is mapped in Fig. 27. Beyond the beach ridge, the surface is flat and consists of gravel scattered in sand. Sample B3-2 for grain-size analysis (Fig. 67) is collected from the sandy surface beyond the beach ridge, 16 m from the ocean. It consists of well sorted sand and 2 % gravel.

Fig. 66 A beach ridge is located 6 m from the ocean, which can be connected to the lower 890 m long ridge that is mapped in Fig. 27 and described from profile 2. The surface beyond the beach ridge is flat and consists of gravel scattered in sand

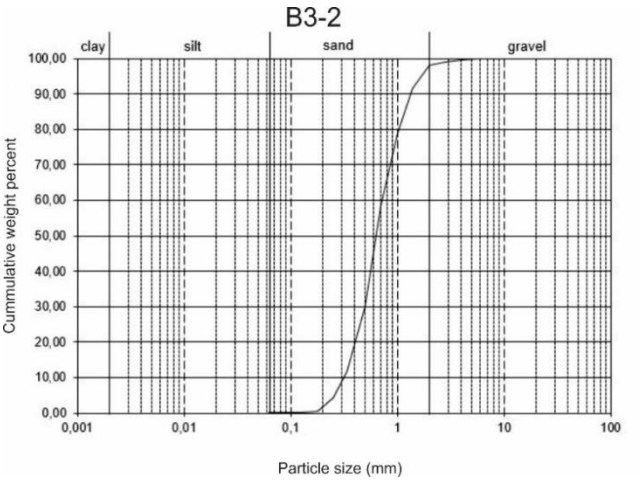

Fig. 67 Grain-size analysis of sample B3-2, which is collected from the sandy surface beyond the lower beach ridge see Fig. 63 for location). The sample contains well sorted sand with 2 % gravel

A belt of seaweed is deposited on the sandy surface 24 m from the ocean. It extends towards northeast, and can be connected to the belt of seaweed described in profile 2. Sample B3-3 for grain-size analysis (Fig. 68) is collected from the sandy surface beyond the belt of seaweed, 30 m from the ocean. The sample consists of well sorted sand and <1 % gravel.

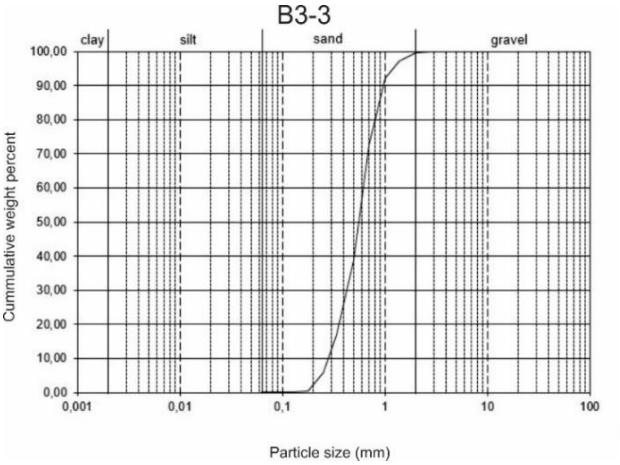

Fig. 68 Grain-size analysis of sample B3-3, which is collected from the sandy surface beyond the belt of seaweed. 30 m from the ocean (see Fig. 63 for location). The sample contains well sorted sand with <1 % gravel

31 m from the ocean, there is a sharp transition to a small beach ridge that extends towards southeast. The ridge is at approximately the same height as the upper 1 km long beach ridge on the map (Fig. 27), but the two ridges are not connected (Fig. 69). The surface beyond the beach ridge is flat and consists of gravel and boulders scattered in a sandy surface. Sample B3-4 for grain-size analysis (Fig. 70) is collected from the sandy surface beyond the beach ridge, 46 m from the ocean. It consists of well sorted sand and <1 % gravel.

Fig. 69 A short beach ridge extends towards SE. It is at approximately the same height as the upper 1 km long beach ridge, but the two ridges are not connected

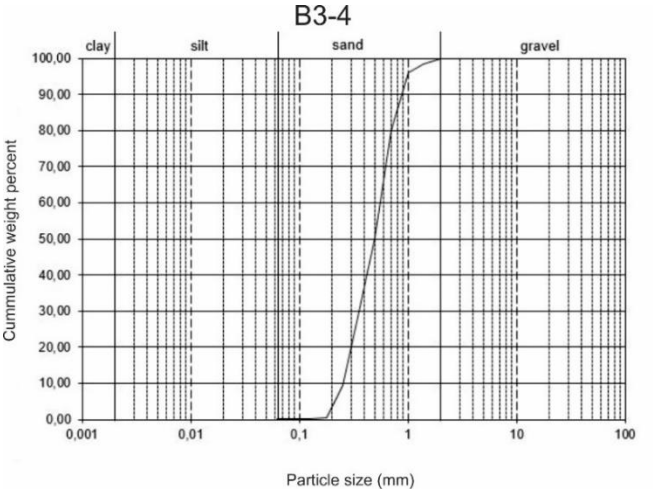

Fig. 70 Grain-size analysis of sample B3-4, which is collected from the sandy surface beyond the small beach ridge, 46 m from the ocean (see Fig. 63 for location). It contains well sorted sand and <1 % gravel

51 m from the ocean, the third beach ridge of the profile is located. It reaches its peak 71 m from the ocean, where the surface is flat and contains boulders and gravel scattered in sand. Sample B3-5 for grain-size analysis (Fig. 71) is collected from the flat sandy surface beyond the beach ridge. The sample shows well sorted sand with 1.5 % gravel.

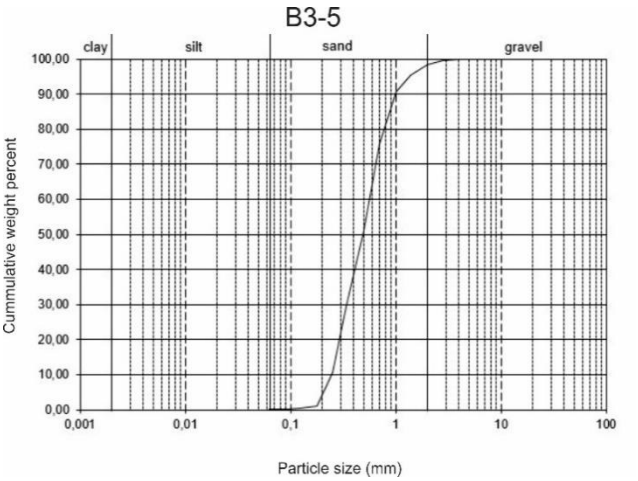

Fig. 71 Grain-size analysis of sample B3-5, which is collected from the sandy surface beyond the third beach ridge at profile 3, 71 m from the ocean (see Fig. 63 for location). The sample shows well sorted sand that contains 1.5 % gravel

After the flat surface beyond the beach ridge, the slope towards the peak of the profile begins, followed by the flat surface at the end of part A (Fig. 72), which is 7.1 m a.s.l (Fig. 62). The surface consists of gravel and boulders scattered in a sandy surface. Asymmetric ripples with a stoss side dipping towards northeast and concentrations of gravel on the sandy surface are found. Similar deposits are described from profile 1 and 2, and are interpreted to be wind ripples and lag-surfaces that are formed by aeolian activity (Collinson et al., 2006). Sample B3-6 for grain-size analysis (Fig. 73) is collected from the sandy surface at the end of part A. The sample contains mainly sand, as well as 5 % gravel.

Fig. 72 The top of profile 3 has a flat surface which contains boulders and gravel scattered in sand. Driftwood are found on the surface

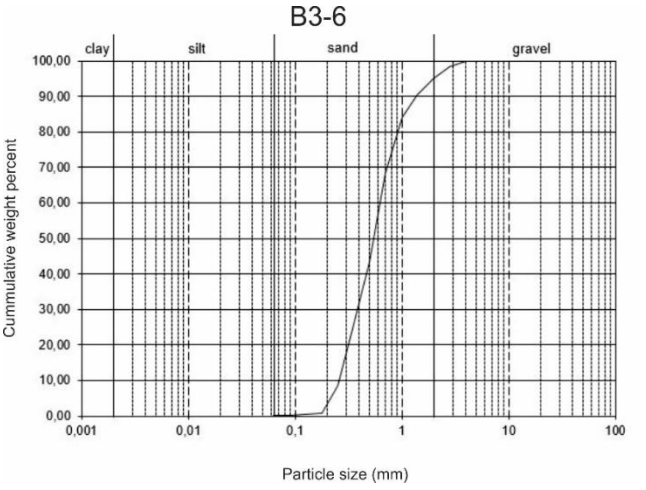

Fig. 73 Grain-size analysis of sample B3-6, which is collected from the sandy surface at the end of part A (see Fig. 63 for location). The sample is dominated by sand, and contains 5 % gravel

Part B (120-253 m):

After the barrier reaches its peak at 7.1 m a.s.l., 120 m from the ocean, the slope to Nordlaguna begins (Fig. 62). The surface consists of gravel and boulders scattered in sand, and driftwood and vegetation is found (Fig. 74). Three samples for grain-size analysis were collected from the sandy surface at part B, B3-7 (Fig. 75), B3-8 (Fig. 76) and B3-9 (Fig. 77). The samples are dominated by sand, and contain 4 %, 2 % and 5 % gravel respectively.

Fig. 74 The surface on the slope to Nordlaguna contains boulders and gravel scattered in sand, and driftwood and vegetation are found

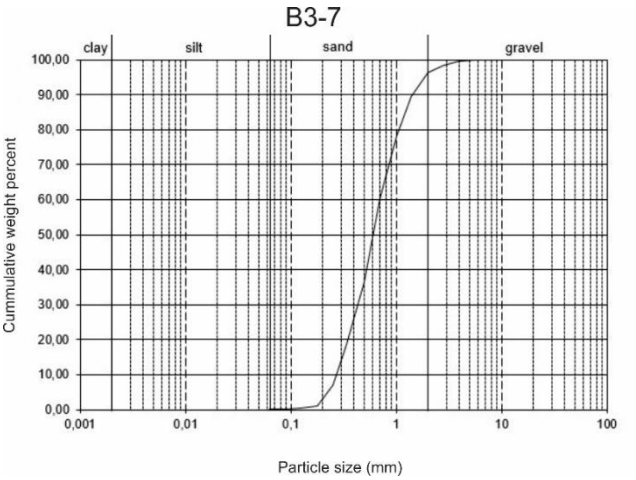

Fig. 75 Grain-size analysis of sample B3-7, which is collected from the sandy surface at part B (see Fig. 63 for location). The sample is dominated by sand and contains 4 % gravel

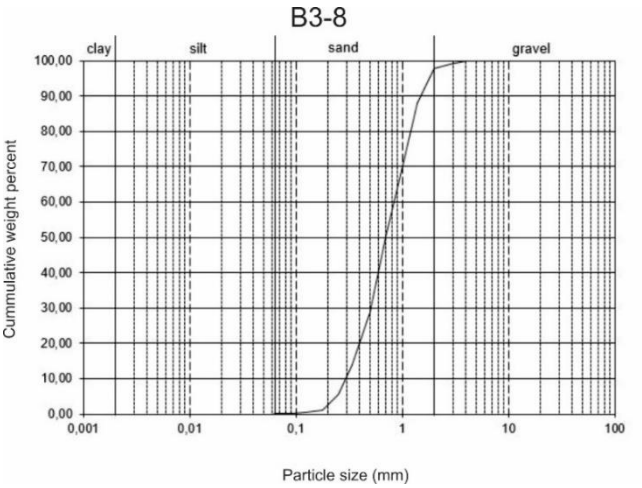

Fig. 76 Grain-size analysis of sample B3-8, which is collected from the sandy surface at part B (see Fig. 63 for location). The sample is dominated by sand, and contains 2 % gravel

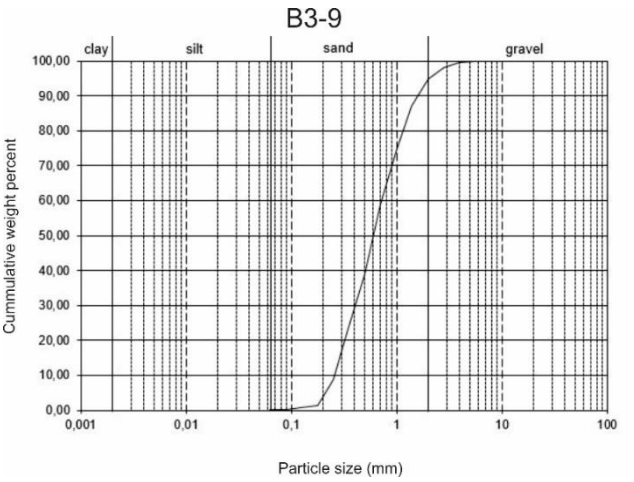

Fig. 77 Grain-size analysis of sample B3-9, which is collected from the sandy surface at part B (see Fig. 63 for location). The sample is dominated by sand, and contains 5 % gravel

4.2.2 Tornøedalen

Tornøedalen enters the lake from east, and is by far the largest fluvial/niveofluvial deposit of the three valleys (Fig. 18). The valley is 2 km long, and begin at the confluence of Alfred Øiendalen and the channel systems from the proglacial lake Tornøevatnet (Fig. 10). The valley ends in a fan deposit between Hochstetterkrateret (138 m a.s.l.) and Wildberget (300 m a.s.l.) (Fig. 78).

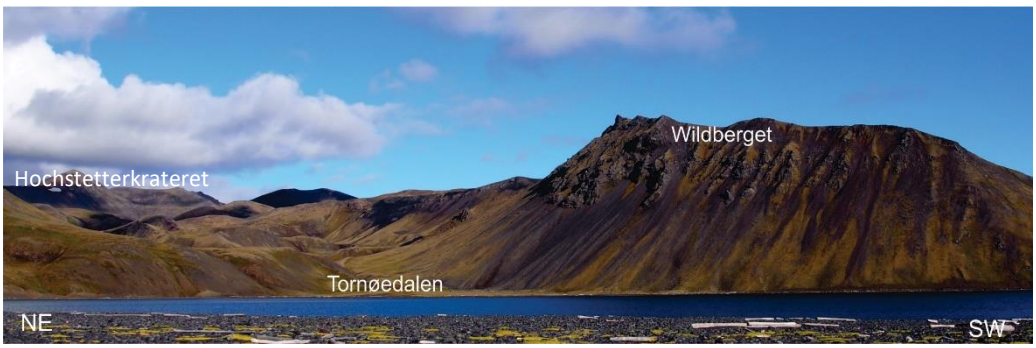

Fig. 78 Tornøedalen ends in the valley floor between Hochstetterkrateret (138 m a.s.l.) and Wildberget (300 m a.s.l.)

The valley floor is up to 380 m wide, and the length from the fan apex to the lake shoreline is 460 m. A braided channel system is found on the valley floor (Fig. 79). The channels are not permanently filled with water, but the northern part of the fan were observed to be active during heavy rain (Fig. 80), and are mapped as temporary active channels that are active during flash flooding and snowmelt. The channels on the central part of the fan are covered with vegetation (Fig. 81), and are therefore interpreted to be inactive. Debris flow- and rockfall deposits are found at the slope down from Wildberget, and large amounts of rockfall material are found at the southern part of the valley floor at the base of the slope. Debris flow deposits extend up to 20 m from the base of the slope on the valley floor (Fig. 82). The slope down from Hochstetterkrateret contains solifluction material and unspecified mass movement deposits, as well as an alluvial fan at the end of a seasonal active channel, which is mapped as a fluvial/niveofluvial deposit (Fig. 79). A belt of driftwood is found on the valley floor, approximately 80 m from the lake shoreline.

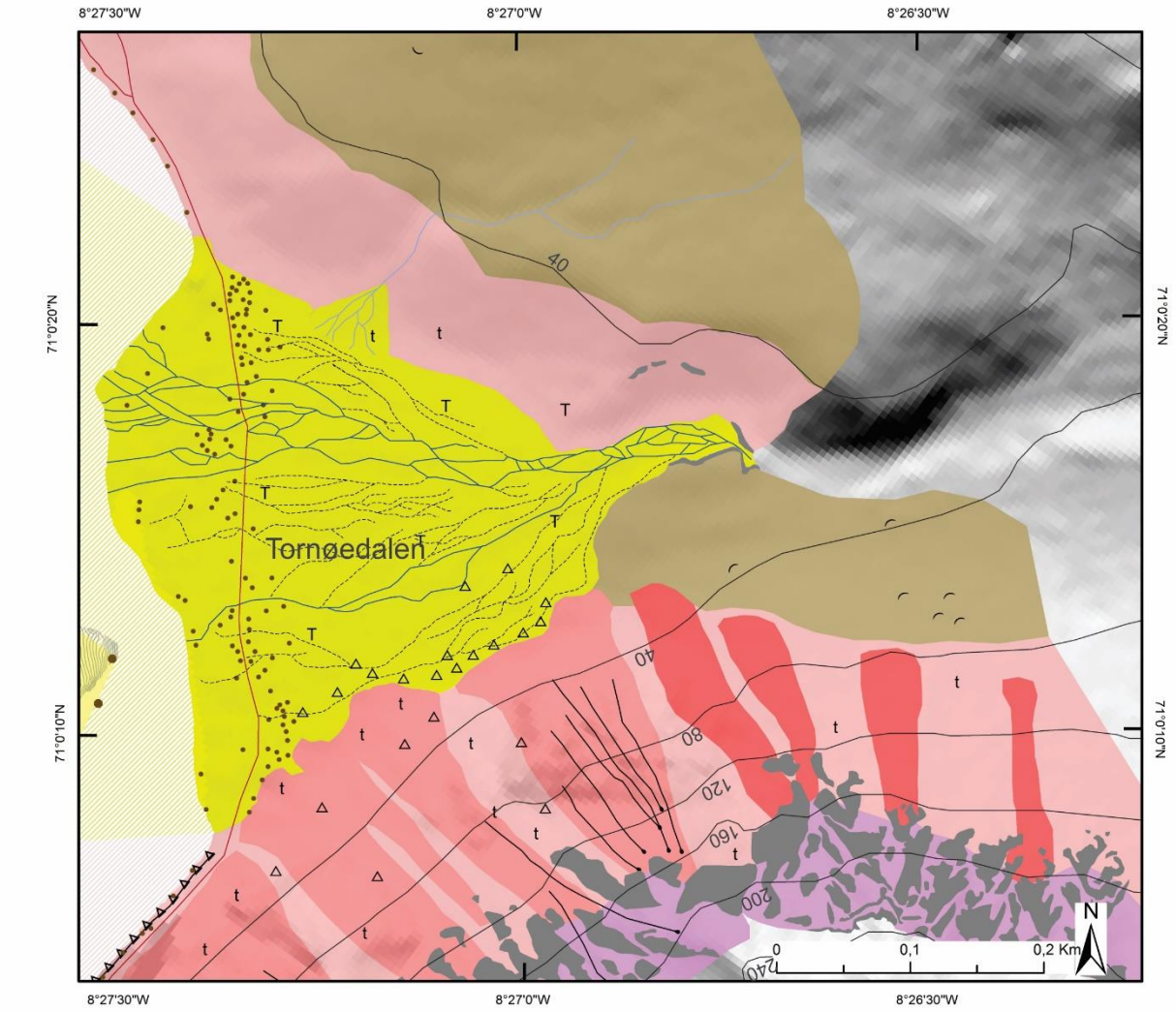

Fig. 79 Detailed geological map of Tornøedalen. Terrestrial contour interval 40 m. Legend of the elements at the subaerial environment in Fig. 19.

Fig. 80 The channel system at Tornøedalen was observed to be active during heavy rain A) Dry channels B) Channels filled with water. Note the plume of sediments formed in the lake

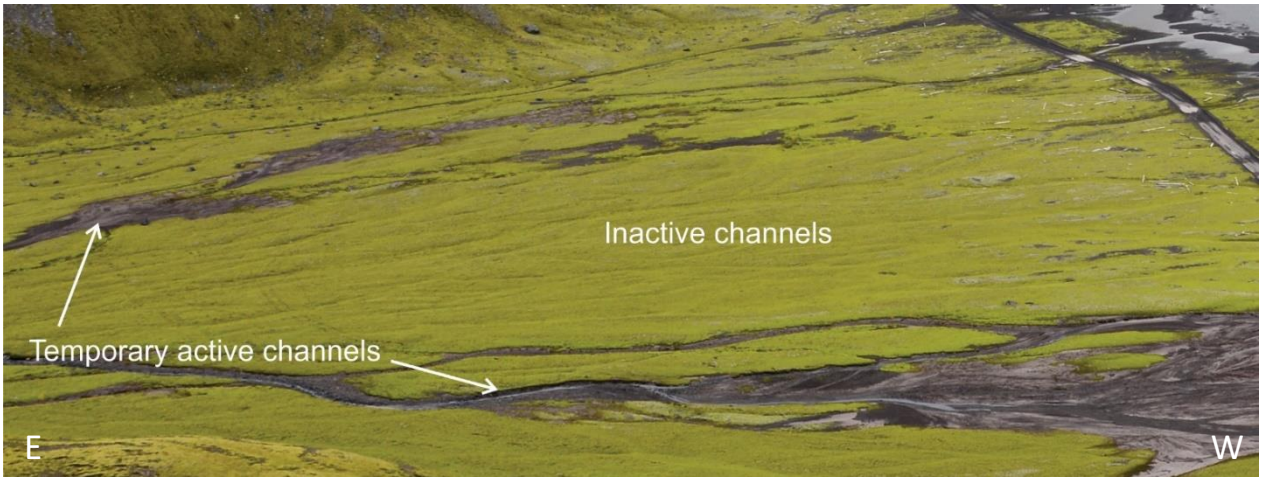

Fig. 81 The majority of the temporary active channels are found on the northern part of the valley floor, and a few channels are located on the southern part. The inactive channels are covered with vegetation, and is mainly found at the middle of the valley floor (photo: A. Lyså)

Fig. 82 Deposits of debris flows extend up to 20 m from the base at the slope down from Wildberget on the valley floor. Note the large amounts of rockfall material on the slope and valley floor

To gain knowledge about the sedimentation from Tornøedalen to the lake, detailed investigations of the morphology at the northern part of the valley floor were carried out during fieldwork. Four samples for grain-size analyses (TD-1 – TD-4) were collected from the channels, and a lithological log was created (see Fig. 83 for location). The valley floor is described from the fan apex towards the lake.

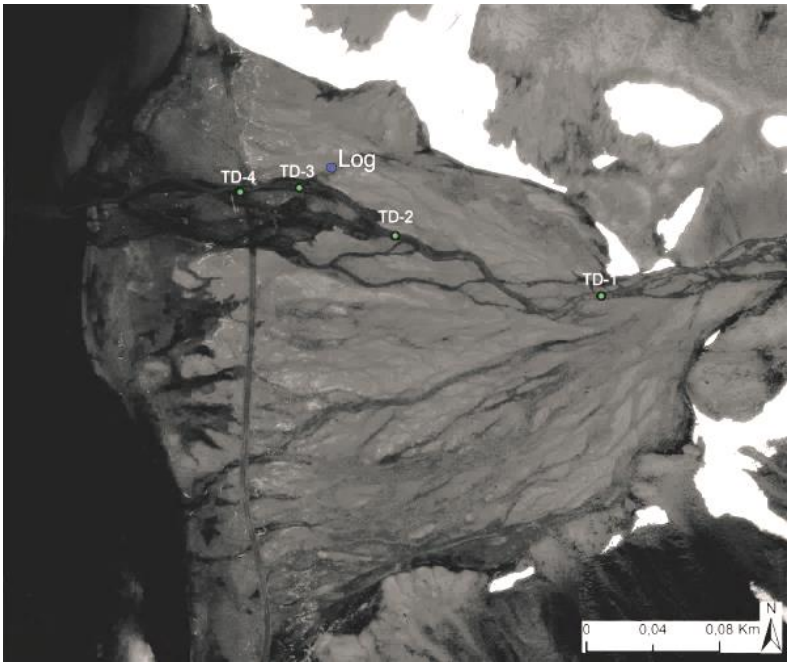

Fig. 83 Locations of the samples for grain-size analyses (TD-1 - TD-4, green dots) and lithological log (blue dot). The detailed studies were conducted at the active northern part of the fan (satellite image: KSAT)

Exposed bedrock is found on each side of the channel at the fan apex. The bedrock is eroded, and gravel and boulders are scattered on the valley floor (Fig. 84A). Some of the bedrock is rounded (Fig. 84B). MPS was measured at the long axis of the ten largest particles within a radius of 2 m, which gave the following measurements (in cm): 27, 34, 35, 42, 45, 48, 54, 56, 88. This gives an average of 42.6 cm. A few of the clasts were imbricated with the long axes dipping towards the fan apex in east, suggesting that the current that created the imbrication was directed from east to west (Fig. 85). The surface at this location consists of mainly gravel and boulders with sand between.

Fig. 84 Exposed bedrock are found at the fan apex in Tornøedalen A) Eroded bedrock at each side of the channels at the fan apex. Boulders are scattered on the valley floor at this location B) Rounded bedrock at the fan apex

Fig. 85 Imbricated clasts at the fan apex. The long axis are dipping towards the fan apex in east, suggesting that the current that created the imbrication were directed from east to west

Well defined channels are found 10 m downstream from the fan apex, where the valley floor is 30 m wide. Vegetated elongated banks parallel to stream flow are found between the channels (Fig. 86). There is a decrease in grain-size in the channels downstream.

Fig. 86 Vegetated elongated banks are found between the well defined channels 10 m downstream from the fan apex. The valley floor is 30 m wide at this location

MPS was measured at the long axis of the ten largest particles within a radius of 2 m, which gave the following measurements (in cm): 19, 22, 23, 24, 25, 28, 30, 30, 32, 34. This gives an average of 26.7 cm. Channels at this point are 1.5, 2.5 and 5 m wide. Sample TD-1 for grain-size analysis (Fig. 87) is collected from a temporary active channel 100 m from the fan apex. The sand in the sample is poorly sorted, and consist 13 % gravel.

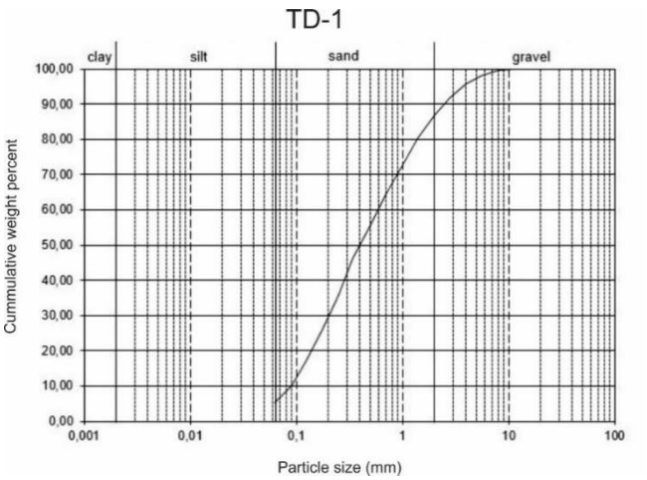

Fig. 87 Grain-size analysis of sample TD-1 (see Fig. 83 for location), which is collected from a temporary active channel 100 m from the fan apex. The sand in the sample is poorly sorted, and consist 13 % gravel

110 m from the fan apex, the valley floor and the channels spreads out. The banks between the channels are large and covered with thick vegetation (Fig. 88A). The channels are well defined, and has a width of 0.5 and 4 m and are 20 cm deep. The surface of the channels consists of sand and gravel. The grain-sizes in the channels can have great variations in small areas (Fig. 88B). Sample TD-2 for grain-size analysis (Fig. 89) was sampled in a temporary active channel 124 m downstream from TD-1 (see Fig. 83 for location). The sand in the sample is poorly sorted, and the amount of gravel is 40 %.

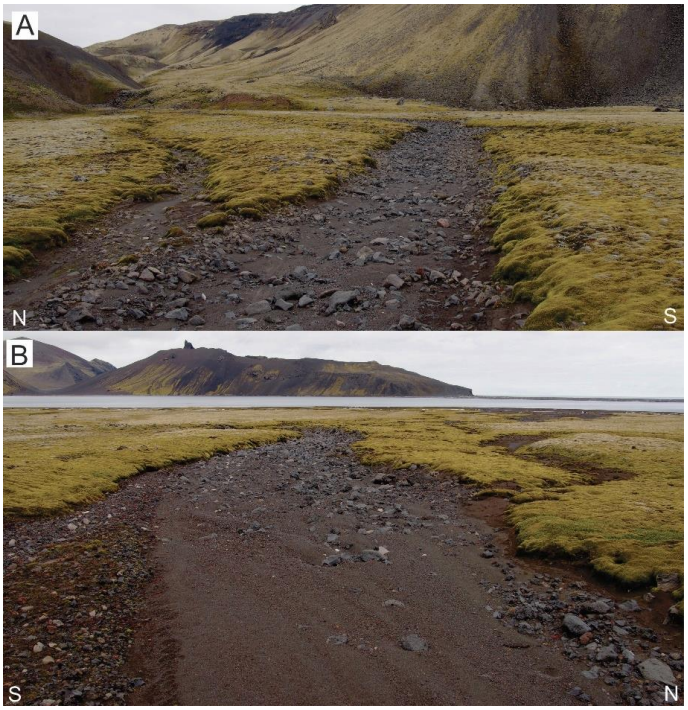

Fig. 88 The valley floor and the channels spreads out 110 m from the fan apex. The channels is well defined, and the banks between them are covered with thick vegetation. The two channels in this photo are 0.5 and 4 m wide and 20 cm deep B) The grain-size in the channels can have great variations in small areas. The channel is 5.5 m wide at this point

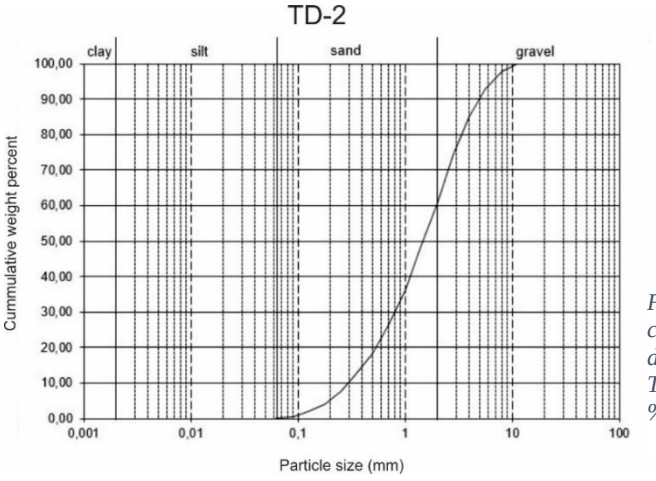

Fig. 89 Grain-size analysis of sample TD-2, which is collected from a temporary active channel 124 m downstream from sample TD-1 (see Fig. 83 for location). The sand in the sample is poorly sorted, and consists of 40 % gravel

Asymmetric ripples are found on the surface of the channels. The ripples have a wavelength of 15 cm, and maximum height is 1.5 cm (Fig. 90A). The stoss side is dipping toward east. In the same area, concentrations of gravel are found at the surface, suggesting that the sand has been removed (Fig. 90B). The two features are interpreted as wind ripples and lag-surface, which are created by aeolian activity (Collinson et al., 2006).

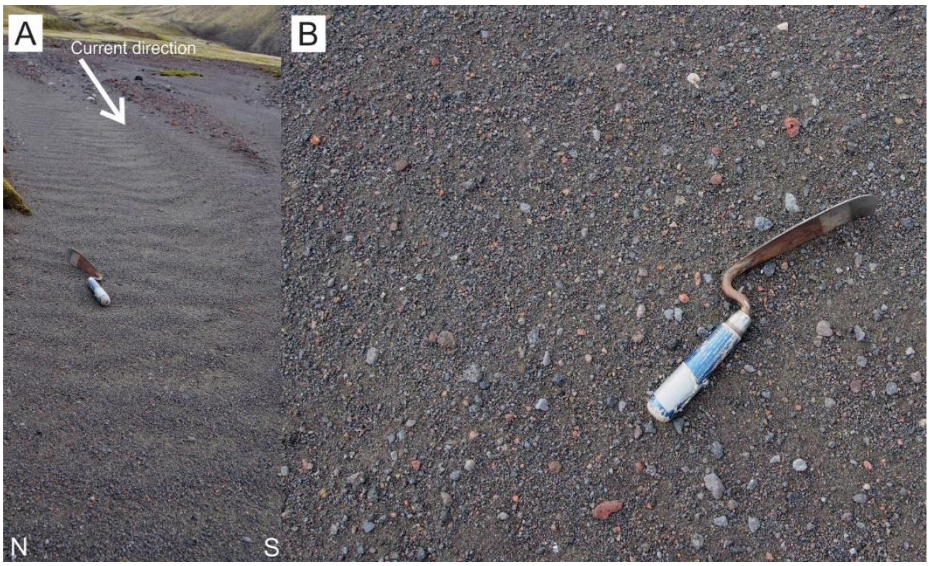

Fig. 90 Surface deposits characteristic of aeolian activity A) Asymmetric ripples with a stoss side dipping towards east. The ripples have a wavelength of 15 cm and maximum height 1.5 cm B) Concentrations of gravel at the surface, indicating that the sand has been removed, creating a lag-surface

At the beginning of the belt of driftwood, approximately 120 m from the lake shoreline (Fig. 79), the depth of channels decrease, the banks are smaller, and there is less vegetation (Fig. 91). Sample TD-3 for grain-size analysis (Fig. 92) was collected from a temporary active channel at this location. The sample contains poorly sorted sand with high amounts of gravel (28 %).

Fig. 91 At the driftwood belt approximately 80-120 from the lake shoreline, the size of channels and banks decrease. The channels are 0.5 to 1 m at this point

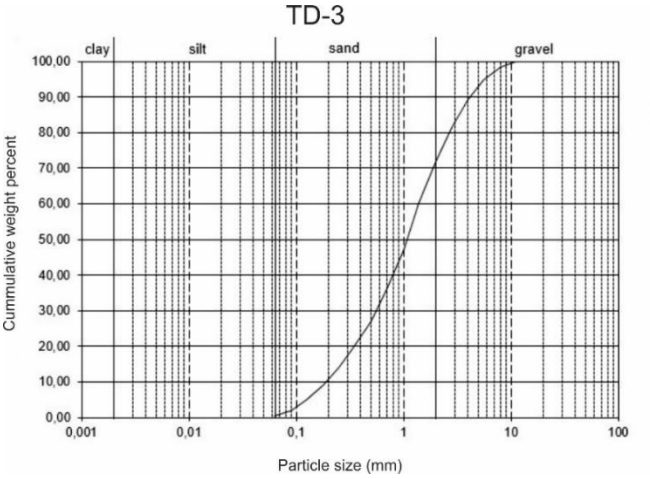

Fig. 92 Grain-size analysis of sample TD-3, which is collected approximately 120 m from the lake shoreline (see Fig. 83 for location). The sample contains poorly sorted sand and 28 % gravel

The channels are wider and shallower towards the lake shoreline. Sample TD-4 for grain-size analysis (Fig. 93) was collected approximately 90 m from the lake shoreline. The sample shows a dominance of sand, and the amount of gravel is 2 %.

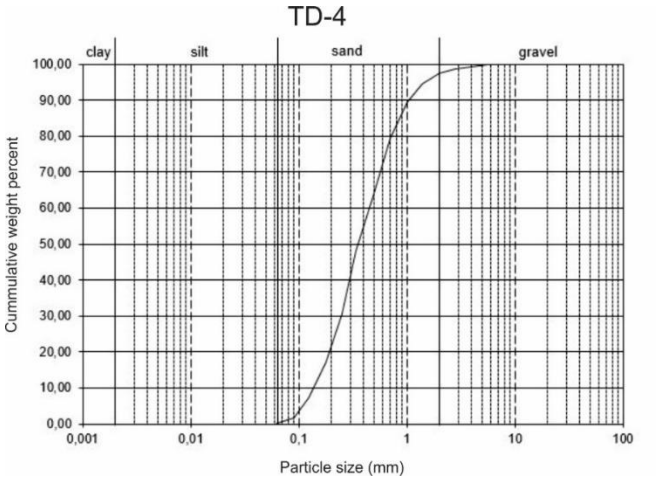

Fig. 93 Grain-size analysis of sample TD-4, which is collected approximately 90 m from the lake shoreline (see Fig. 83 for location). The sample is dominated by sand, and the amount of gravel is 2 %

A lithological log from an inactive channel in Tornøedalen was described. The location is on the northern side of the valley floor, 125 m from the lake shoreline (Fig. 83). South of the channel, other inactive channels, that appear to be completely covered with vegetation, are found. Vegetation covers the channel upstream (Fig. 94A), while it is more or less vegetation-free downstream (Fig. 94B), where it meets the temporary active channels (Fig. 79). The inactive channel is 3 m wide and 10 m deep. The surface consists of lag-deposits with granules and pebbles, and a matrix of medium sand.

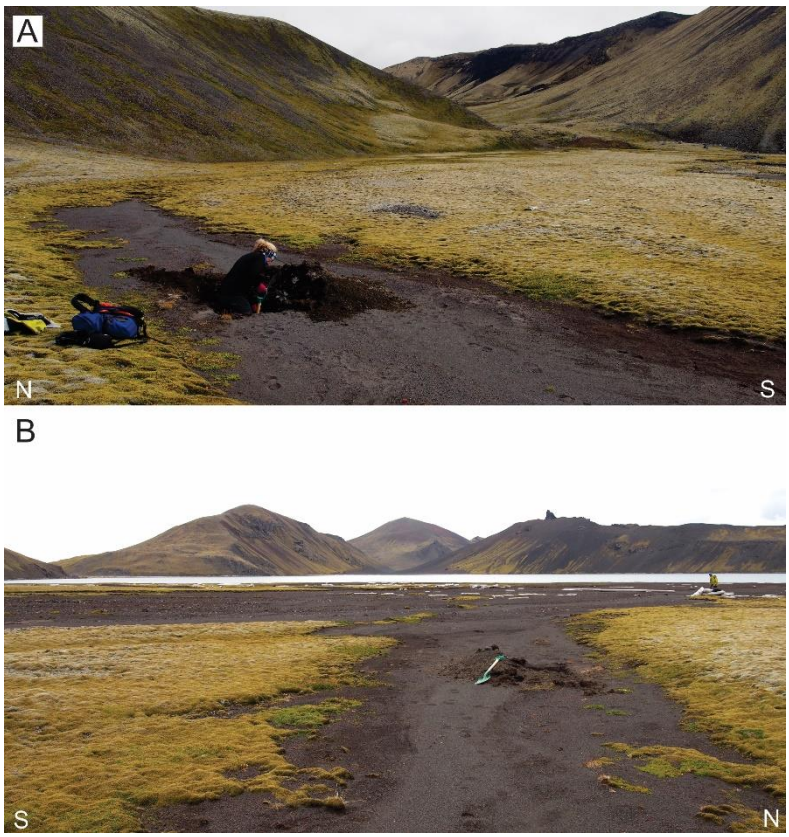

Fig. 94 The section described from the valley floor in Tornøedalen is located in an inactive channel 125 m from the lakeshore A) Vegetation grows in the channels upstream B) The channel is more or less vegetation free downstream

The pit for the sedimentary log is 90 m deep, and the described section is oriented east-west, parallel to the current direction of the channel. The lithological log is presented in Fig. 95.

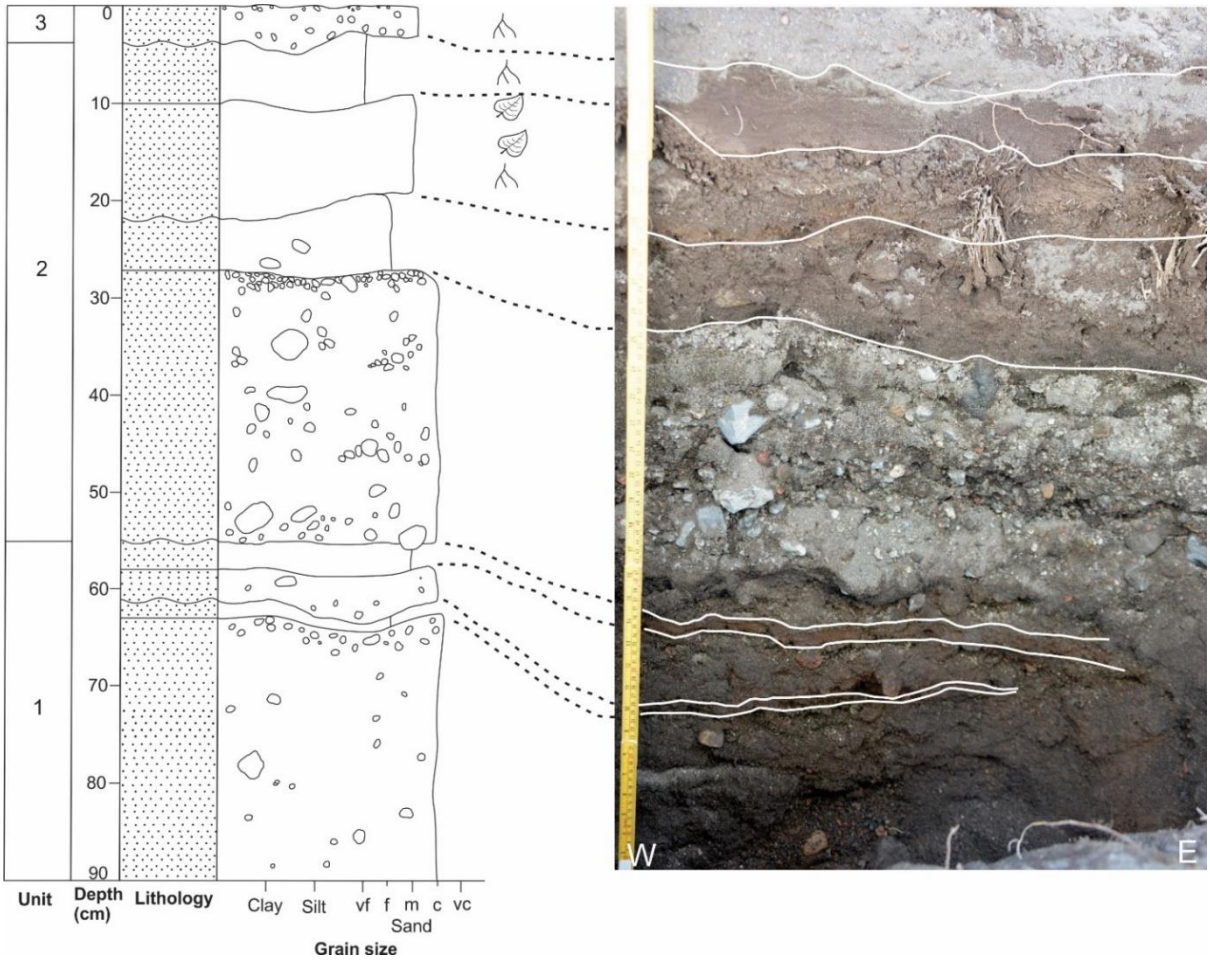

Fig. 95 Lithological log from an inactive channel at the valley floor in Tornøedalen (see Fig. 83 for location). The section is 90 m deep and oriented east-west, parallel to the current direction of the channels. The perspective of the image may be misleading when compared to the log, as it is seen from above (photo: A. Lyså)

Unit 1 (90-55 cm)

Unit 1 consist of four layers. The lower boundary is not exposed. The unit is dominated by coarse sand with granules and pebbles scattered throughout the deposit and concentrated at the top. A few cobbles up to 2.3 cm in diameter are found. The clasts are subangular to angular. A thin layer of variable thickness (2-0.5 cm) occurs at 63-61 cm. It has a lower boundary that follows the rough surface of the underlying layer. Fine sand dominates the deposit. The third layer in the unit is between 61-58 cm depth, and has a lower erosional boundary. The layer is dominated by coarse sand, with some scattered pebbles. The uppermost layer of unit 1 at 55-58 cm depth has a sharp transition to the underlying layer, and consists of medium sand.

Unit 2 (55-4 cm)

The lowermost layer of unit 2 at 55-27 cm depth is dominated by coarse sand with large amounts of gravel up to 4 cm in diameter. The clasts are touching other clasts. Large amounts of granules and pebbles are concentrated at the top of the layer, where the amount of sand is small. The second layer in

unit 2 is deposited with a sharp transition to the underlying layer, and has a variable thickness between 5 to 9 cm. It consists of fine sand with a few isolated cobbles. The third layer at 10-22 cm depth has a lower erosional boundary, and consists of medium sand. Plant material and roots that are similar to the vegetation on the channel banks are found within the layer. The uppermost layer shows a sharp transition from the underlying sand. It consists of very fine sand, and roots are found in the layer.

Unit 3 (4-0 cm)

The uppermost unit includes the surface deposit. It consists of medium sand with gravel scattered in the deposit. The boundary to the underlying layer is erosive. Roots are found within the sediment.

4.2.3 Stasjonsdalen

Stasjonsdalen is the 250 m long valley that ends in the 300 m long and 130 m wide valley floor between Wildberget (300 m a.s.l.), Brinken (80 m a.s.l.) and Mohnberget (180 m a.s.l.) (Fig. 96).

Fig. 96 Stasjonsdalen ends in the valley floor between Wildberget (300 m a.s.l.), Brinken (80 m a.s.l.) and Mohnberget (180 m a.s.l.)

The valley floor consists of the braided channel system from Stasjonsdalen and from the 600 m long Jøssingdalen, which leads to the eastern side of Jan Mayen (Fig. 10). The channel systems on the valley floor are dry, and enters the lake from south. The channels at the western side of the valley floor are not covered with vegetation, and were not observed to be active during heavy rain. It appears likely that they are filled with water during snowmelt in spring and summer, and are mapped as seasonal active channels (Fig. 97). The channels at the middle and eastern part of the valley floor are covered with vegetation, and are therefore interpreted to be inactive. There are two well-defined belts of driftwood by the shoreline, at 9 and 14 m from the lake. The slopes around the valley floor are dominated by solifluction material (Fig. 22).

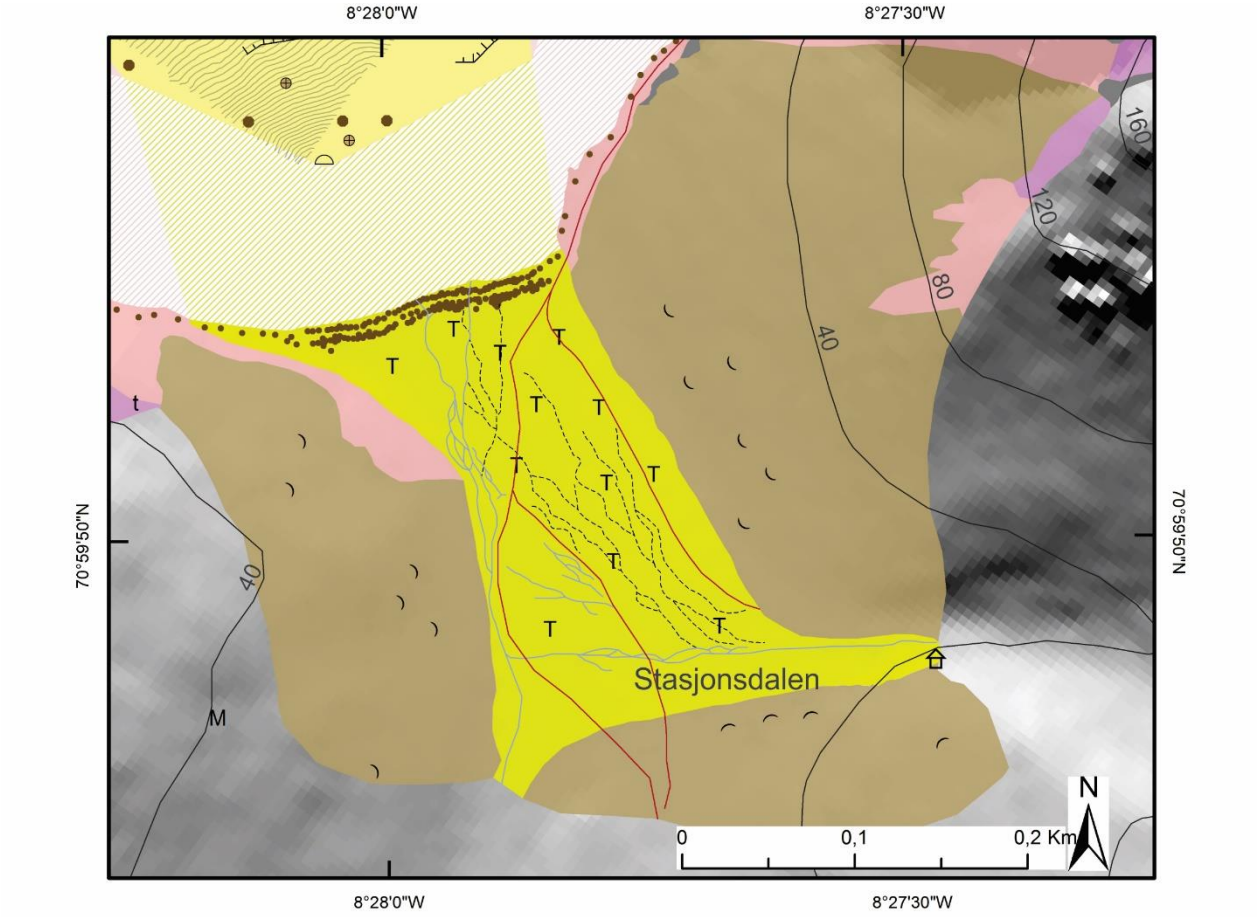

Fig. 97 Detailed geological map of Stasjonsdalen. Terrestrial contour interval 40 m. Legend of the elements at the subaerial environment in Fig. 19.

The morphology of the seasonal active channels from Stasjonsdalen was investigated during fieldwork, and is described below. Two samples for grain-size analyses (SD-1 and SD-2) were collected from the channel system from Stasjonsdalen and Jøssingdalen. Their location is shown in Fig. 98.

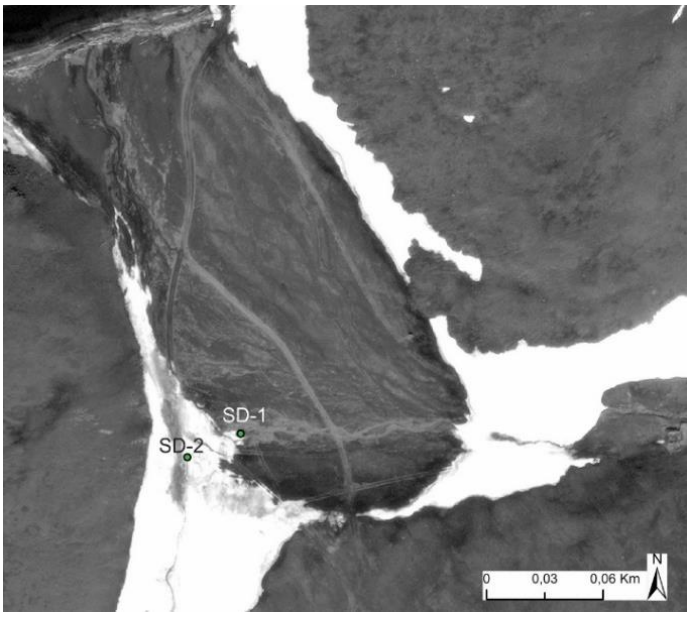

Fig. 98 Locations of the two samples for grain-size analyses on the valley floor in Stasjonsdalen. Sample SD-1 is collected from the channel system from Stasjonsdalen, and sample SD-2 is from the channel system from Jøssingdalen

Channels are found at the end of Stasjonsdalen, where the valley floor spreads out. The channels form a chaotic braided pattern, and the short banks are elongated parallel to stream flow (Fig. 99). The channel system consists of a 9 m wide main channel with a network of smaller channels 1-1.5 m wide and 20-30 m deep. Vegetation is growing mainly at the channel banks, but some is also found within the channels. The surface consists of medium sand with gravel, as well as a few small boulders up to 29 cm in diameter.

Fig. 99 Channels from Stasjonsdalen are found where the valley floor spreads out. The channels has a chaotic pattern, and consists of a main channel with a network of smaller channels. Upstream view

Further downstream, the valley floor spreads out, and the channels are less chaotic. A 3 to 4 m wide main channel follows the southern part of the valley floor (Fig. 100), where the channel system from Jøssingdalen enter the valley floor (Fig. 97). The channel surface contains mainly gravel, with a few deposits of sand in between. Sample SD-1 for grain-size analysis (Fig. 101) was collected from the sand between gravel in the channel. The sample contains mainly sand, and the amount of gravel is 8.5 %.

Fig. 100 The valley floor wide out downstream, and there are one 3 to 4 m wide main channel that follows the southern part of the valley floor. Downstream view

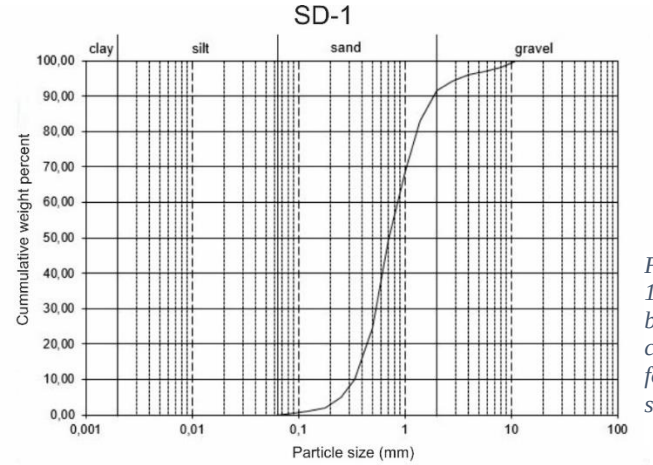

Fig. 101 Grain-size analysis of sample SD-1, which is collected from the sand between gravel at the seasonal active channel from Stasjonsdalen (see Fig. 98 for location). The sample contains mainly sand and 8.5 % gravel

Where the channel systems from Stasjonsdalen and Jøssingdalen meet, the channels are poorly defined (Fig. 102). The surface consists mainly of gravel with sand in between. Sample SD-1 for grain-size analysis (Fig. 103) was collected from the sand at the channel from Jøssingdalen. The sample contains mainly sand, and 10 % gravel.

Fig. 102 The channels are poorly defined where the channel system from Jøssingdalen enters the valley floor. A gravel road goes through Jøssingdalen

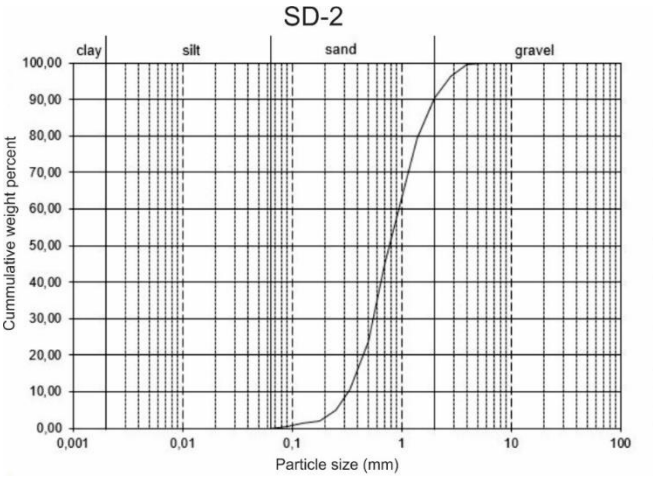

Fig. 103 Grain-size analysis of sample SD-2, which is collected from sand between gravel at the seasonal active channel from Jøssingdalen (see Fig. 98 for location). The sample is dominated by sand, and contains 10 % gravel

At the western part of the valley floor, the channels that lead to the lake are well defined with vegetated elongated banks (Fig. 104). The channels contains mainly gravel, with a few deposits of sand in between.

Fig. 104 The channels at the western part of the valley floor is well-defined with vegetated elongated banks

4.2.4 Wilzcekdalen

Wilzcekdalen is the 300 m long valley between Nordlaguna and Maria Musch-Bukta (Fig. 10) that ends in the 240 m long valley floor between Mohnberget (180 m a.s.l.) and Fugleberget (136 m a.s.l.) (Fig. 105).

Fig. 105 Wilzcekdalen ends in the valley floor between Mohnberget (180 m a.s.l.) and Fugleberget (136 m a.s.l.) (photo: A. Lyså)

A braided channel system is found on the valley floor. The channels were not observed to be active during heavy rain, but it appears likely that they are active during snowmelt in spring and summer. They are therefore mapped as seasonal active channels (Fig. 106). The slopes at each side of the valley floor have different characteristics. The slope down from Fugleberget is mapped as unspecified mass movement deposits, and channels are found in the debris on the slope. Two alluvial fans are found at the end of the channels from the slope, and are mapped as fluvial/niveofluvial deposit (Fig. 106).

Weathered material is mapped on the top of the mountain, where deposits of pyroclastic material is found (Lysså and Larsen, pers. comm. 2018). Debris flow- and rockfall deposits are found at the base of the slope down from Mohnberget at the southeastern side of the valley floor. The top of the slope contains weathered material. Driftwood is found by the lakeshore, where it is concentrated in a belt along the shoreline, 15-18 m from the lake. Large amounts of driftwood is scattered on the valley floor, up to 104 m from the lake (Fig. 106).

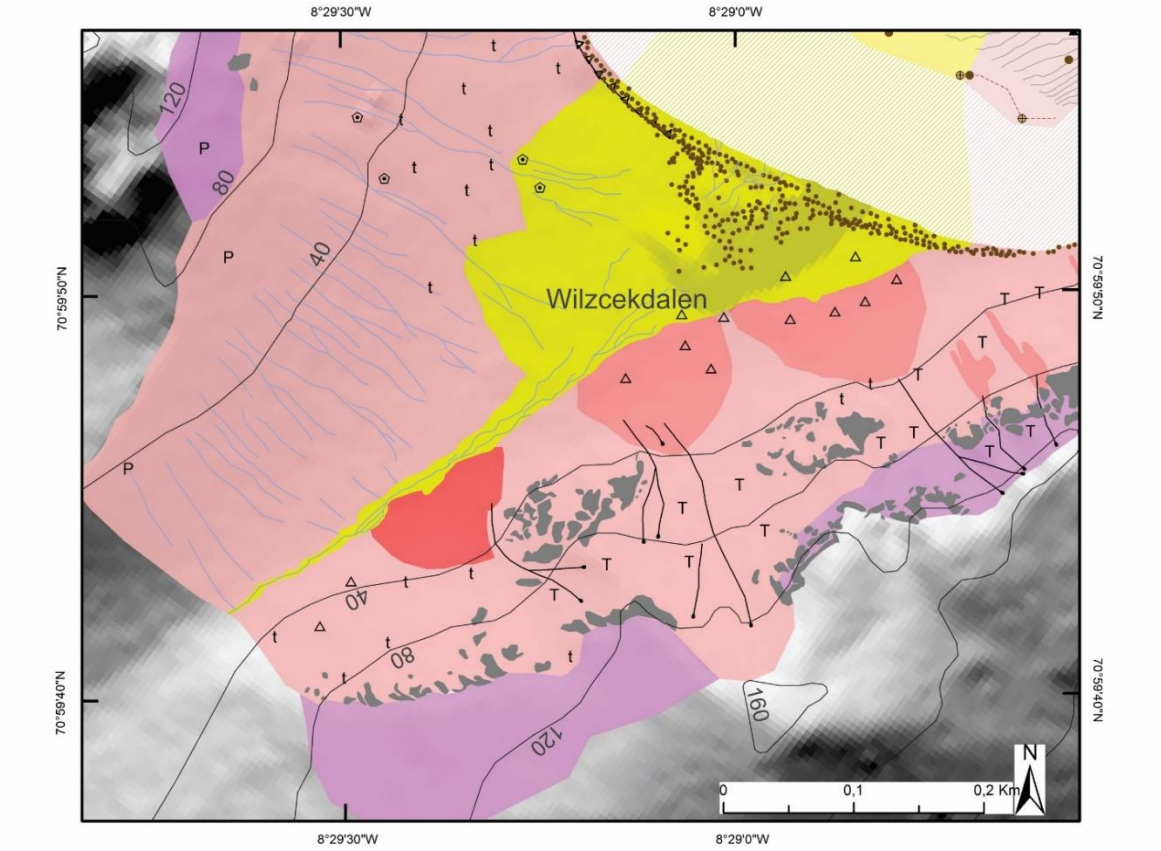

Fig. 106 Detailed geological map of Wilzcekdalen. Terrestrial contour interval 40 m. Legend of the elements at the subaerial environment in Fig. 19.

The morphology of the valley floor in Wilzcekdalen was investigated during fieldwork, and lithological logs from two sections were described (see Fig. 107 for location).

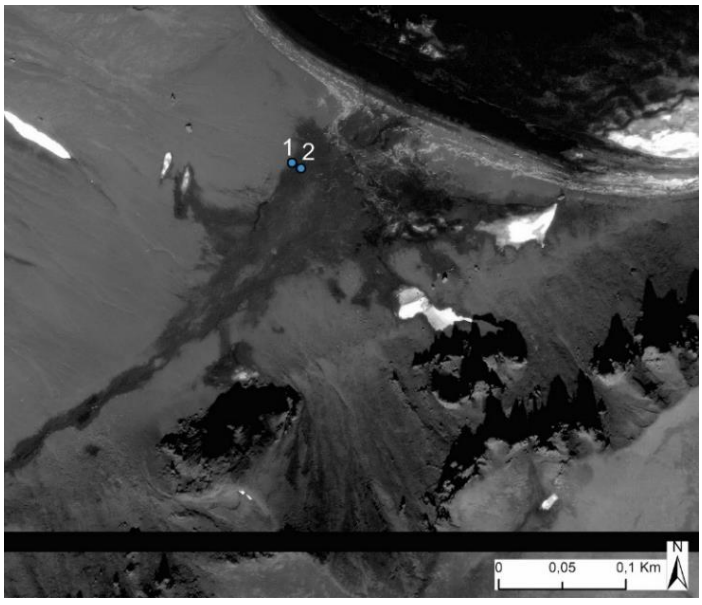

Fig. 107 Two lithological logs from the valley floor in Wilzcekdalen was described. Their locations are indicated by blue dots

The seasonal active channels spread out at the fan apex, 120 m from the ocean (Fig. 106). The channels are braided, have a chaotic pattern, and are between 0.4 and 1.2 m wide and 16 cm deep (Fig. 108). The surface in the channels is dominated by medium sand, and the banks consists of granules and pebbles in medium sand. Concentrations of gravel are found at the surface throughout the valley floor, which are interpreted to be lag-deposits (Collinson et al., 2006). The channels continue toward the lake, but are poorly defined where the driftwood is deposited.

Fig. 108 Braided seasonal active channels at the valley floor in Wilzcekdalen. The channels at this location is between 0.4 to 1.2 m wide and up to 16 cm deep

At the northwestern side of the valley, lobes of silt are deposited at the base of the slope down from Fugleberget, at the end of the alluvial fans (Fig. 106). The lobes are partly overlapping the seasonal active channels (Fig. 109).

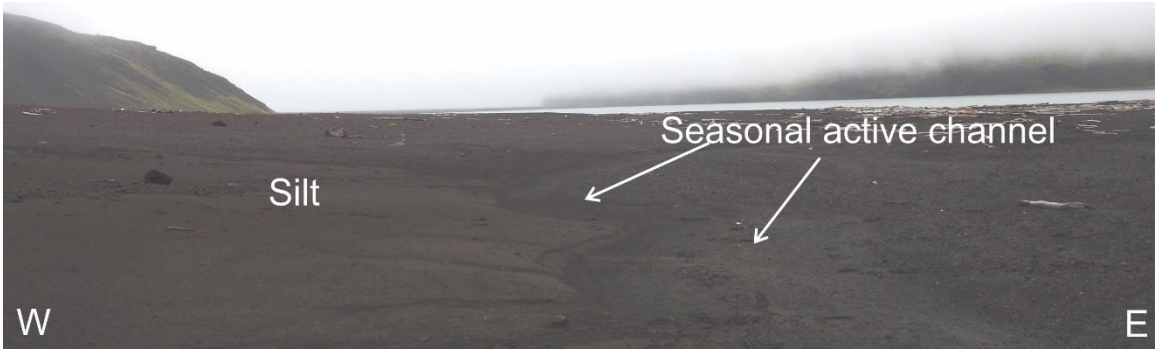

Fig. 109 Lobes of silt are deposited on the valley floor at the base of the slope down from Fugleberget at the northwestern side of the valley. The lobes overlap the seasonal active channels

Two lithological logs from the northwestern part of the valley floor in Wilzcekdalen, at the base of the slope down from Fugleberget, were described (see Fig. 107 for location). The surface at Log 1 consists mainly of medium sand with granules and pebbles concentrated at the surface as lag-deposits (Fig. 110A) and lobes of silt overlapping seasonal active channels at the base of the slope down from Fugleberget (Fig. 110B). Log 1 (Fig. 111) is described from a 105 m deep pit, and the described section is oriented southwest-northeast, parallel to the current direction of the channels.

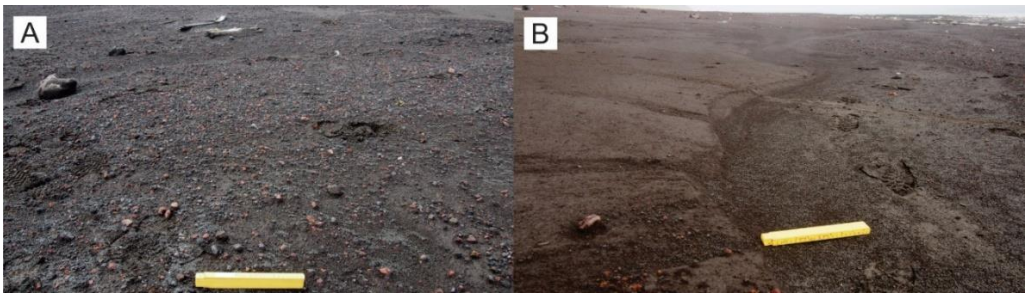

Fig. 110 The surface at Log 1 from Wilzcekdalen (see Fig. 107 for location) consists of A) concentrations of granules and pebbles at the surface, creating lag-deposits B) Deposits of lobes of silt overlapping seasonal active channels at the base of the slope down from Fugleberget, as seen in Fig. 109

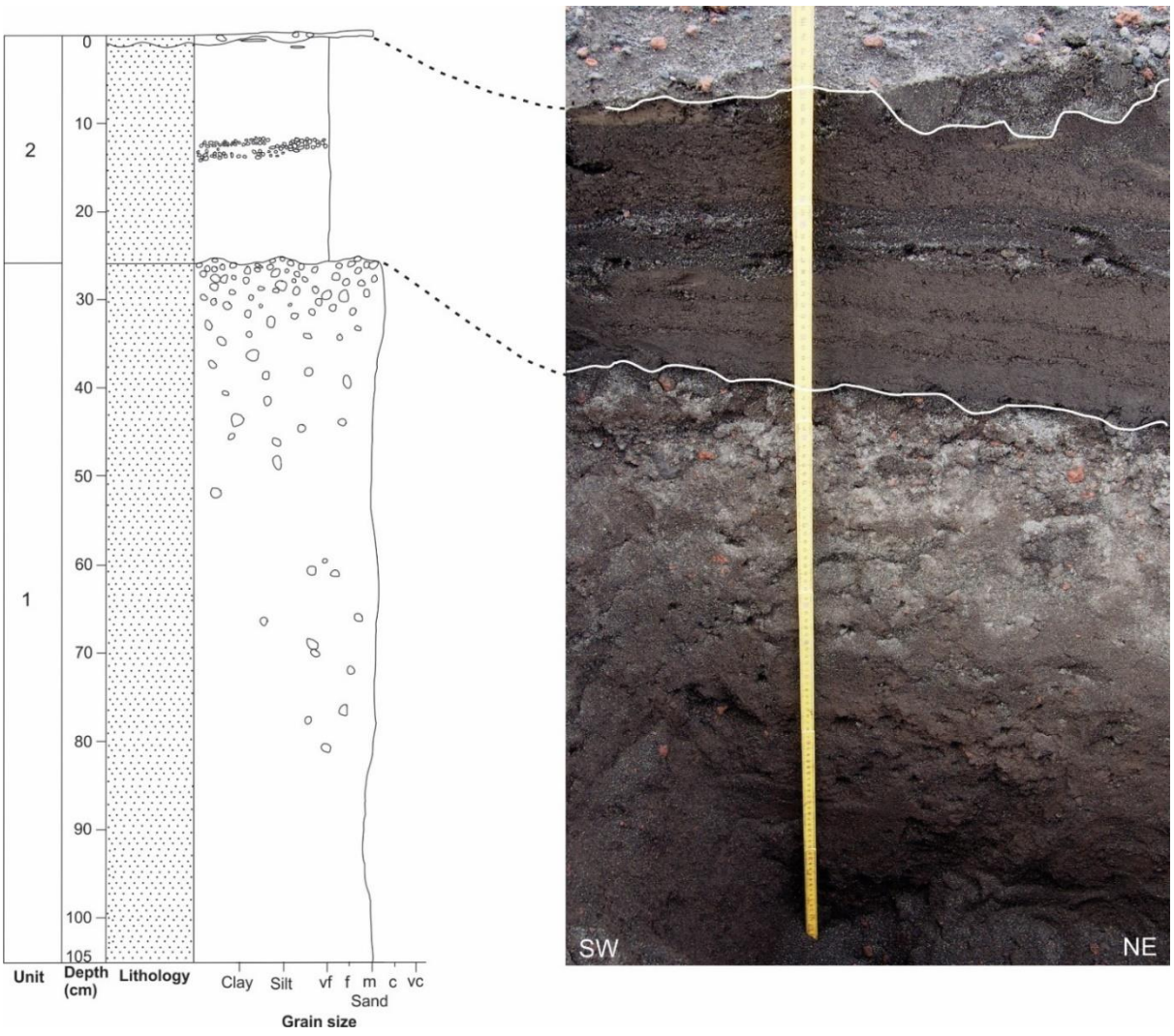

Fig. 111 Lithological log 1 from the valley floor in Wilzcekdalen (see Fig. 107 for location), where lag-surface, lobes of silt and seasonal active channels are found (Fig. 110). The section is 105 m deep, and is oriented SW-NE, parallel to the current direction of the channels. The perspective of the image may be misleading when compared to the lithological log, as it is viewed from above

Unit 1 (105-26 cm)

Unit 1 consists of one layer from 105-26 cm depth in the section. The lower boundary is not exposed. The layer contains mainly medium sand, but coarse and medium sand is also found within the layer. Granules and pebbles are randomly distributed between 83-58 cm depth and from 52 cm depth to the top of the unit, where it is concentrated.

Unit 2 (26-0 cm)

There is a sharp transition to unit 2, which is the second layer between 26-2 cm depth as well as the surface layer. The first layer contains very fine sand with lenses of coarse sand and gravel between 15-11 cm depth and lenses of silt at the top of the layer. The surface layer has an erosional boundary to the underlying layer, and has a varying thickness. It contains medium sand with granules and pebbles.

Log 2 is located 8.5 m southeast of Log 1 (see Fig. 107 for location). The surface of the log consists of medium sand with concentrations of granules and pebbles as lag-deposits (Fig. 112). Seasonal active channels are found at this location. Log 2 (Fig. 113) is described from an 87 cm deep pit, and the described section is oriented southwest-northeast, parallel to the current direction of the channels on the valley floor.

Fig. 112 The surface at Log 2 from Wilzcekdalen consists of medium sand with granules and pebbles as lag-deposit (see Fig. 107 for location)

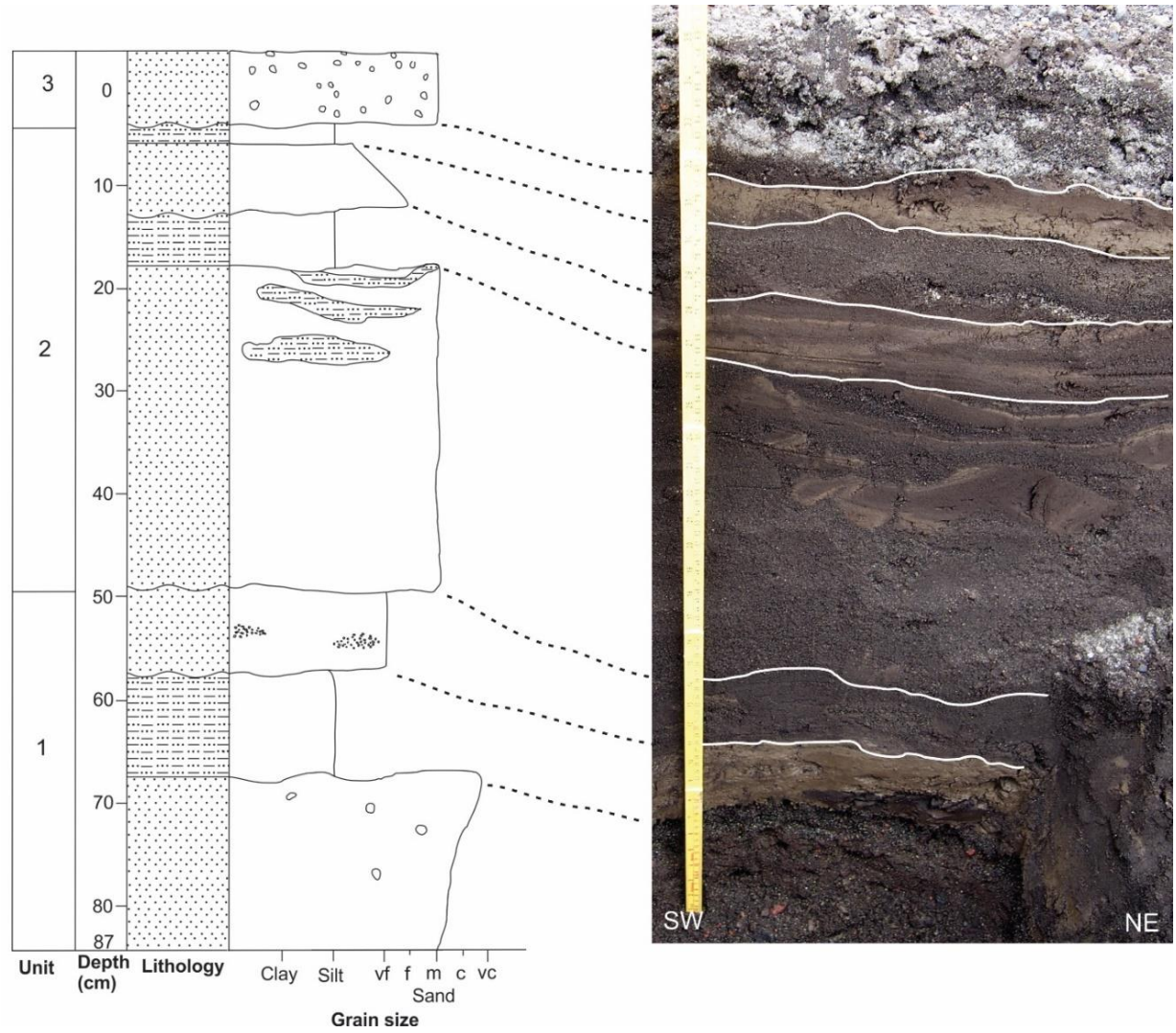

Fig. 113 Lithological log 2 from the valley floor in Wilzcekdalen (see Fig. 107 for location). Seasonal active channels and a lag-surface with medium sand, granules and pebbles are found at the location. The section is 87 cm deep, and is oriented SW-NE, parallel to the current direction of the channels. The perspective of the image may be misleading when comparing to the log, as it is viewed from above

Unit 1 (87-52 cm)

Unit 1 extends from 87-52 cm, and consists of three layers. The lower boundary is not exposed. The lowermost layer is coarsening upwards from medium to coarse sand, with a few granules and pebbles randomly distributed within the layer. The top of the layer is uneven, and there is a sharp transition to the layer above, which consists of silt. The boundary to the third layer of the unit is uneven, and as it does not follow the thickness of the silt-layer below, it is interpreted to have an erosional boundary. The third layer contains very fine sand with lenses of medium sand.

Unit 2 (52-7 cm)

Unit 2 consists of four layers. As the first layer has an uneven boundary to the top of unit 1, it is interpreted to be erosional. It contains medium sand with a chaotic pattern of lenses of silt. The lenses

have a color variation of darker and lighter silt. The second layer in the unit is a deposit of silt with a structure of the same color variations as seen in the lenses. The third layer in the unit cuts the structures in the silt, and is interpreted to be erosive. It is fining upwards from fine to very fine sand. The fourth and last layer in the unit is a 2-3 cm thick layer of silt.

Unit 3 (7-0 cm)

The uppermost unit of the section is the 7 cm thick surface layer. It has an erosional boundary to the top of unit 2, and consists of medium sand with a few granules and pebbles scattered in the layer.

4.2.5 Subaerial slopes

The steep subaerial slopes down from Hochstetterkrateret (138 m a.s.l.), Wildberget (300 m a.s.l.), Mohnberget (180 m a.s.l.) and Fugleberget (136 m a.s.l.) extend directly into the lake. Debris flow deposits, rockfall deposits, solifluction materials and unspecified mass movement materials are identified on the slopes and mapped on the geological map (Fig. 18). Both thick and thin vegetation is found on the slopes, as well as seasonal active channels. The top of Wildberget, Mohnberget and Fugleberget consists of weathered material. Boulders, gravel and driftwood is concentrated at the base of the slopes, 5-10 m from the lake shoreline, approximately 1 m above the lake water level (Fig. 114). There is a sharp transition to the sands found at the slope above, which seem to have been removed from the base. This is mapped as an abrasional scarp (Fig. 18).

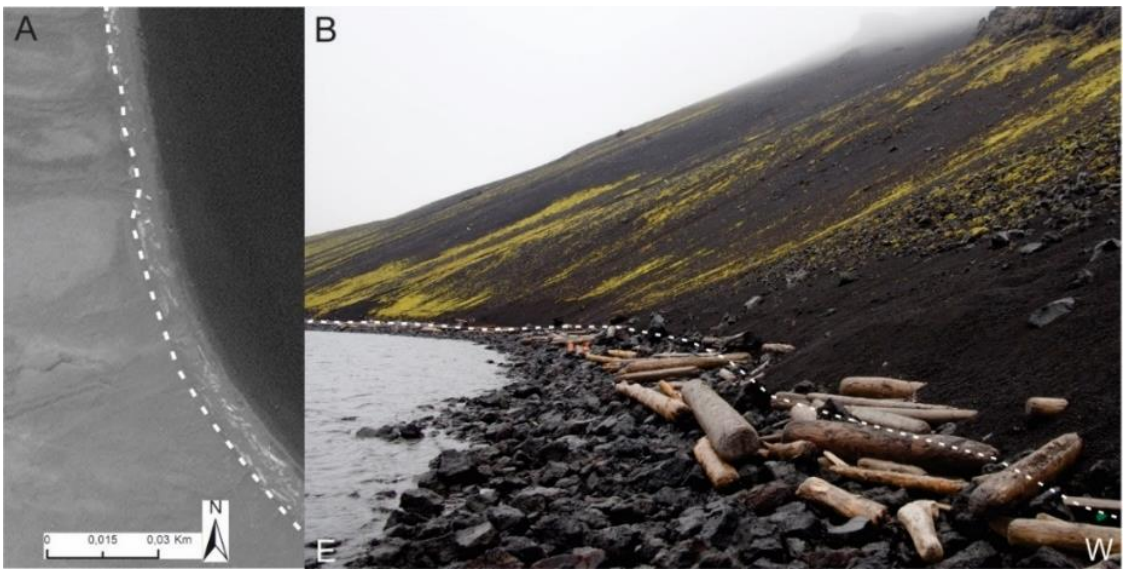

Fig. 114 Abrasional scarp along the base of the slopes by the lake shoreline creates a sharp transition between the concentrations of boulders, gravel and driftwood and the sand on the slopes above. A) Abrasional scarp along the slope down from Fugleberget between Wilzcekdalen and Bommen (satellite image: KSAT) B) The same slope as in A seen from ground-level

At the lake shoreline by the base of the slope down from Fugleberget, between Wilzcekdalen and Bommen, fan-shaped deposits are found (Fig. 115A). The deposits are found at the end of seasonal active channels, and are cut by the abrasional scarp (Fig. 115B). The features are up to 13 m long and 18 m wide at the widest, and are mapped as fan-shaped features on the geological map (Fig. 18)

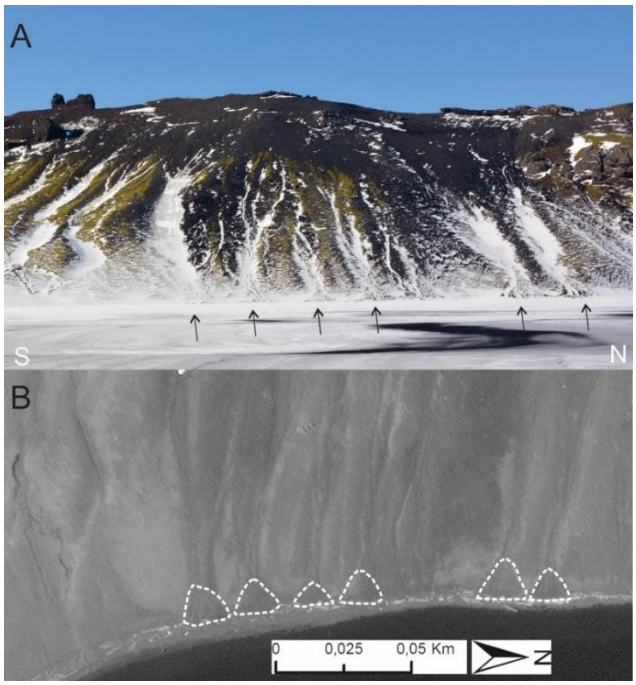

Fig. 115 Fan shaped deposits at the end of seasonal active channels at the base of the slope down from Fugleberget, between Wilzcekdalen and Bommen A) Seen from winter ice on the lake. Arrows are pointing at the fan-shapes (photo: A. Lysså) B) Seen from satellite image. Outline of the fan-shapes are marked with white. Note that the features are cut by abrasional scarp (satellite image: KSAT)

4.3 Sedimentation in Nordlaguna

In this chapter, the data from Nordlaguna is presented. It consists of the map of the sediment distribution in the lake, and the data from the two sediment cores from the lake, NL2 and NL1B.

4.3.1 Sediment distribution

The map of sediment distribution in the lake (Fig. 116) is based on knowledge about the terrestrial environment and observations on the SSS-data. In general, the deposits on the terrestrial environment are estimated to continue onto their subaqueous counterparts, as the surface deposits do not contain specific structures that can be separated on the SSS-data, except for the debris flow deposits on the slope down from Fugleberget (Fig. 23). The subaqueous areas close to the lake shoreline are not covered by the survey, and are estimated to consist of the same type of deposits as observed on the subaerial environment and mapped in the lake.

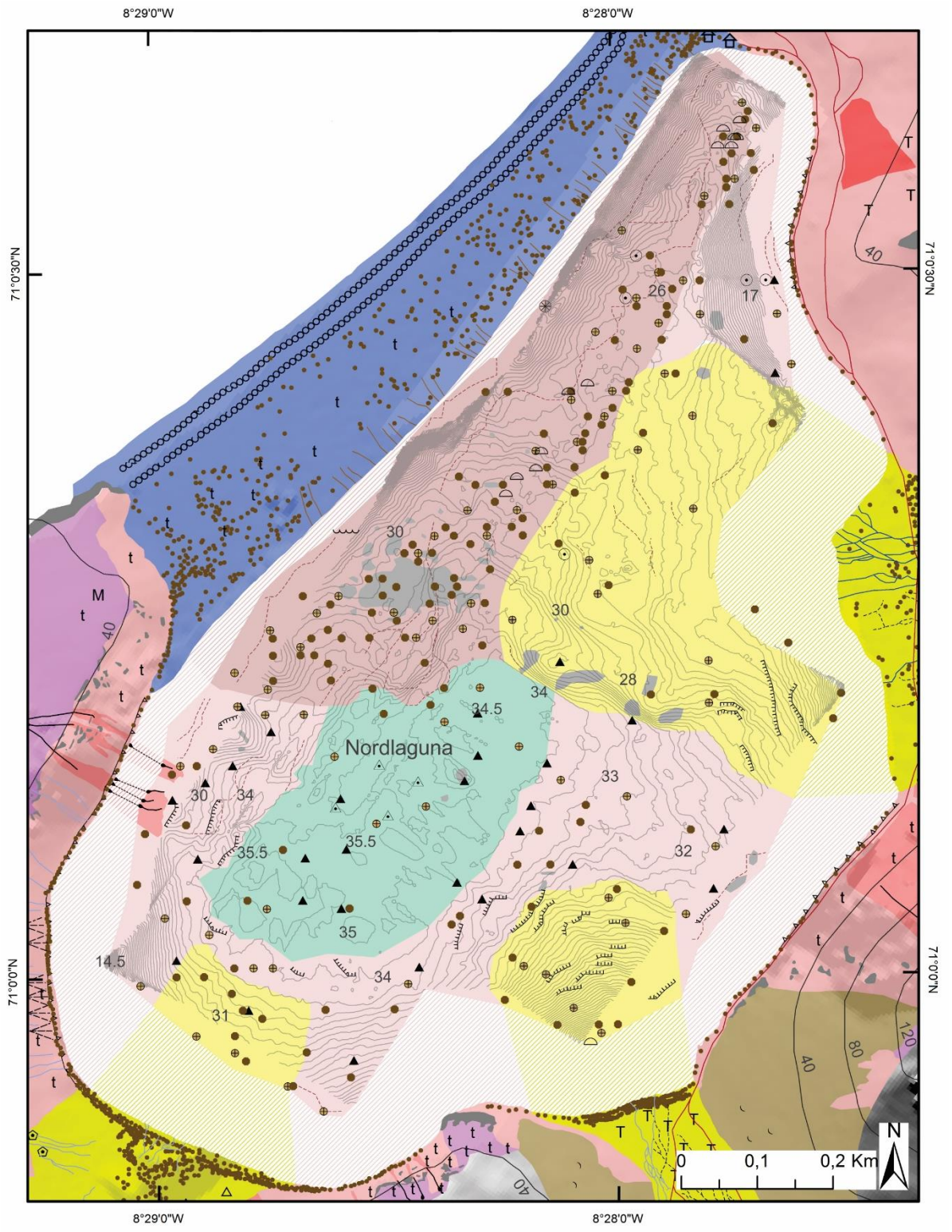

Fig. 116 Detailed geological map of the sediment distribution in Nordlaguna. Terrestrial contour interval 40 m, bathymetric interval 0.5 m. Legend of the elements at the subaerial environment in Fig. 19, and legend of the elements at the subaqueous environment in Fig. 20

Large amounts of driftwood (Fig. 117A) and boulders (Fig. 117B) are scattered on the lake floor, both fully exposed and covered with sediments. Boulders are mainly found at the southern side of the lake, below the slopes down from Wildberget, Mohnberget and Fugleberget, but also on the deep and flat part of the lake (Fig. 116).

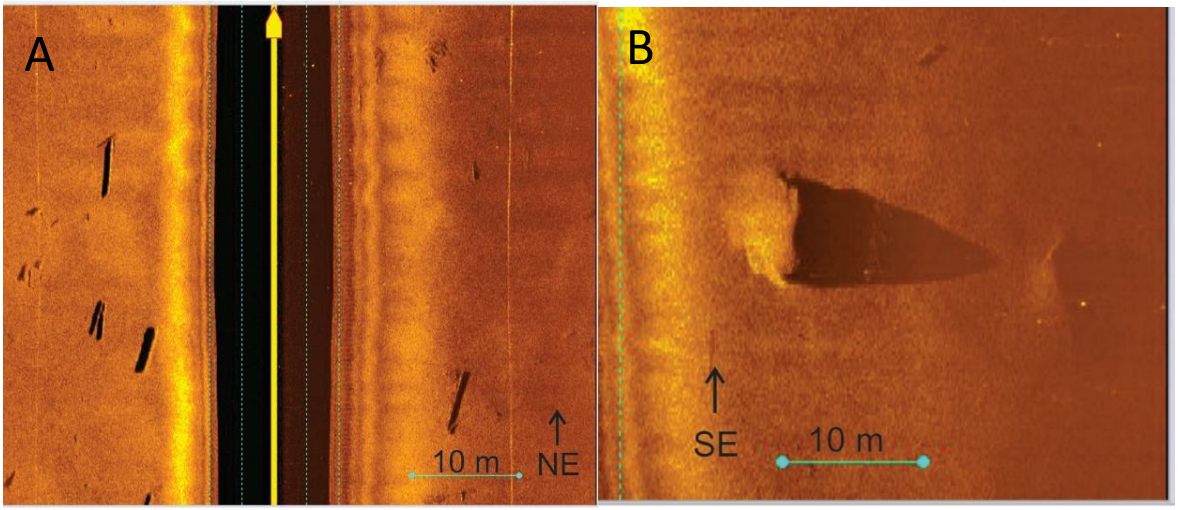

Fig. 117 Large amounts of boulders and driftwood are scattered on the lake floor, both fully exposed and covered with sediments A) Driftwood on the slope down from Bommen B) Partly buried boulder below the slope down from Fugleberget

Five depressions in the sediments on the lake surface were observed at the northern part of Nordlaguna. Two types of depressions were found, three symmetrical (Fig. 118A) and two asymmetrical (Fig. 118B). The depressions are interpreted as pockmarks, which can be formed as a result of fluids escaping through the sediments (Judd & Hovland, 2007).

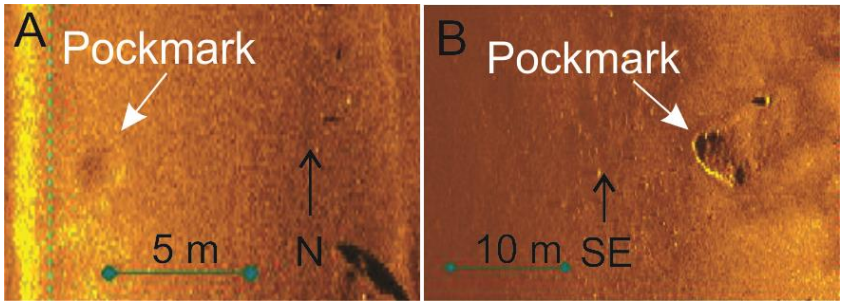

Fig. 118 Two types of pockmarks were found in Nordlaguna A) Symmetrical pockmark, with a width of 1.7 m B) Asymmetrical pockmark on the slope down from Bommen. The pockmark is 2.3 m wide and 5.1 m long

On the subaqueous fan deposits in Tornøedalen, Stasjonsdalen and Wilzcekdalen, as well as on the subaqueous slope down from Wildberget, cracks with backwalls that are oriented downslope are observed in the sediments (Fig. 119). The cracks are aligned parallel to the slopes, and are mainly occurring in clusters. The features are interpreted as back-scarps of subaqueous slides. Such slides can be initiated by for instance high loads of sediments, earthquakes or fluid escapes (eg. Van Daele et al., 2015; Wilhelm et al., 2015).

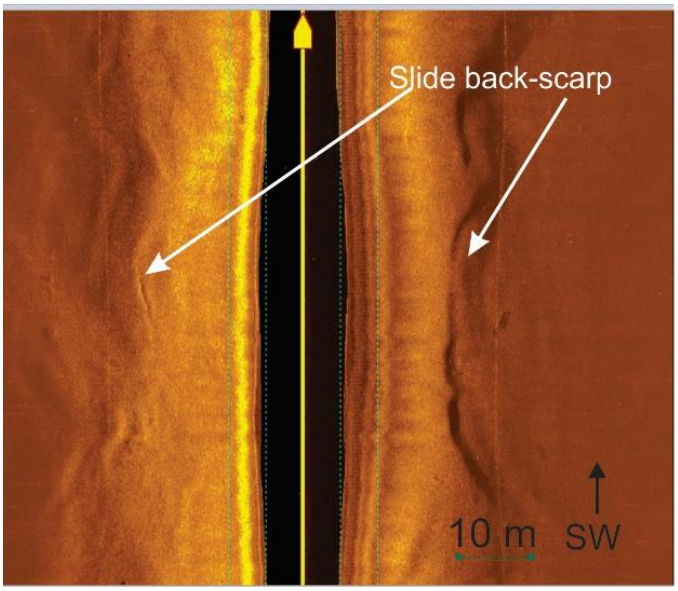

Fig. 119 Example of slide back-scarp on the subaqueous slope down from Wildberget

Ripples are found at approximately 24 m water depth on the subaqueous slope from Bommen (Fig. 116). The ripples are long with a sinuous shape, and some bifurcate. Since the ripples are only seen in plan view, it can not be determined is they are symmetric or not. The size of the ripples seems to decrease downslope (Fig. 120). The ripples can have been formed by either wave activity or current activity in the lake, which is usually distinguished by the symmetry of the ripples. However, since wave ripples can also be recognized in plan view as long and continuous, sinuous-shaped and bifurcating, the ripples are interpreted to be created by waves (Nichols, 2009).

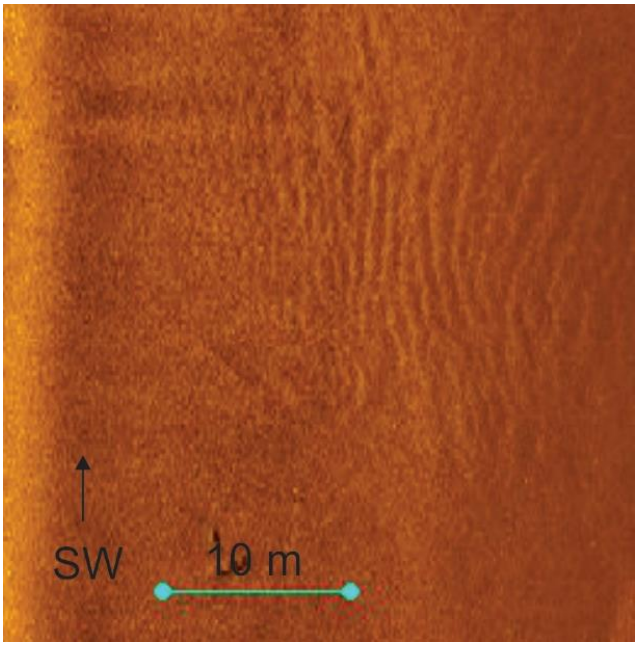

Fig. 120 Ripples at approximately 24 m water depth on the subaqueous slope down from Bommen. The size of the ripples decrease downslope (towards southeast, left in the image)

Bedrock is found on the subaqueous slopes in Nordlaguna, mainly at the slope down from Bommen (Fig. 121A). The bedrock seems to be partly covered by sediments. At the slope down from Bommen, bedrock with a crater-like shape (Fig. 121B) is found, at 16 m water depth. The feature is mapped as crater-like feature (Fig. 116).

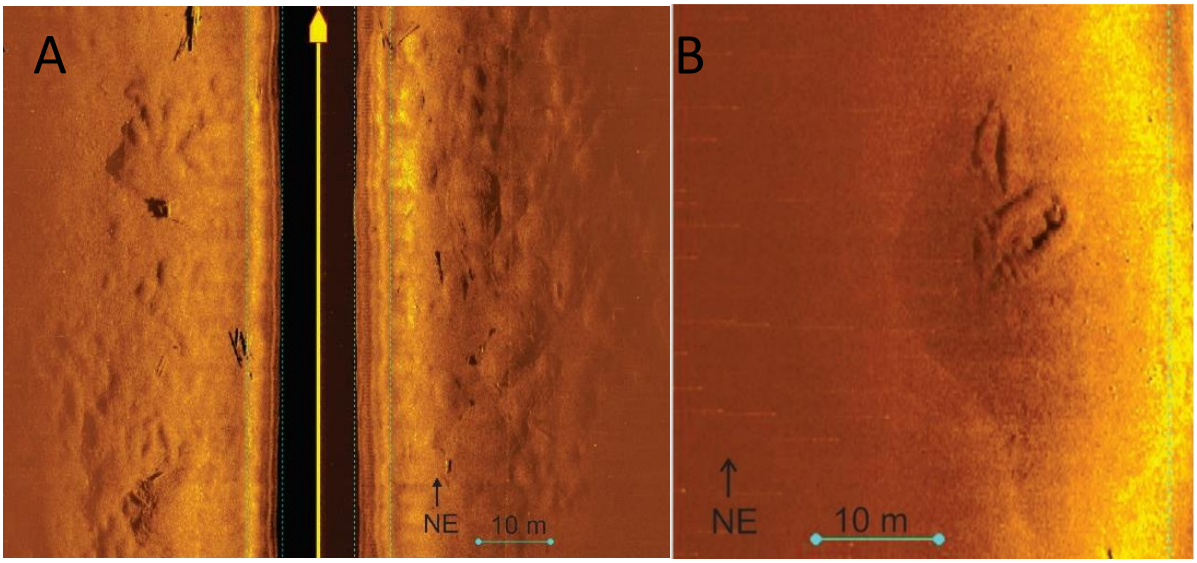

Fig. 121 A) Bedrock is found at the subaqueous slope down from Bommen B) Bedrock in a crater-like shape is found on the slope down from Bommen, at 16 m water depth

Outer rims of mass movement deposits (Fig. 122) are found on the subaqueous slopes down from Bommen, Fugleberget and Hochstetterkrateret (Fig. 116). Some of the outer rims are overlapping, which may indicate that they are originating from different episodes of deposition.

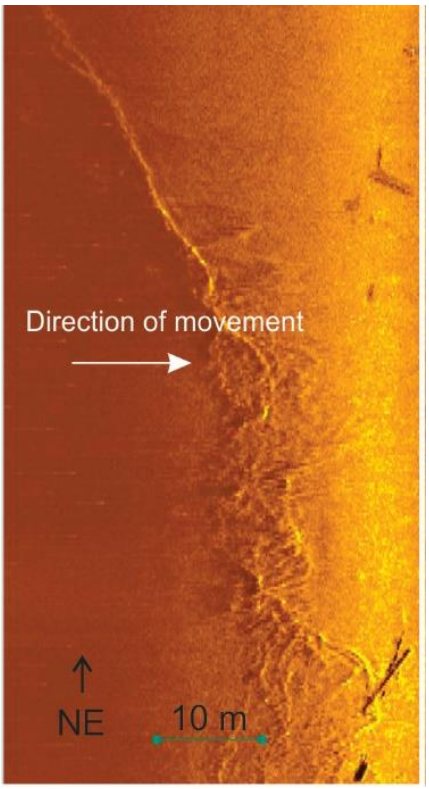

Fig. 122 Outer rim of mass movement deposits on the subaqueous slope down from Bommen. Direction of movement is downslope

4.3.2 Sediment cores

Two cores that were collected from Nordlaguna, NL2 and NL1B, are presented in this section. Their location is shown in Fig. 123.

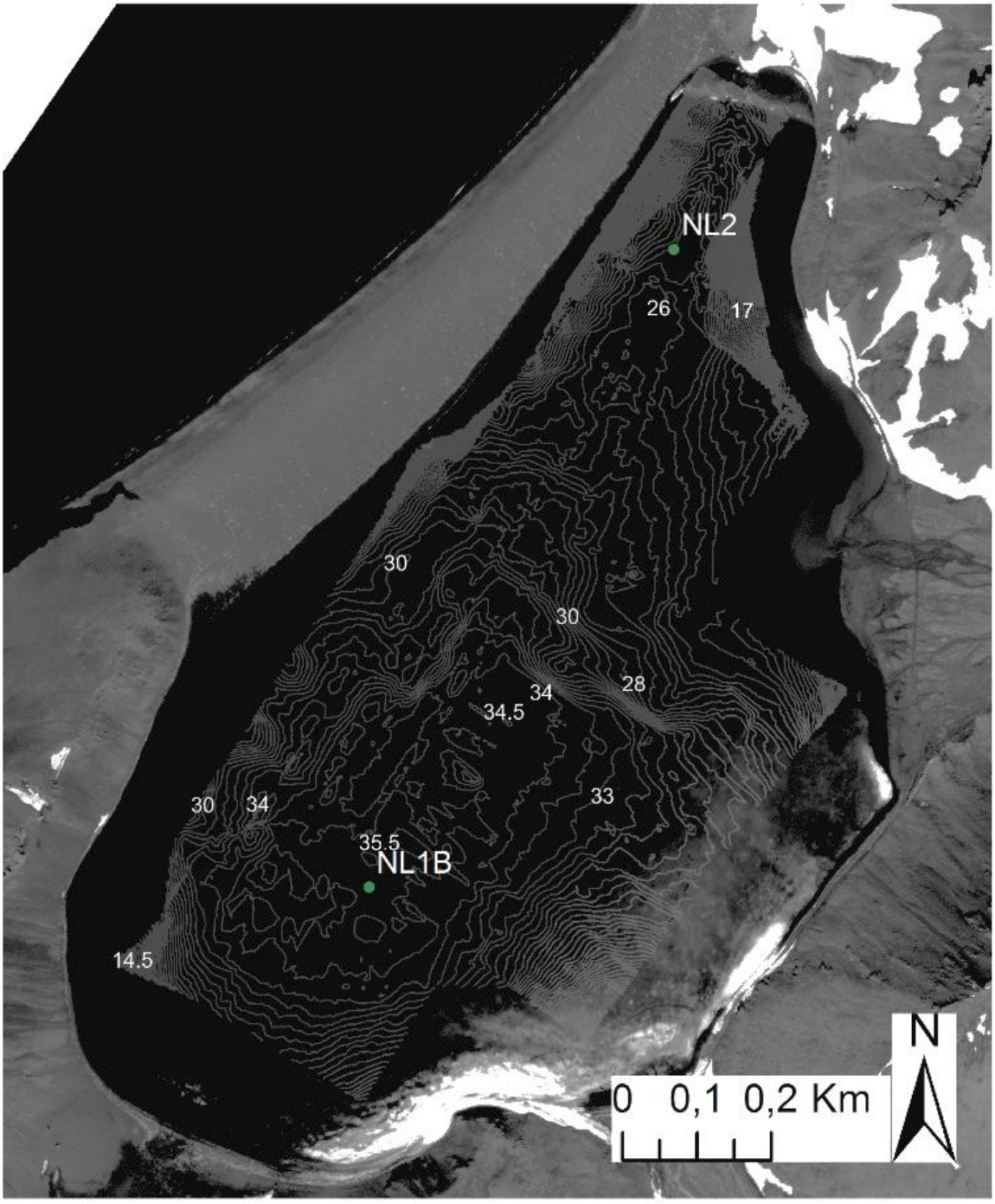

Fig. 123 Location of the two cores in Nordlaguna that are used in this thesis. Core NL2 is from the northern part of the lake, at 25 m water depth. Core NL1B is from the flat bottom where the lake is at its deepest, at 35.5 m water depth. Bathymetric interval 0.5 (Satellite image: KSAT)

Core NL2

Core NL2 is collected from the northern part of Nordlaguna, approximately 120 m from Bommen and 160 m from the slope down from Hochstetterkrateret (Fig. 123), where the surface is interpreted to consist of mass movement deposits that are mainly derived by wash-over. The sediment in core NL2 has a total length of 99.5 cm (Fig. 124), and is divided into two units that are presented below. Grain-size analyses of the sediment cores (Appendix A) were used to gain information about the grain-size within the units when the lithological log was created.

Fig. 124 Lithological log of core NL2 with x-ray image, photo of the core surface, lithological units, chronology and physical properties (fractional porosity, density and magnetic susceptibility)

Lithology:

Unit 1 (109-63.5 cm)

Unit 1 extends from 109 to 63.5 cm. The base of the unit was penetrated by the coring. The lower part of the unit consists of laminated silt that is deposited as couplets with coarse dark silt followed by a

deposit of fine silt/clay with a lighter color. The couplets has a variation in thickness throughout the unit: between 76-77 cm in the core, there is an average of 5 couplets per cm; between 77-71.5 cm, there is an average of 1.2 couplets per cm; between 71.5-68 cm, there is an average of 1.7 couplets per cm.

Grains of fine to medium sand are deposited in the unit, some are randomly distributed while some are deposited in horizons that follows the lamination. The amount of sand gradually increases upwards in the unit. Between 79.5-78 cm, a layer of very fine sand is deposited. The layer slightly cuts the underlying lamination, giving it an erosive boundary.

Unit 2 (63.5-9.5 cm)

There is a sharp transition to the second unit in the core. The first layer in the unit is a 36 cm thick layer of sand. The base of the layer consists of coarse sand that slightly cuts the lamination at the top of unit 1, creating an erosive boundary between the two units. The layer is fining upwards to fine sand. Clasts up to 2 cm long are scattered in the layer, mainly at the lower part. There is a gradual transition to a deposit of silt on top of the layer. Between 26.5-21 cm, two normally graded layers are deposited. The layers are fining upwards from medium sand to silt, and both cut the underlying silt, creating an erosive boundary. The uppermost layer in the unit is the 11.5 cm thick layer that are fining upwards from coarse sand at the base to medium sand at the top. Intraclasts of silt are found in the upper part of the layer.

Physical properties:

The three physical properties, fractional porosity, density and magnetic susceptibility, follow the lithology of the core, and has a marked transition between the two units. The values of fractional porosity are low where the core consists of coarse sediments, and positive peaks where fine sediments are deposited. The density mirrors the fractional porosity, with high values where coarse sediments are deposited, and negative peaks at fine sediments. The values of magnetic susceptibility decreases at the transition between the two units.

Dates:

The ^{14}C- dates and calibrated dates of core NL2 is presented in Fig. 124 and Table 2.

Table 2 Depth, ^{14}C-dates and calibrated dates of core NL2

Depth (cm)	**^{14}C year BP**	**Cal. year BP**
26.5-27.8		End of 1950s/beginning of 1980s
64.8-69.8	300±35	400.5±28.5
78.2-83.2	205±50	179.5±35.5
93-96	630±70	582±27
100-105	235±55	180±34
105-108	13 670±170	16 505.5±261.5

Interpretation:

Unit 1

The laminated couplets of coarse silt and fine silt/clay are interpreted to be annually deposited varves. The varves consists of a coarse silt layer that is deposited during the hydrological season in spring or summer, and the fine silt/clay is deposited when the lake is covered with winter ice (Lowe & Walker, 2015). The lamination may also be due to temporary deposition in the lake, but it does take a significant time of quiet conditions in the lake for the very finest particles to settle from suspension, which appears likely to be achieved only when the lake is covered with winter ice (Francus et al., 2007). Although there may be several episodes of sedimentation during a year, only one deposit of clay will be formed (Strum, 1979). The isolated grains of sand are interpreted to be aeolian deposited sediments on the winter ice that settles on the lake floor as the ice melts. Such deposits are a common feature in Arctic lakes (eg. Retelle and Child, 1996). The layer of very fine sand between 79.5-78 cm may be deposited by the same process, if there has been a concentration of sand on the winter ice. However, this layer could also be a deposition by wash-over event, as the core is collected from the shallow part of the basin, where the lake floor is interpreted to consist of mass movement deposits that are mainly derived by wash-over.

Unit 2

The sand in unit 2 is interpreted to be a wash-over deposit, based on the same criteria as mentioned above. The intraclasts of silt can be rip-up clasts that are eroded from the underlying layers, when the waves have washed the sand into the lake.

Core NL1B

Core NL1B is collected 940 m southwest of core NL2, at a water depth of 35.5 m, which is the deepest and flat part of the lake (Fig. 123). According to the geological map (Fig. 116), the lake bottom in this area is classified as lacustrine deep floor deposit. The sediment in the core has a total length of 92 cm (Fig. 125) and is divided into three units that are presented below. Grain-size analyses of the sediment cores (Appendix A) were used to gain information about the grain-size within the units when the lithological log was created.

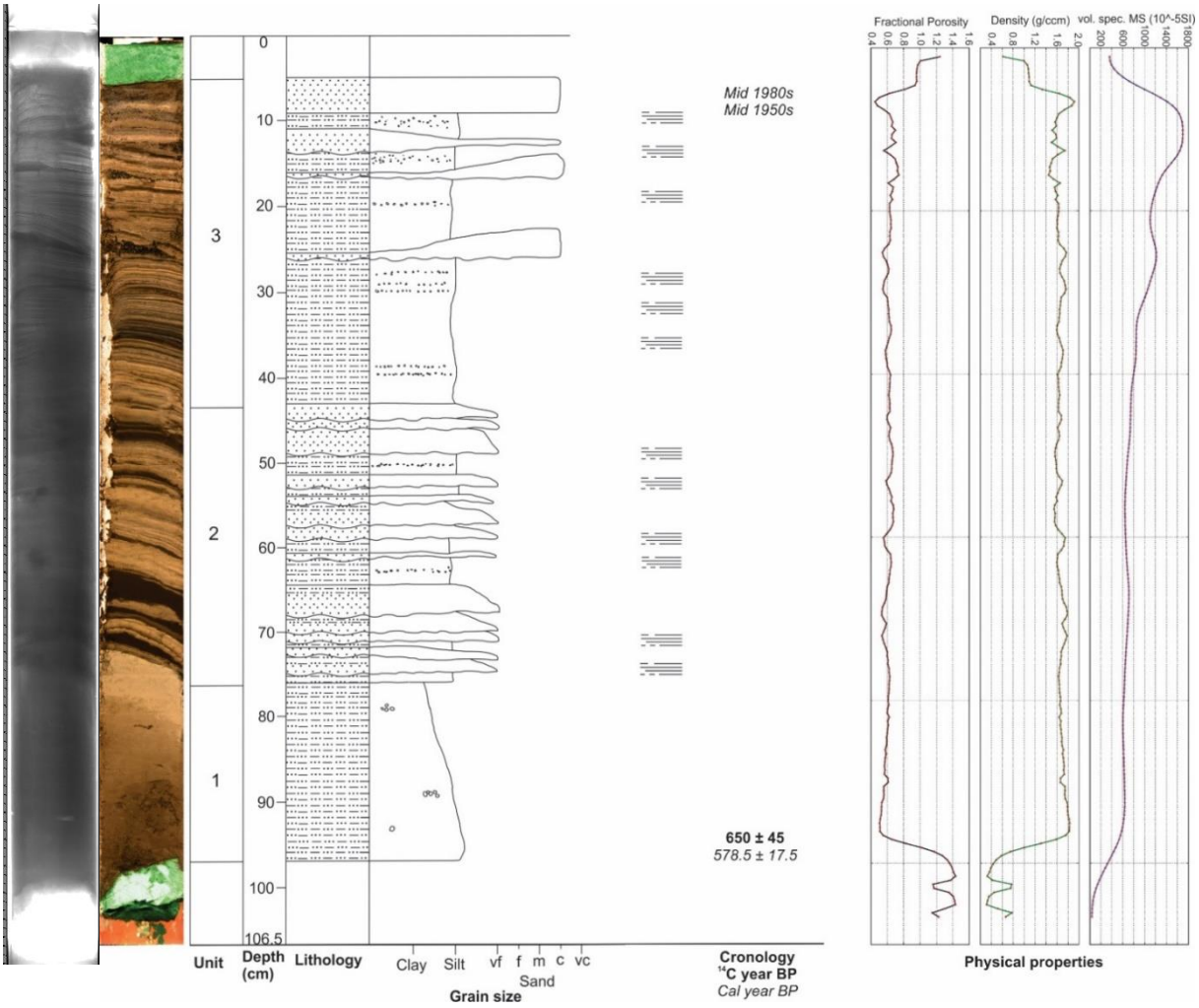

Fig. 125 Lithological log of core NL1B with x-ray image, photo of the core surface, lithological units, chronology and physical properties (fractional porosity, density and magnetic susceptibility)

Lithology:

Unit 1 (97-75 cm)

The base of the core was penetrated by coring. The lower unit consists of normally graded structureless silt. A few clasts of coarse sand is scattered throughout the unit.

Unit 2 (75-43 cm)

There is a sharp transition between unit 1 and unit 2. Unit 2 is characterized by a series of normally graded deposits that are fining upwards from mainly fine sand to silt. The deposits have a variable thickness, and the underlying layer has been slightly cut, creating an erosive boundary. Layers of laminated silt are deposited between the normally graded deposits. The lamination consists of couplets with coarse dark silt followed by a deposit of fine silt/clay with a lighter color. Isolated grains of mainly medium sand are deposited in horizons that follow the lamination.

Unit 3 (43-5 cm)

The uppermost unit in the core is dominated by laminated silt with lenses of coarse sand. The laminated silt has the same characteristics as in unit 2, and consists of laminated couplets of coarse and fine silt with isolated clasts of coarse to medium sand deposited in horizons that follow the lamination. The couplets have a variation in thickness throughout the unit: between 41-38 cm in the core, there is an average of 1.5 couplets per cm; between 33-31 cm, there is an average of 3 couplets per cm; between 30-28 cm, there is an average of 3 couplets per cm; between 24-21 cm, there is an average of 3 couplets per cm. Coarse sand is deposited on the upper part of the unit as lenses that are up to 1.5 cm thick. The base of the lenses has slightly cut the underlying laminated silt, creating an erosive boundary. The top of the core consists of an unsorted layer of coarse sand and silt.

Physical properties:

The three physical properties - fractional porosity, density and magnetic susceptibility - follows the lithology of the core. Fractional porosity shows negative peaks where coarse particles are deposited, giving it a wiggling curve as there are deposits of silt and sand throughout the core. The density-curve mirrors the curve of the fractional porosity. The magnetic susceptibility-curve has high values at the top of the core, where the coarsest material is deposited, and is gradually decreasing with depth.

Dates:

The ^{14}C-dates and calibrated dates of core NL1B is presented in Fig. 125 and Table 3.

Table 3 Depth, ^{14}C-dates and calibrated dates of core NL1B

Depth (cm)	**^{14}C year BP**	**Cal. year BP**
5-7		Mid 1980s
7-8		Mid 1950s
94-96	650±45	578.5±17.5

Interpretation:

Unit 1

As the silt in the lower part of the core is structureless and fining upwards, the unit may have been deposited in one event. This could for instance be by subaqueous slides, as slide back-scarps are mapped on the subaqueous slopes (Fig. 116). The isolated grains of sand can have been redeposited with the silt during a slide event.

Unit 2

The series of normally graded layers that characterize unit 2 can be interpreted as turbidites, as characteristic features of such deposits, for instance an erosive base and normally graded layer (Walker & Mutti, 1973) are found. The couplets of laminated silt between the turbidites are interpreted to be annually deposited varves, based on the same criteria as described in unit 1 core NL2. The isolated grains that follow the lamination are interpreted to be deposited by wind-action on the winter ice and settled on the lake floor as the ice melts, which is a common feature in arctic lake sediments (eg. Retelle and Child, 1996).

Unit 3

The laminated silt with isolated grains in unit 3 seems to be a continuation of the similar deposits in unit 2, suggesting that it is deposited by the same mechanisms. The lenses of coarse sand may be large accumulations of depositions of wind-blown sediments on the winter ice, and is deposited on the lake floor as the ice melts, by the same mechanisms as the isolated grains.

5. Discussion

This chapter is a discussion on the results from chapter 4. It is divided into three sections: section 5.1 is a discussion of the sedimentary sources that are observed around and in the lake. The mechanisms and processes that control the distribution of sediments in the lake are discussed in section 5.2, and the potential of using the two sediment cores to study past environmental conditions are evaluated in section 5.3.

5.1 Sedimentary sources

This section will discuss the sources of sedimentation to the lake. The discussion is based on the geological map, field observations, roundness-, shape- and grain-size analyses and sediment cores. Three types of sedimentation from within the drainage area are recorded: fluvial sedimentation (section 5.1.1), mass movement material derived from wash-over (section 5.1.2) and mass movement deposits from the subaerial slopes around the lake (section 5.1.3). The external sources of sedimentation are wind-blown sediments (section 5.1.4) and pyroclastic fallout (section 5.1.5).

5.1.1 Fluvial sedimentation

Fluvial/niveofluvial deposits are found in the three valleys around Nordlaguna: Tornøedalen, Stasjonsdalen and Wilzcekdalen (Fig. 18), suggesting that these are the main sources of fluvial sediments to the lake. The field observations, mapping, grain-size analyses and lithological logging reveals that the valleys have significantly different characteristics, both morphological and sedimentological, which are discussed in order to estimate their relative importance of fluvial sedimentation to the lake. The discussions are focused around the water discharge of the channel systems, channel morphology and the amount and type of source material from the slopes to the valley floors. Another possible source of fluvial sedimentation to the lake is runoff from the subaerial slopes that extends directly into the lake, which is briefly discussed below.

Water discharge

The water discharge in a river controls the amount and size of sediments that can be transported (Baker & Ritter, 1975). In this discussion, the observations of grain sizes in the channel system are used to estimate the relative discharge of the temporal and seasonal active streams in the channel systems, which can provide information about the size and amounts of fluvial sediments that are transported from the three valleys.

The coarsest material in the temporal and seasonal active channels are the boulders found at the fan apex in Tornøedalen (Fig. 84). According to the measurements of MPS, the boulders decrease from an average of 42.6 cm at the fan apex to an average of 26.7 cm 10 m downstream. The grain-size analysis

from the valley floor shows an increased sorting of the sand and less gravel content downstream, indicating that the coarsest materials are not transported to the lake. However, the high content of boulders and gravel upstream may indicate that the river in Tornøedalen can, at times, have the highest velocity of the three channel systems, and thereby transport coarser and larger amounts of fluvial sediments to the lake. This can also be seen on the morphology of the lake shoreline, as the active part of the valley floor in Tornøedalen is the only of the three valleys that are prograding into the lake (Fig. 18), indicating that the sediment supply to the lake exceeds the erosion of the shoreline (Boyd et al., 1992). The coastlines at Stasjonsdalen and Wilzcekdalen are linear and not prograding, indicating less sediment supply to their subaqueous slopes.

A few small boulders were observed in the channel system at the end of Stasjonsdalen (Fig. 99). The field observations shows that the channels on the valley floor are dominated by gravel, and the grain-size analyses from the channel systems from Stasjonsdalen and Jøssingdalen shows a high gravel content, which could indicate that the seasonal active rivers have a high velocity. However, the drainage area of the valleys are small, there are no sources of water at present and the channel system was not observed to be active during heavy rain. This could imply that the river may not reach high velocities at present. It is, however possible that there has been more fluvial activity in the channel system at previous times. A possible explanation of this can be that there was more water discharge in the valley during the deglaciation of Jan Mayen.

The content of gravel in Wilzcekdalen is significantly less than at Tornøedalen and Stasjonsdalen, which can be seen by comparing the lithological log from Tornøedalen (Fig. 95) with the lithological logs from Wilzcekdalen (Fig. 111, Fig. 113). This reveals that the channel system in Tornøedalen consists of significantly coarser particles than in Wilzcekdalen. The sand in the lithological log from Tornøedalen is mainly coarse, while Wilzcekdalen is dominated by medium sand and has a high content of silt. This implies that the seasonal active river in Wilzcekdalen has a significantly lower discharge, and mainly transports fine material to the lake.

Channel morphology

A fluvial channel system is better evolved with time (Schumm, 1977), and the study of channel morphology can provide information about the fluxes of water, sediment and energy (Likens, 2009). The channel system in Tornøedalen is the best developed of the channel systems in the three valleys, with well-defined channels and vegetated banks (Fig. 88). In comparison, the channel system in Stasjonsdalen is less defined (Fig. 100), but significantly better developed than the channel system in Wilzcekdalen, which consists of a network of short, narrow and shallow channels with a chaotic pattern (Fig. 108). This implies that the channels in Tornøedalen have experienced fluvial activity during a longer period of time than the other two valleys, as well as higher stream energy. This suggestion can be backed up by the observation of the active rivers that were formed in Tornøedalen during heavy rain,

as there may be more frequently events of fluvial activity and thereby more time to develop the channels than at Stasjonsdalen and Wilzcekdalen. It can also be explained by their differences in drainage area, as the 2 km long Tornøedalen has s significantly larger drainage area than the 250 m long Stasjonsdalen and the 300 m long Wilzcekdalen (Fig. 10). The possibility of Wilzcekdalen being the previous connection between the lake and the ocean before it may have been blocked by the eruption in Maria Musch-bukta some 600-800 years ago (Larsen, pers. comm. 2018) can partially explain the poorly developed channels in the valley, as this would provide less time for fluvial activity and channel development than Tornøedalen and Stasjonsdalen.

Source material to the valley floors

The slopes surrounding the valley floors can provide source material to the valley floors, that can be further transported to the lake by fluvial processes. The slopes around the three valleys have significantly different characteristics, affecting their importance to the sedimentation in the lake. In Tornøedalen, material from the slopes down from Wildberget and Hochstetterkrateret are deposited on the valley floor (Fig. 79). This includes debris flow deposits and rock fall deposits from Wildberget and the alluvial fan from Hochstetterkrateret. The same characteristics can be seen on the slopes around Wilzcekdalen, where debris flow deposits and rock fall material are deposited from Mohnberget, and two large alluvial fans are found at the slope down from Fugleberget (Fig. 106). This can possibly provide large source material to the channel systems at the two valley floors. In comparison, the slopes around Stasjonsdalen, Wildberget, Brinken and Mohnberget, are all dominated by solifluction material (Fig. 97). The solifluction process transport the slope material slowly downslope, generally at a rate of 1 m/year (Matsuoka, 2001), resulting in significantly less material from the slopes to the valley floor. This limits the amount of fluvial sediments that can be deposited from Stasjonsdalen to the lake.

Runoff from the subaerial slopes

Seasonal active channels that extend directly into the lake are found on the slope down from Fugleberget, between Bommen and Wilzcekdalen, where fan-shaped features are found by the lake shore (Fig. 115). These channels and features are possibly formed by alluvial processes, and alluvial material can therefore be transported directly from the subaerial slopes to the lake. However, as there are few and short channels on the slope, they may be of less importance to the fluvial/alluvial deposition in the lake than the fluvial material from the channel systems in the valley floor.

5.1.2 Wash-over deposition

Wash-over is a common depositional mechanism in coastal settings as response to storm events (Morton & Sallenger, 2003). Waves overtopping the barrier, and thereby depositing wash-over material, is recorded to occur at Bommen, both by field observations of wash-over channels (Fig. 28) and imbricated clasts at the barrier (Fig. 53), subaqueous mapping of the lake floor (Fig. 116), historical data (Richter

1946; Barr, 2015) and in the sedimentary record (Fig. 124). The morphology of beach ridges and particle sizes at a shoreline can provide information about the wave energy (Flemming, 2011), and the wave direction controls the longshore transport of the particles (Komar, 1971). The wave energy and – direction at the shoreline of Bommen can provide information about the source material to wash-over deposition in the lake, as well as the distribution of the sediments (section 5.2.3)

Wave energy

The northeastern and southwestern part of Bommen has different morphology and properties of the beach ridges and grain-sizes found at the barrier. The longest beach ridge on the barrier is described from all three profiles. At the northeastern part of the barrier, the beach ridge is steep and mainly consists of boulders (Fig. 35), while the grain-sizes and gradient decreases towards southwest, as seen on profiles 2 (Fig. 51) and 3 (Fig. 69). This can also be illustrated by the measurements of maximum particle size of the beach ridge at profile 1 and 2, where the average particle size drastically decreases from an average of 100.5 cm at the northeastern part of the barrier to an average of 39.3 cm 450 m towards southwest. The grain-size analyses from the three profiles at the barrier show that the sand at the northwestern and middle part of the barrier is coarser and has a significantly higher content of gravel. This can imply that the northeastern part is exposed to the highest wave energy on the barrier, while it is gradually decreasing towards southwest. This can also be illustrated by the wash-over channels, which are better defined at the northeastern part than at the southwestern part of the barrier, indicating high wave energy. The observations of construction material from Atlantic City (Fig. 21) reveals that the waves can at times be strong, as all the buildings were destroyed during the storm.

According to Hayes (1978), a single wash-over event can within a few hours cause more erosion and deposition than what would occur in decades during normal conditions. This can be seen in core NL2 (Fig. 124), where the thickness of what was interpreted as wash-over material by one single event was 36 cm thick, and significantly larger than the deposits of the other depositional mechanisms observed in the core. Wash-over deposition can therefore contribute to significantly large amounts of sediments in the lake.

Wave direction

The degree of roundness and shape of clasts can be used to measure the textural maturity of a deposit, and thereby indicate the amount of reworking (Collinson et al., 2006). The roundness- and shape analyses from the three profiles shows that the sample from profiles 1 and 3 are significantly less rounded and have a more equant shape than the samples from profile 2. The sample from profile 2 is thereby more reworked and textural mature than the samples from profile 1 and 3, that can indicate that the waves are oriented from two directions at the coastline of the barrier. Such bimodal directional waves can be a result of the dynamics of waves and ocean-swell or when waves are generated from different weather systems (Garcia-Gabin, 2015). Another argument for this is the observations of beach ridges

building out from both southwest and northeast at profile 3 (Fig. 69*)* as this implies longshore drift from both directions. The material from profiles 1 and 3 may be more recently eroded from the exposed bedrock that is found of the seaward side of both the northeastern and southwestern part of the barrier (Fig. 27), and thereby less reworked than the material from profile 2. The bimodal directional waves can therefore transport material to the barrier from both southwest and northeast, but the dominating direction of waves is thought to be from northeast where the wave energy is higher, as discussed above.

5.1.3 Mass movement material

The subaerial slopes that extend directly into the lake mainly consists of unspecified mass movement material, as well as debris flow and rockfall material (Fig. 18). Deposition by mass movement processes from subaqueous slopes around a lake are common in mountainous areas (eg. Bøe et al., 2014), which appears likely to occur in Nordlaguna. This can be exemplified by the observation of debris flow deposits at the subaqueous slope below Fugleberget (Fig. 23), that seems to be a continuation of the debris flow deposits observed at the terrestrial slope. The boulders that are observed on the lake floor (Fig. 117) are thought to be deposited by rock fall from the exposed bedrock at Fugleberget, Mohnberget and Wildberget. The majority of the boulders are deposited on the subaqueous slopes, while a few boulders are found on the flat part of the lake. Due to fluid resistance (Falkovich, 2011), the boulders on the flat part of the lake are unlikely to have been transported solely by initial rockfall. A more likely explanation may be that if some rockfalls have occurred during winter, the boulders temporarily settles on the winter ice before being deposited on the lake floor once the ice starts melting. These boulders may have been transported even further from the slopes by ice drifting during spring.

5.1.4 Wind-blown sediments

Wind-related surfaces were observed in the field. Lag-surfaces at Bommen, Tornøedalen and Wilzcekdalen, as well as wind ripples at Bommen and in Tornøedalen were found. At Bommen, the stoss sides of the ripples were dipping towards northwest, and towards east in Tornøedalen. This direct the wind-blown particles towards the lake. Wind-blown particles were observed in the two sediment cores, both as isolated grains and as lenses of sand. These were interpreted to have been deposited on winter ice and settled on the lake floor when the ice melts. It appears likely that wind-blown material is deposited in the lake throughout the year, but due to fluid resistance (Falkovich, 2011) the velocity of the particles drop once entering the lake, and are probably deposited near the lake shoreline. The amount of wind-blown grains that are deposited on the deep parts of the lake floor seems to mainly depend on how the sediments are accumulated on the winter ice. This can be exemplified by the three lenses of sand that were observed in unit 3 in core NL1B (Fig. 125), as they may have been accumulations of wind-blown sediments on the winter ice, in contrast to the isolated grains in the core. The observations of the wind-related surfaces, wind-blown particles in the sediment cores and the knowledge about strong winds at Jan Mayen (Gabrielsen et al., 1997) could imply that wind-blown sediments are a significant external source of sedimentation in the lake.

5.1.5 Pyroclastic fallout

According to Gjerløw (2015), the Eggøya eruption in 1732 resulted in a tephra sheet deposit that covered the majority of Jan Mayen. Pyroclastic fallout is observed at Fugleberget, which is suggested to origin from the explosive eruption at Maria Musch-Bukta some 600-800 years ago (Lysså and Larsen, pers. comm. 2018). It appears likely that pyroclastic fallout is deposited directly in the lake during volcanic eruptions on the island. Volcanic particles that settle in a column of water can often be deposited as graded layers (Kuenen, 1953). The normally graded layers in core NL1B (Fig. 125), which were interpreted to be deposited by turbidity currents, could possibly be formed by volcanic ash settling in the lake during volcanic eruptions on the island. However, establishing this would require more precise dating of the core (as discussed in section 5.3.1) or possibly geochemical analysis, which is not a part of this thesis. Another complication to this suggestion is that all sediments at Jan Mayen are of volcanic origin. It can therefore be difficult to separate the volcanic particles that are deposited directly into the lake, from those that are resedimented from the terrestrial environment.

5.2 Sediment distribution

The sediment distribution on the lake floor is mapped in Fig. 116. However, this is a simplified version of the lake floor, and is based on the bathymetry, SSS-data and knowledge of the terrestrial sedimentary processes. The sediment distribution in a lake can be complex, and different processes that control the distribution may dominate at different parts of the year (Hilton et al., 1986). Five main mechanisms that control the sediment distribution are recognized in Nordlaguna, and will be discussed in this section. Sediments that are transported in suspension and as underflows are discussed in sections 5.2.1 and 5.2.2, respectively. How the morphology of the barrier and the wave energy and –direction can control the distribution of sediments derived by wash-over is discussed in section 5.2.3, which mechanisms contribute to redistribution of sediments are discussed in section 5.2.4 and the process of sediment focusing in the lake are discussed in section 5.2.5.

5.2.1 Sediments transported in suspension

When the river in Tornøedalen was observed to be active during heavy rain, a plume of sediments was formed (Fig. 80). Providing that the lake is stratified, the sediment plume can be transported in the epilimnion before it falls out of suspension (Fig. 1), and possibly distribute fluvial sediments throughout the lake floor (Nichols, 2009). This can be seen in the sediment record of the two cores from the lake. Although none of the cores were collected from the subaqueous fan deposits, where the majority of fluvial deposits are expected to be deposited, laminated silt was found in both cores (Fig. 124, Fig. 125), which is a deposit that is often predominantly formed by fluvial processes (Retelle and Child, 1996).

5.2.2 Sediments transported by underflow

Underflows can be a mechanism of transporting coarse material to the deep part of a lake (Fig. 1) (Nichols, 2009). Such deposits are found in Nordlaguna, in core NL1B, as deposits that were interpreted to be formed by turbidity currents (Fig. 125). Such deposits can form when high-density mixtures of water and sediment are induced by a river (Nichols, 2009), and can therefore origin from one of the three fluvial systems around the lake. It is also possible that the turbidity currents are triggered by subaqueous slide events and transported as underflows (Piper & Normark, 2009), as slide back-scarps are found on the subaqueous slopes (Fig. 119).

5.2.3 Distribution of wash-over sediments

The morphology of the barrier can give indications of how the wash-over sediments are distributed on the lake floor. The northeastern part of Bommen is the lowest and narrowest part where wash-over channels are best defined. It can therefore be argued that there are more frequent episodes of waves overtopping the barrier at its northeastern part, and thereby more erosion of the barrier. The majority of wash-over sediments are therefore most likely found at the northeastern part of the subaqueous slope.

5.2.4 Redistribution of sediments

Waves and currents can form in a lake and affect the distribution of sediments (Larsen and MacDonald, 1993). Winds can be strong on Jan Mayen, and 22 % of the days in January have a maximum wind strength of 6 on Beaufort scale (strong breeze) (Gabrielsen et al., 1997). This can form waves and currents in Nordlaguna, which can be illustrated by the ripples found on the subaqueous slope down from Bommen (Fig. 120). The abrasional scarps on the subaqueous slopes and the well-defined belts of driftwood in Stasjonsdalen and Wilzcekdalen can be other examples of processes in Nordlaguna that contribute to the reworking of sediments. These features can form by either lake-level fluctuations, which are common in closed basins (Einsele & Hinderer, 1997), or by wave-actions. When the water level in the lake is low, larger amounts of sediments are exposed for redistribution by wave-actions.

Another mechanism of redistribution of sediments in the lake is subaqueous slides, which are known to occur in the lake as slide back-scarps are observed (Fig. 119). Subaqueous slide back-scarps, wave-actions and currents as well as lake level fluctuations in Nordlaguna indicate that there are possibly significant reworking of sediments in the lake. This can also be exemplified by the inverted radiocarbon ages observed in core NL2, as discussed in section 5.3.1.

5.2.5 Focusing of sediments

Focusing of sediments occurs at the deepest part of a lake (Blais & Kalff, 1995). This is mapped as lacustrine deep floor deposit in Nordlaguna (Fig. 116). Depositional mechanisms that can be related to sediment focusing were found in the core from this part, NL1B (Fig. 125). Unit 1 in the core was interpreted to be deposited by one single event, such as a subaqueous slide. Unit 2 was interpreted to be

dominated by turbidites. These processes can be examples of focusing of sediments, as they are transported downslope until they reach the deepest part of the lake, where no further transport is possible, and the sediments are focused.

5.3 Evaluation of the sediment cores

In this section, the possibility of using the two sediment cores to study past environmental conditions are discussed, as well as how the variations in depositional mechanisms that were observed in the cores can be connected to past environmental conditions.

5.3.1 Chronology

When using lake sediments are used to reconstruct past environmental conditions, it is important to obtain a reliable chronology (Bradley, 2014). Reworked sediments or dating of terrestrial organic material are examples of factors that can complicate radiocarbon dating, as the organic material found in the sediment may be older than the sediment that is deposited at the same time (Olsson, 1991). The organic material used for dating the cores in this thesis is terrestrial in origin, as no organic material from within the lake was found. This, as well as the knowledge of reworking processes in the lake (as discussed in section 5.2.4) may complicate the chronology of the two cores.

NL2

The date at the base of core NL2 shows a remarkably old age compared to the dates just a few cm above (Fig. 124, Table 2), suggesting it is unreliable. The remaining dates of the core shows two reversals in the chronology, which may be caused by deposition of old terrestrial material or by reworking the sediments. This irregular pattern of the dates would be a great uncertainty if the core were used to study past environmental conditions.

NL1B

Few amounts of organic material were found in core NL1B, creating a big gap in the chronology between 94-96 cm and 7-8 cm (Fig. 125, Table 3). It is therefore difficult to evaluate if the date at the base of the core is reliable or not, but knowledge about the unreliable chronology of core NL2, as well as the processes of resedimentation at the location of core NL1B (as discussed in section 5.2.4 and 5.2.5), creates uncertainty of the reliability of the dates.

5.3.2 Implications of past environmental conditions

Although the poor chronology of the sediment cores may complicate studies of past environmental conditions, the variations in depositional mechanisms and properties that are observed in the cores can provide implications of how changes in the environmental conditions can control the sedimentation in the lake.

There is a sharp transition between the two units in core NL2, which is dominated by significantly different processes. Unit 1 is dominated by laminated silt interpreted as annually deposited varves, and unit 2 is dominated by sediments deposited by wash-over events (Fig. 124*)*. Wash-over events can possibly modify the barrier morphology significantly (Matias et al., 2007), which can be illustrated by the decreasing width of Bommen. It has drastically changed since it was first measured in 1928, when it was 200 m wide at the narrowest part (Barr, 2015). In 2016, it was measured to be 135 m wide at the narrowest part (Fig. 30). The majority of the erosion of the barrier is most likely occurring on the seaward side, but this can also imply increased wash-over events in the lake and erosion at the lake ward side. The increased amount of material deposited by wash-over events and erosion of the barrier can possibly be connected to the decreasing sea ice around Jan Mayen, as increased coastal erosion as a result of decreasing sea ice extent is recorded at other locations in the Arctic (eg. Jones et al., 2007; Overeem et al., 2011).

Both core NL1B and NL2 show variations in the thickness of the laminated silt that were interpreted as annually deposited varves (section 4.3.2). This is especially prominent in core NL2, where the varve thickness ranges from an average of 5 couplets per cm to 1.2 couplets per cm. Varve thickness can potentially be used to reconstruct past environmental conditions, such as temperatures (e.g. Besonen et al., 2008) or glacier dynamics (e.g**.** Ohlendorf et al., 1997). As glaciers are within the drainage area of Tornøedalen, which is the major source of fluvial sedimentation to the lake, their dynamics will control the deposition in the lake. As the cores used in this study do not cover more than probably a few hundred years, it would be difficult to connect to large scale variations in environmental conditions in the Arctic. However, on a smaller and local scale, the variations in varve thickness can possibly be connected to the glacier fluctuations the last 350 years, as described by Orheim (1993).

6. Summary and conclusions

The study of Nordlaguna and the adjacent land area has resulted in knowledge about the sedimentary sources and processes that control the sedimentation and sediment distribution in the lake. The deposits in the two sediment cores were interpreted by using knowledge of the modern sedimentary processes, and their potential of being used to study past environmental conditions was evaluated. The conclusions of the thesis are:

- Five main sources of sedimentation to the lake are found: temporal and seasonal fluvial activity from the three valleys around the lake and subaerial slopes; wash-over deposition from the barrier that separates the lake from the ocean; mass movement deposition from the subaerial slopes; wind-blown sediments and pyroclastic fallout.
- Based on the discussion of drainage areas and morphology of the three valley floors as well as their grain-sizes, it is concluded that the channel system in Tornøedalen is the major source of fluvial sedimentation to the lake. This valley has the largest drainage area, and the temporal and seasonal active river that forms in the valley seems to have the highest stream discharge as well as the most frequent events of fluvial activity of the three valleys.
- The channel systems at Stasjonsdalen and Wilzcekdalen are suggested to be of significantly less importance of fluvial sedimentation to the lake at present times. However, it appears likely that the channel system in Stasjonsdalen was active during times of more fluvial activity, such as during the deglaciation of Jan Mayen.
- The mapping of the lake gives an indication of the sediment distribution on the lake floor, but this is controlled by a variety of mechanisms and processes in the lake.
- Sediments transported in suspension may be distributed throughout the lake floor, which can be reflected in the sediment cores, as fluvial sediments were found although they were not collected from the subaqueous fan deposits. The deposits by turbidity currents from core NL1B are likely to be transported as underflows, and can origin from subaqueous slide events of from fluvial sediments with a high-density mixture of water and sediments.
- The majority of sediments deposited by wash-over events are most likely distributed at the northeastern part of the subaqueous slope, where the barrier is at its lowest and narrowest and the wash-over channels are best defined.
- Wave action, lake level fluctuations and subaqueous slides are suggested as mechanisms that can redistribute the sediments in the lake.
- The poor chronology of the sediment cores may complicate their use in studies of past environmental conditions.

- The increase in wash-over deposition recorded from the sediment core as well as the increased erosion of the barrier could imply that the loss of sea ice at Jan Mayen increases the coastal erosion, and thereby the possibility of more deposition of wash-over sediments in the lake.
- Variation in thickness of the annually deposited varves can possibly be connected to the fluctuations in glacier extent the last 350 years that is recorded on Jan Mayen.

References

Anda, E., Orheim, O., & Mangerud, J. (1985). Late Holocene glacier variations and climate at Jan Mayen. *Polar Research*, *3*(2), 129-140.

Baker, V. R., & Ritter, D. F. (1975). Competence of rivers to transport coarse bedload material. *Geological Society of America Bulletin*, *86*(7), 975-978.

Barr, S. (2015). *Jan Mayen – Norges utpost I vest. Øyas historie gjennom 1500 år*. Oslo: Kolofon forlag

Benn, D. I. (2014). Clast morphology. In *A practical guide to the study of glacial sediments* (pp. 92-106). London: Routledge.

Benn, D. I., & Ballantyne, C. K. (1994). Reconstructing the transport history of glacigenic sediments: a new approach based on the co-variance of clast form indices. *Sedimentary Geology*, *91*(1-4), 215-227.

Besonen, M. R., Patridge, W., Bradley, R. S., Francus, P., Stoner, J. S., & Abbott, M. B. (2008). A record of climate over the last millennium based on varved lake sediments from the Canadian High Arctic. *The Holocene*, *18*(1), 169-180.

Blais, J. M., & Kalff, J. (1995). The influence of lake morphometry on sediment focusing. *Limnology and Oceanography*, *40*(3), 582-588.

Blockley, S. P. E., Lane, C. S., Lotter, A. F., & Pollard, A. M. (2007). Evidence for the presence of the Vedde Ash in Central Europe. *Quaternary Science Reviews*, *26*(25-28), 3030-3036.

Bourke, R. H., Paquette, R. G., & Blythe, R. F. (1992). The Jan Mayen Current of the Greenland Sea. *Journal of geophysical research*, *97*, 7241-7250.

Boyd, R., Dalrymple, R., & Zaitlin, B. A. (1992). Classification of clastic coastal depositional environments. *Sedimentary Geology*, *80*(3-4), 139-150.

Bradley, R. (2014). *Paleoclimatology: Reconstructing Climates of the Quaternary*. Sand Diego: Academic press

Bøe, R., Longva, O., Lepland, A., Blikra, L. H., Sønstegaard, E., Haflidason, H., Bryn, P., & Lien, R. (2004). Postglacial mass movements and their causes in fjords and lakes in western Norway. *Norwegian Journal of Geology*, *84*(1), 35-55

Carroll, A. R., & Bohacs, K. M. (1999). Stratigraphic classification of ancient lakes: Balancing tectonic and climatic controls. *Geology*, *27*(2), 99-102.

Collinson, J., Thompson, D., & Mountney, N. (2006). *Sedimentary structures*. Harpenden: Terra Publishing

Cromwell, G., Tauxe, L., Staudigel, H., Constable, C. G., Koppers, A. A. P., & Pedersen, R. B. (2013). In search of long-term hemispheric asymmetry in the geomagnetic field: Results from high northern latitudes. *Geochemistry, Geophysics, Geosystems*, *14*(8), 3234-3249.

Dalrymple, R. W., Zaitlin, B. A., & Boyd, R. (1992). Estuarine facies models: conceptual basis and stratigraphic implications: perspective. *Journal of Sedimentary Research*, *62*(6), 1130-1146.

Dearing, J. A. (1991). Lake sediment records of erosional processes. *Hydrobiologia*, *214*(1), 99-106.

Eaton, G. P. (1963). Volcanic ash deposits as a guide to atmospheric circulation in the geologic past. *Journal of Geophysical Research*, *68*(2), 521-528.

Einsele, G. (2013). *Sedimentary basins: evolution, facies, and sediment budget*. Berlin: Springer-Verlag

Einsele, G., & Hinderer, M. (1997). Terrestrial sediment yield and the lifetimes of reservoirs, lakes, and larger basins. *Geologische Rundschau*, *86*(2), 288-310.

Eugster, H. P., & Hardie, L. A. (1978). Saline lakes. In *Lakes* (pp. 237-293). New York: Springer

Falkovich, G. (2011). Fluid Mechanics: A short course for physicists. New York: Cambridge University Press

Fitch, F. J. (1964). The development of the Beerenberg volcano, Jan Mayen. *Proceedings of the Geologists' Association*, *75*(2), 133-165.

Fitch, F. J., Grasty, R. L., & Miller, J. A. (1965). Potassium—Argon Ages of Rocks from Jan Mayen and an outline of its volcanic history. *Nature*, *207*(5004), 1349.

Flemming, B. W. (2011). Geology, morphology and sedimentology of estuaries and coasts. *Treatise on estuarine and coastal science*, *3*, 7-38.

Francus, P., Bradley, R. S., Lewis, T., Abbott, M., Retelle, M., & Stoner, J. S. (2008). Limnological and sedimentary processes at Sawtooth Lake, Canadian High Arctic, and their influence on varve formation. *Journal of Paleolimnology*, *40*(3), 963-985.

Gabrielsen, G. W., Brekke, B., Alsos, I. G., & Hansen, J. R. (1997). *Natur-og kulturmiljøet på Jan Mayen: med en vurdering av verneverdier, kunnskapsbehov og forvaltning*. Norsk Polarinstitutt Meddelser, 144,

Garcia-Gabin, W. (2015). Wave bimodal spectrum based on swell and wind-sea components. *IFAC-PapersOnLine*, *48*(16), 223-228.

Gjerløw, E., Höskuldsson, A., & Pedersen, R. B. (2015). The 1732 Surtseyan eruption of Eggøya, Jan Mayen, North Atlantic: deposits, distribution, chemistry and chronology. *Bulletin of Volcanology*, *77*(2), 14.

Hagen, J. O., Liestøl, O., Roland, E., & Jørgensen, T. (1993). *Glacier atlas of Svalbard and Jan Mayen.* Norsk Polarinstitutt Meddelser, 129, 1-141

Hayes, M. O. (1978). Impact of hurricanes on sedimentation in estuaries, bays, and lagoons. In *Estuarine Interactions* (pp. 323-346). New York: Academic Press

Hilton, J., Lishman, J. P., & Allen, P. V. (1986). The dominant processes of sediment distribution and focusing in a small, eutrophic, monomictic lake. *Limnology and Oceanography*, *31*(1), 125-133.

Hulth, J., Rolstad, C., Trondsen, K., & Rødby, R. W. (2010). Surface mass and energy balance of Sørbreen, Jan Mayen, 2008. *Annals of Glaciology*, *51*(55), 110-119.

Häggblom, A. (1982). Driftwood in Svalbard as an indicator of sea ice conditions: a preliminary report. *Geografiska Annaler: Series A, Physical Geography*, *64*(1-2), 81-94.

Imsland, P. (1978). The geology of the volcanic island Jan Mayen, Arctic Ocean. *Nordic Volcanological Institute,* 78(13)

Iversen, T. (1936). Sydøstgrønland, Jan Mayen-Fiskeriundersøkelser. *Fiskeridirektoratets Skrifter 5(1).*

Jakobsson, S. P., & Gudmundsson, M. T. (2008). Subglacial and intraglacial volcanic formations in Iceland. *Jökull*, *58*, 179-196.

Johansen, S. (1998). The origin and age of driftwood on Jan Mayen. *Polar Research*, *17*(2), 125-146.

Jones, B. M., Arp, C. D., Jorgenson, M. T., Hinkel, K. M., Schmutz, J. A., & Flint, P. L. (2009). Increase in the rate and uniformity of coastline erosion in Arctic Alaska. *Geophysical Research Letters*, *36*(3)

Judd, A., & Hovland, M. (2007). Seabed Fluid Flow: The Impact on Geology, Biology, and the Marine Environment. Cambridge: Cambridge University Press.

Kinsman, D. J. J., & Sheard, J. W. (1963). The glaciers of Jan Mayen. *Journal of Glaciology*, *4*(34), 439-448.

Klein, M. (2002). Side scan sonar. In *International handbook of underwater archaeology* (pp. 667-678). Boston: Springer

Komar, P. D. (1971). The mechanics of sand transport on beaches. *Journal of Geophysical Research*, *76*(3), 713-721.

Kuenen, P. H. (1953). Significant features of graded bedding. *AAPG Bulletin*, *37*(5), 1044-1066.

Lamb, H. H., Probert-Jones, J. R., & Sheard, J. W. (1962). A new advance of the Jan Mayen glaciers and a remarkable increase of precipitation. *Journal of Glaciology*, *4*(33), 355-365.

Lamoureux, S. F., & Gilbert, R. (2004). A 750-yr record of autumn snowfall and temperature variability and winter storminess recorded in the varved sediments of Bear Lake, Devon Island, Arctic Canada. *Quaternary Research*, *61*(2), 134-147.

Larsen, C. P., & MacDonald, G. M. (1993). Lake morphometry, sediment mixing and the selection of sites for fine resolution palaeoecological studies. *Quaternary Science Reviews*, *12*(9), 781-792.

Leeder, M. (2011). *Sedimentology and sedimentary basins: From turbulence to tectonics*. Chichester: Wiley-Blackwell.

Lehman, J. T. (1975). Reconstructing the rate of accumulation of lake sediment: the effect of sediment focusing. *Quaternary Research*, *5*(4), 541-550.

Likens, G. (2009). *Encyclopedia of inland waters.* Amsterdam: Elsevier.

Lowe, J. J., & Turney, C. S. (1997). Vedde Ash layer discovered in a small lake basin on the Scottish mainland. *Journal of the Geological Society*, *154*(4), 605-612.

Lowe, J. J., & Walker, M. J. (2015). *Reconstructing quaternary environments*. New York: Routledge.

Matias, A., Ferreira, Ó., Vila-Concejo, A., Garcia, T., & Dias, J. A. (2008). Classification of washover dynamics in barrier islands. *Geomorphology*, *97*(3-4), 655-674.

Matsuoka, N. (2001). Solifluction rates, processes and landforms: a global review. *Earth-Science Reviews*, *55*(1-2), 107-134.

Mjelde, R., Breivik, A. J., Raum, T., Mittelstaedt, E., Ito, G., & Faleide, J. I. (2008). Magmatic and tectonic evolution of the North Atlantic. *Journal of the Geological Society*, *165*(1), 31-42.

Morton, R. A., & Sallenger Jr, A. H. (2003). Morphological impacts of extreme storms on sandy beaches and barriers. *Journal of Coastal Research*, 19(3), 560-573.

Nesje, A. (1992). A piston corer for lacustrine and marine sediments. *Arctic and Alpine Research*, 24, 257-259.

Nichols, G. (2009). *Sedimentology and stratigraphy*. West Sussex: Wiley-Blackwell

Ohlendorf, C., Niessen, F., & Weissert, H. (1997). Glacial varve thickness and 127 years of instrumental climate data: a comparison. *Climatic Change*, *36*(3-4), 391-411.

Olsson, I. U. (1991). Accuracy and precision in sediment chronology. *Hydrobiologia*, *214*(1), 25-34.

Orheim, O. (1993). Glaciers of Europe – Glaciers of Jan Mayen, Norway. *US Geological Survey Professional Paper*, 153.

Overeem, I., Anderson, R. S., Wobus, C. W., Clow, G. D., Urban, F. E., & Matell, N. (2011). Sea ice loss enhances wave action at the Arctic coast. *Geophysical Research Letters*, *38*(17).

Pettijohn, F. J., Potter, P. E., & Siever, R. (1987). Sand and Sandstone. New York: Springer-Verlag.

Piper, D. J., & Normark, W. R. (2009). Processes that initiate turbidity currents and their influence on turbidites: a marine geology perspective. *Journal of Sedimentary Research*, *79*(6), 347-362.

Polar Geospacial Center, ArcticDEM retrieved from https://www.pgc.umn.edu/data/Arcticdem/ (12.01.2018)

Rafferty, J. (2011). Lakes and wetlands (The Living Earth). New York: Britannica Educational Publ.

Reid, I., Frostick, L. E., & Layman, J. T. (1985). The incidence and nature of bedload transport during flood flows in coarse-grained alluvial channels. *Earth Surface Processes and Landforms*, *10*(1), 33-44.

Retelle, M. (1986). Stratigraphy and sedimentology of coastal lacustrine basins, northeastern Ellesmere Island, NWT. *Géographie physique et Quaternaire*, *40*(2), 117-128.

Retelle, M. J., & Child, J. K. (1996). Suspended sediment transport and deposition in a high Arctic meromictic lake. *Journal of Paleolimnology*, *16*(2), 151-167.

Richter, S. (1946). Jan Mayen i krigsårene. Minner fra det første stykke norsk land vi besatte og holdt under hele krigen. *Norsk Geografisk tidsskrift 11:2*, 63-86

Schnellmann, M., Anselmetti, F. S., Giardini, D., & McKenzie, J. A. (2005). Mass movement-induced fold-and-thrust belt structures in unconsolidated sediments in Lake Lucerne (Switzerland). *Sedimentology*, *52*(2), 271-289.

Schumm, S. A. (1977). The fluvial system. New York: Wiley

Skreslet, S. (1969). *The ecosystem of the Arctic lake Nordlaguna, Jan Mayen Island. Part 1. General features and hydrology.* Astarte, 2, 27-34

Skreslet, S. (1973). The Ecosystem of the Arctic Lake Nordlaguna, Jan Mayen Island. III. Ecology of Arctic Char. *Salvelinus alpinus*, 43-54.

Sly, P. G. (1978). Sedimentary processes in lakes. In *Lakes* (pp. 65-89). Berlin: Springer-Verlag

Steffensen, E. L. (1982). The climate at Norwegian Arctic stations. *Klima*, *5*(1), 44.

Stroeve, J., Holland, M. M., Meier, W., Scambos, T., & Serreze, M. (2007). Arctic sea ice decline: Faster than forecast. *Geophysical research letters*, *34*(9),

Strum, M. (1979). Origin and composition of clastic varves. In *Moraines and varves; origin, genesis, classification, Proceedings of an INQUA symposium on genesis and lithology of Quaternary deposits, Zurich, 1979* (pp. 281-285). Rotterdam: Balkema

Sylvester, A. G. (1975). History and surveillance of volcanic activity on Jan Mayen island. *Bulletin Volcanologique*, *39*(2), 313-335.

Thompson, R., Bradshaw, R. H., & Whitley, J. E. (1986). The distribution of ash in Icelandic lake sediments and the relative importance of mixing and erosion processes. *Journal of Quaternary Science*, *1*(1), 3-11.

Turney, C. S. M., Burg, D., Van, K., Wastegård, S., Davies, S. M., Whitehouse, N. J., Pilcher, J. R., & Callaghan, C. (2006). North European last glacial–interglacial transition (LGIT; 15–9 ka) tephrochronology: extended limits and new events. *Journal of Quaternary Science*, *21*(4), 335-345.

Van Daele, M., Moernaut, J., Doom, L., Boes, E., Fontijn, K., Heirman, K., Vandoorne, E. Hebbeln, D. Pino, M, Urrutia, R., Brümmer., R., & De Batist, M. (2015). A comparison of the sedimentary records of the 1960 and 2010 great Chilean earthquakes in 17 lakes: Implications for quantitative lacustrine palaeoseismology. *Sedimentology*, *62*(5), 1466-1496.

Walker, R. G., & Mutti, E. (1973). Turbidite facies and facies associations. In *Turbidites and Deep-Water Sedimentation: SEPM Pacific Sec. Short Course* (pp. 119-157)

Wastegård, S., Björck, S., Possnert, G., & Wohlfarth, B. (1998). Evidence for the occurrence of Vedde Ash in Sweden: radiocarbon and calendar age estimates. *Journal of Quaternary Science: Published for the Quaternary Research Association*, *13*(3), 271-274.

Wetzel, R. (2001). *Limnology: Lake and river ecosystems* (3rd ed.). San Diego: Academic Press.

Wilhelm, B., Sabatier, P., & Arnaud, F. (2015). Is a regional flood signal reproducible from lake sediments?. *Sedimentology*, *62*(4), 1103-1117.

Wolfe, A. P., Miller, G. H., Olsen, C. A., Forman, S. L., Doran, P. T., & Holmgren, S. U. (2004). Geochronology of high latitude lake sediments. In *Long-term environmental change in Arctic and Antarctic lakes* (pp. 19-52). New York: Springer

Zolitschka, B., Francus, P., Ojala, A. E., & Schimmelmann, A. (2015). Varves in lake sediments–a review. *Quaternary Science Reviews*, *117*, 1-41.

Appendix A

The grain-size analyzing of samples from the sediment cores, NL1B and NL2, are conducted at the laboratory on NGU and placed at my disposal for this thesis. The method of the grain-size analyses is described in section 3.2.2. The data from the analyses were used when the lithological logs of the cores were created.

Core NL1B

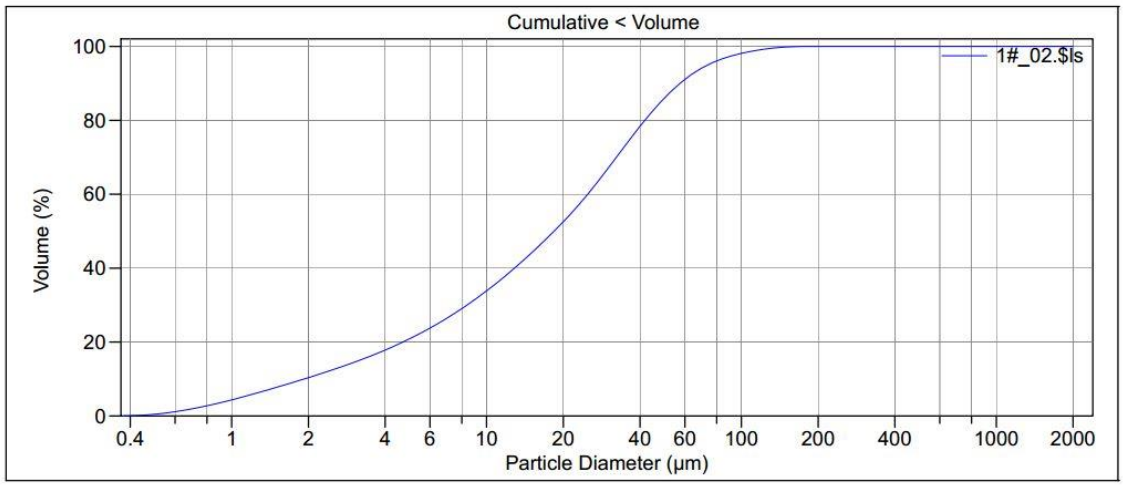

Fig. 126 Grain-size analysis of sample 1 from core NL1B (57-58 cm depth)

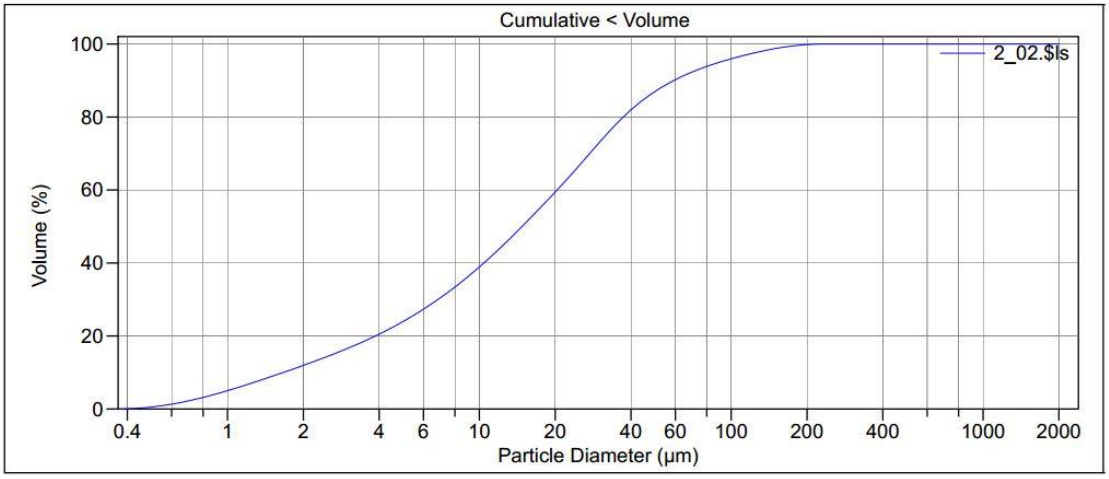

Fig. 127 Grain-size analysis of sample 2 from core NL1B (61-62 cm depth)

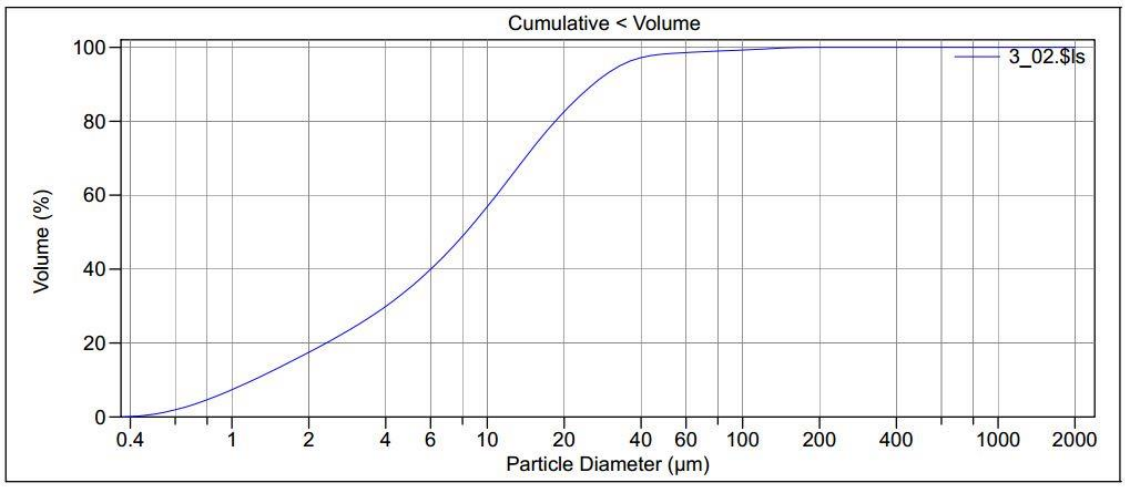

Fig. 128 Grain-size analysis of sample 3 from core NL1B (76-77 cm depth)

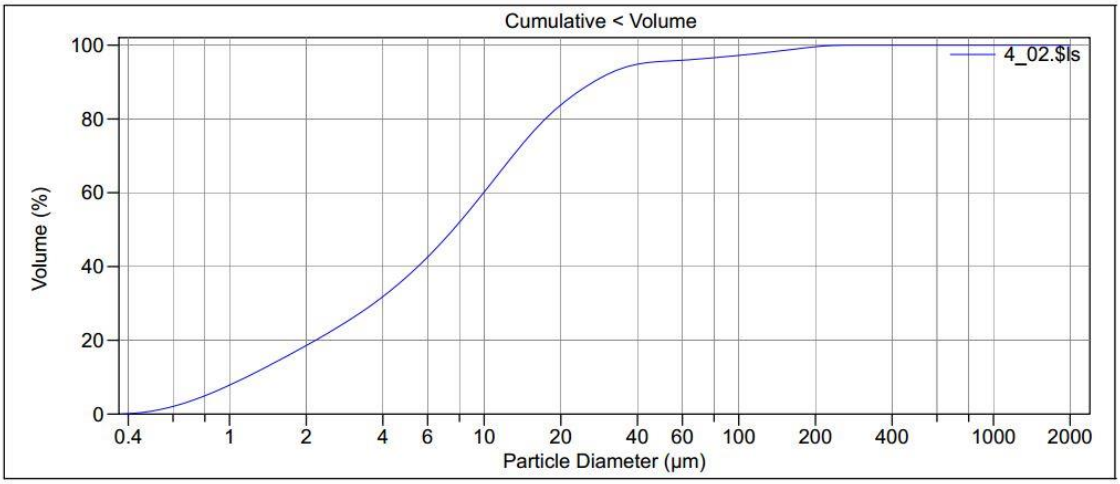

Fig. 129 Grain-size analysis of sample 4 from core NL1B (72-73 cm depth)

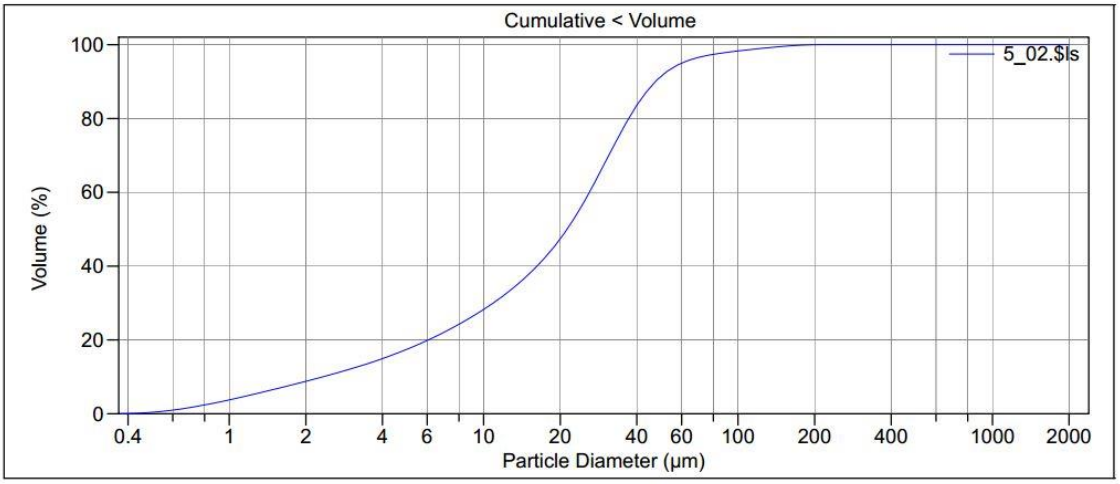

Fig. 130 Grain-size analysis of sample 5 from core NL1B (83-84 cm depth)

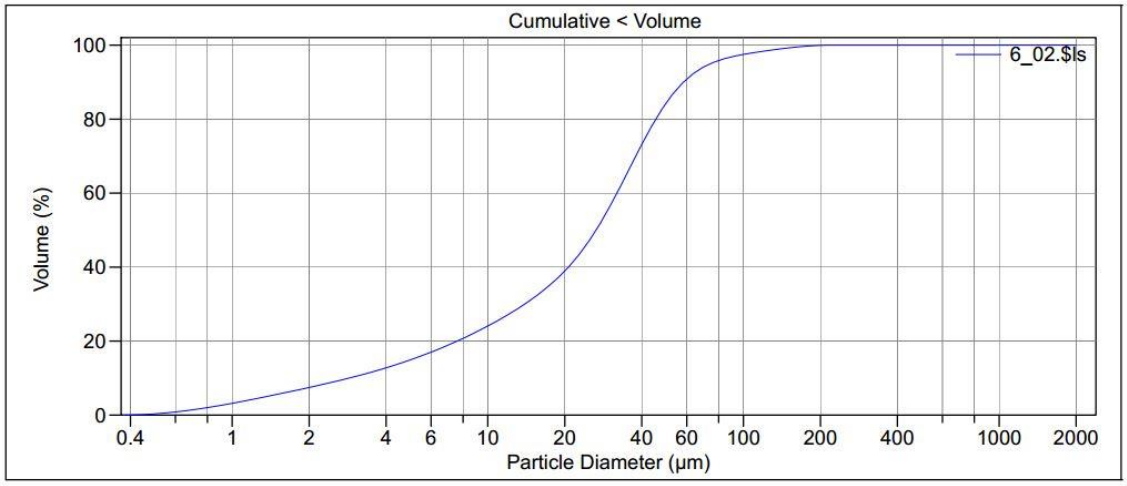

Fig. 131 Grain-size analysis of sample 6 from core NL1B (87-88 cm depth)

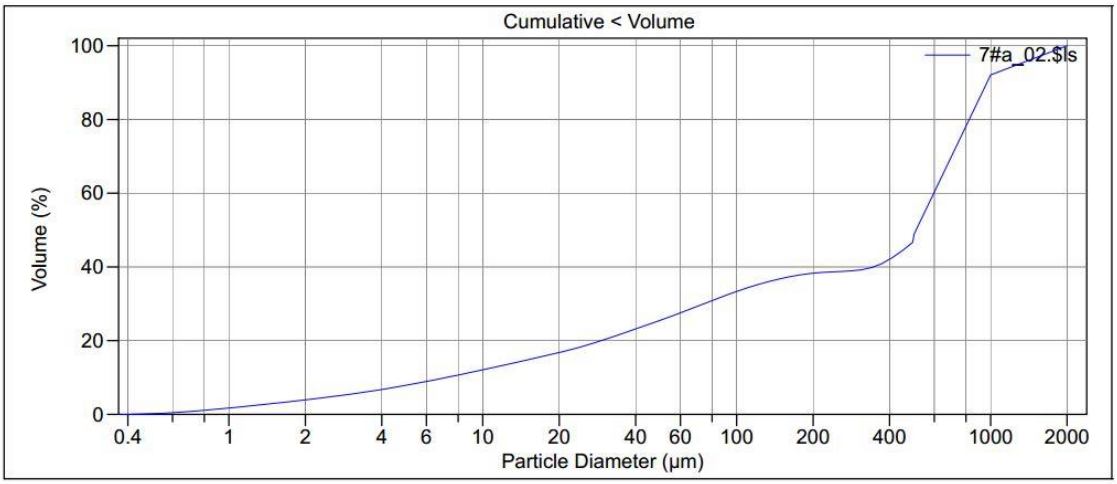

Fig. 132 Grain-size analysis of sample 7 from core NL1B (6-7 cm depth)

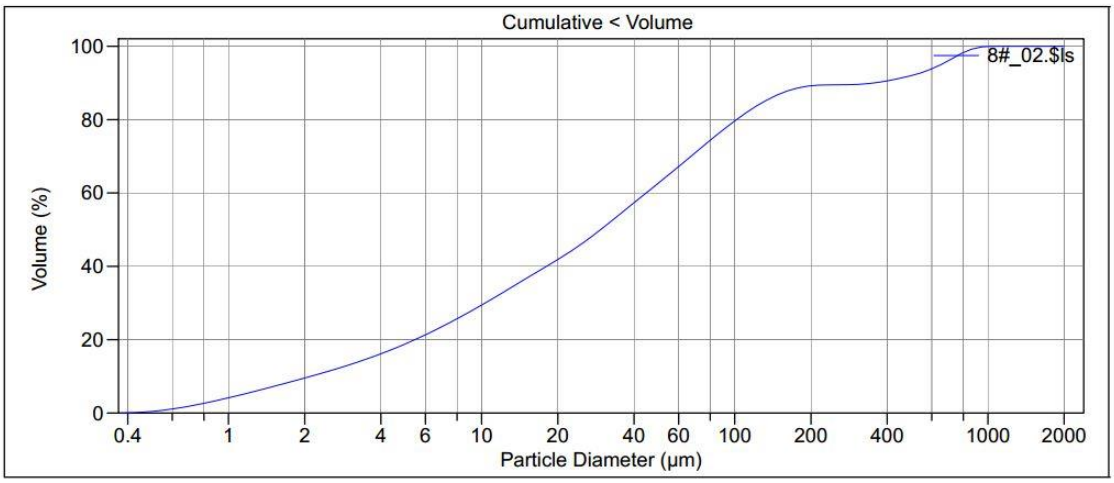

Fig. 133 Grain-size analysis of sample 8 from core NL1B (18-19 cm depth)

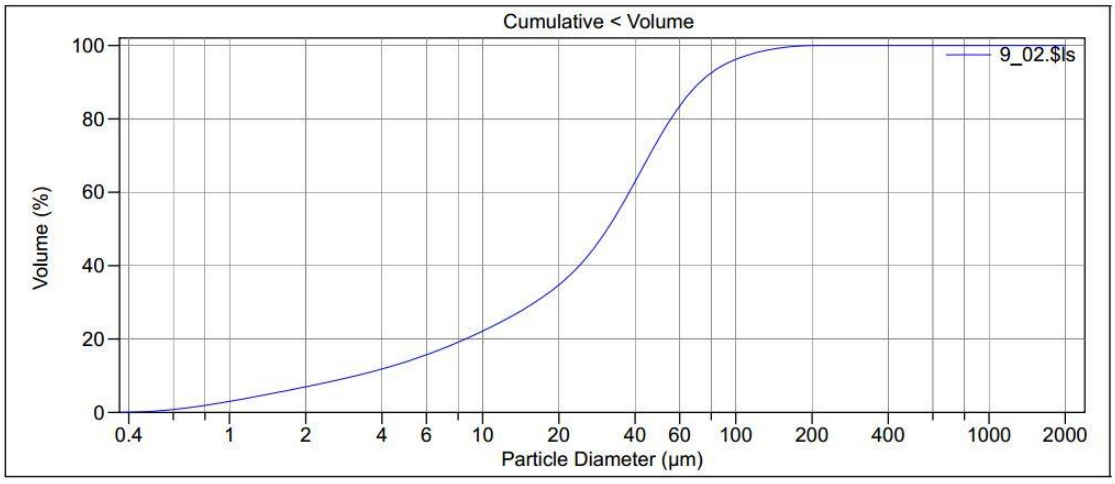

Fig. 134 Grain-size analysis of sample 9 from core NL1B (94-95 cm depth)

Core NL2

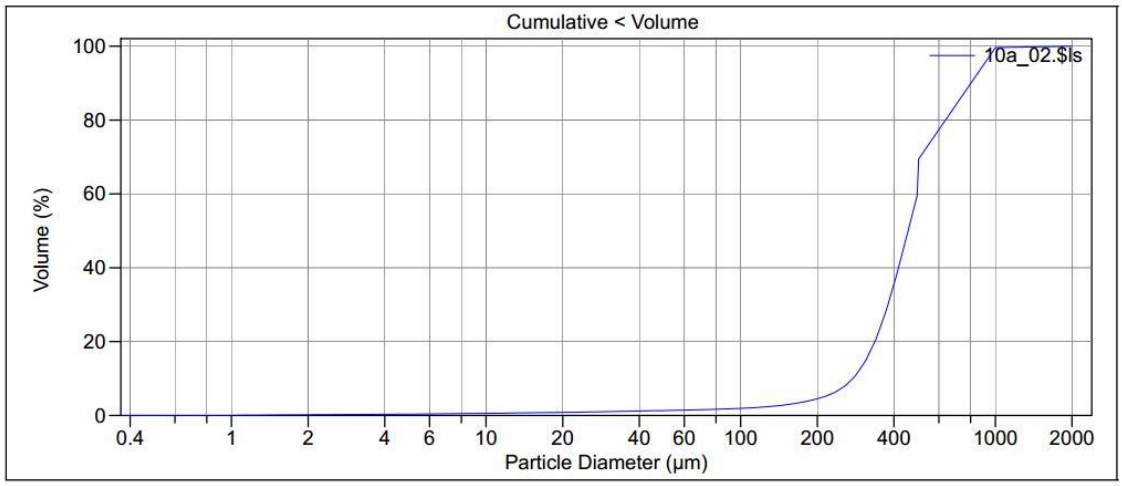

Fig. 135 Grain-size analysis of sample 10 from core NL2 (22.5-24.5 cm depth)

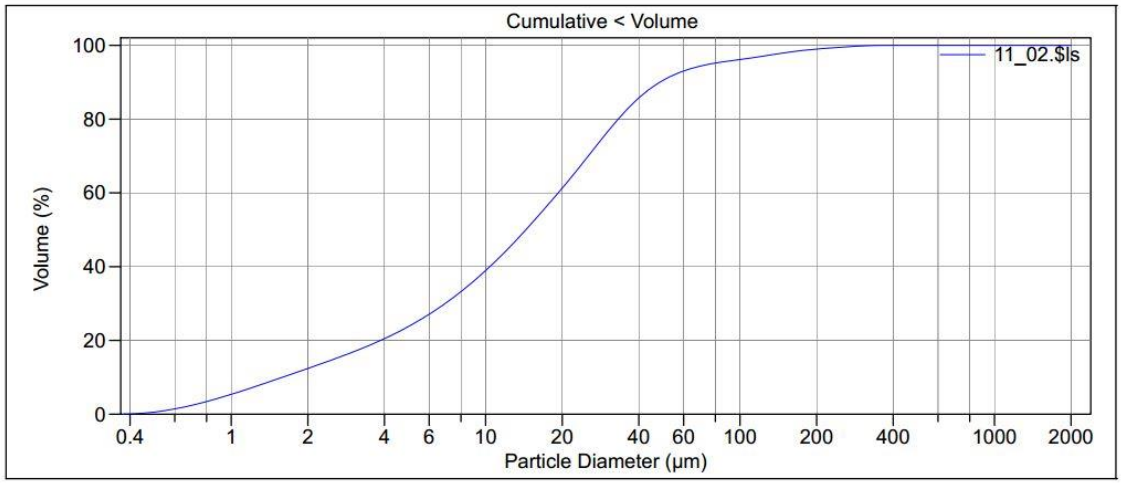

Fig. 136 Grain-size analysis of sample 11 from core NL2 (98-99 cm depth)

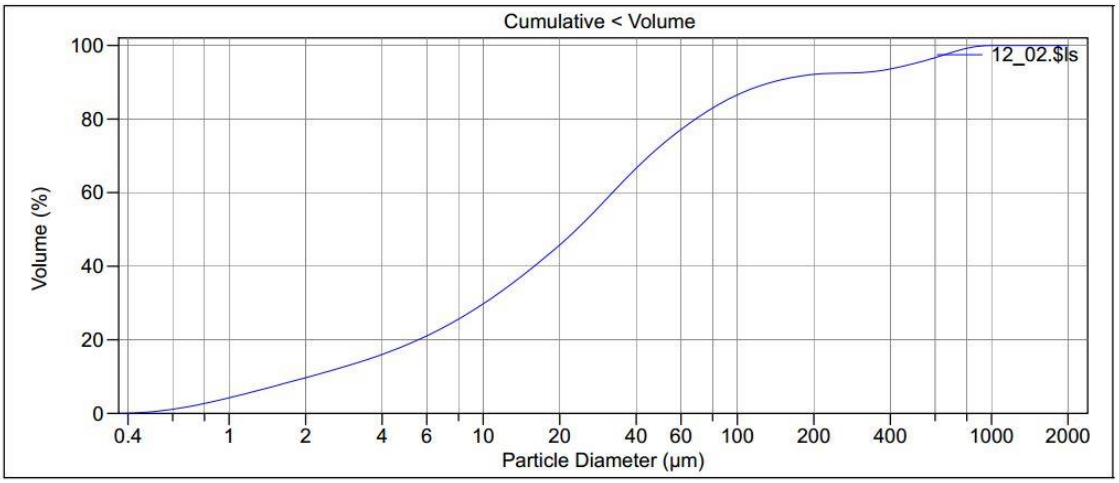

Fig. 137 Grain-size analysis of sample 12 from core NL2 (93-94 cm depth)

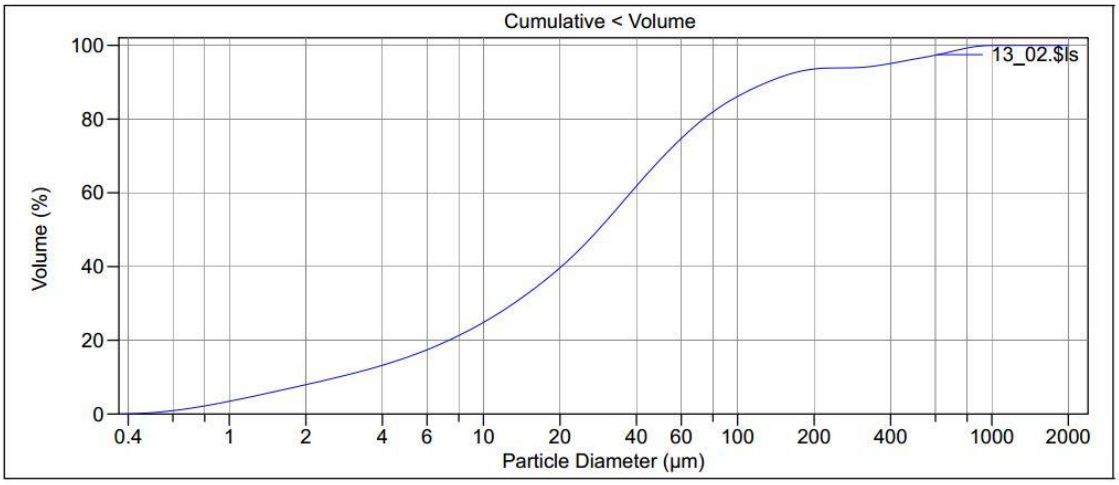

Fig. 138 Grain-size analysis of sample 13 from core NL2 (76-77 cm depth)

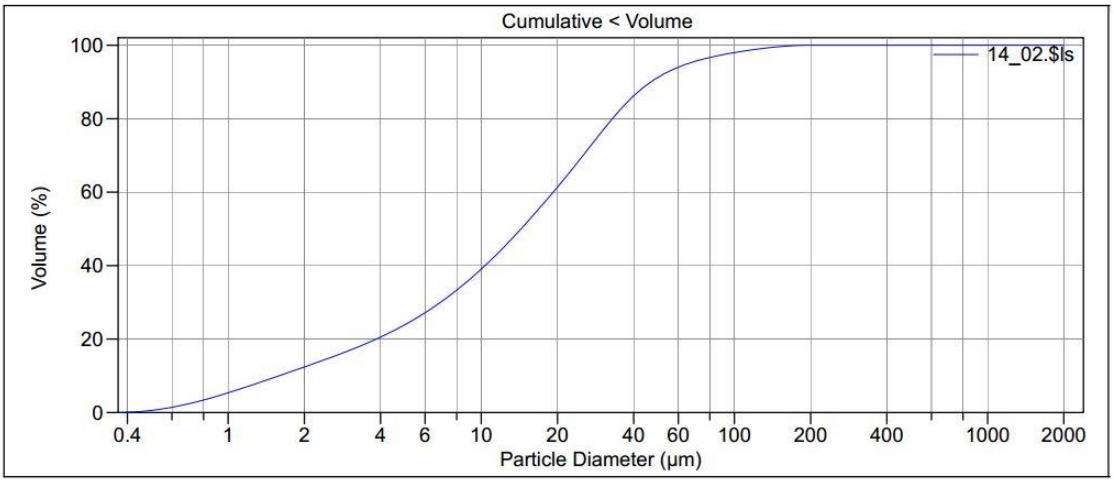

Fig. 139 Grain-size analysis of sample 14 from core NL2 (86-87 cm depth)

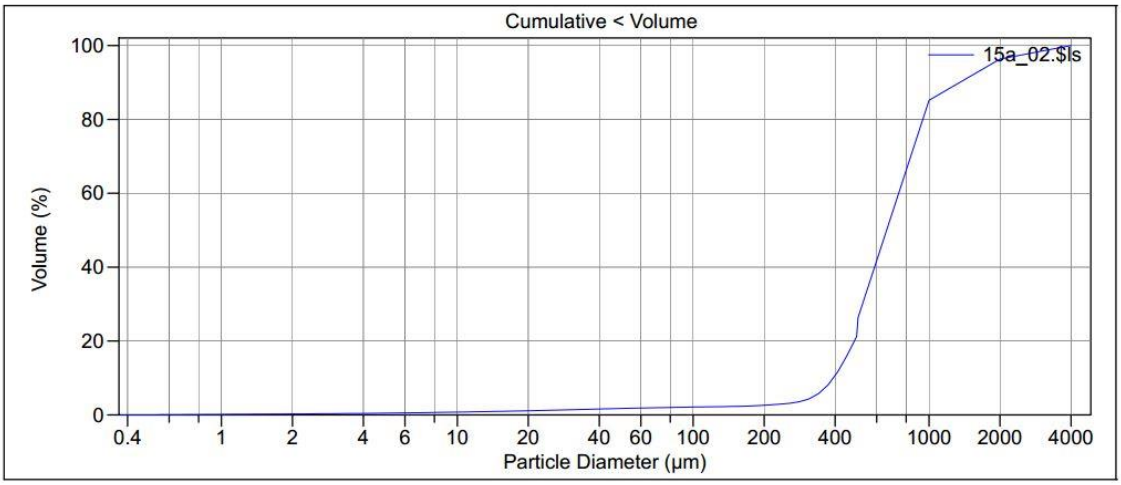

Fig. 140 Grain-size analysis of sample 15 from core NL2 (61-62 cm depth)

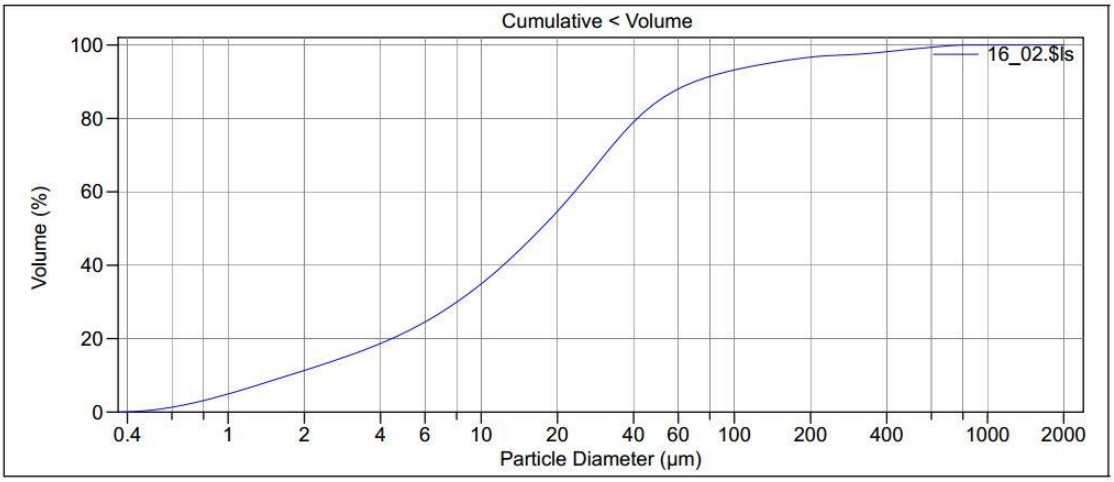

Fig. 141 Grain-size analysis of sample 16 from core NL2 (80-81 cm depth)

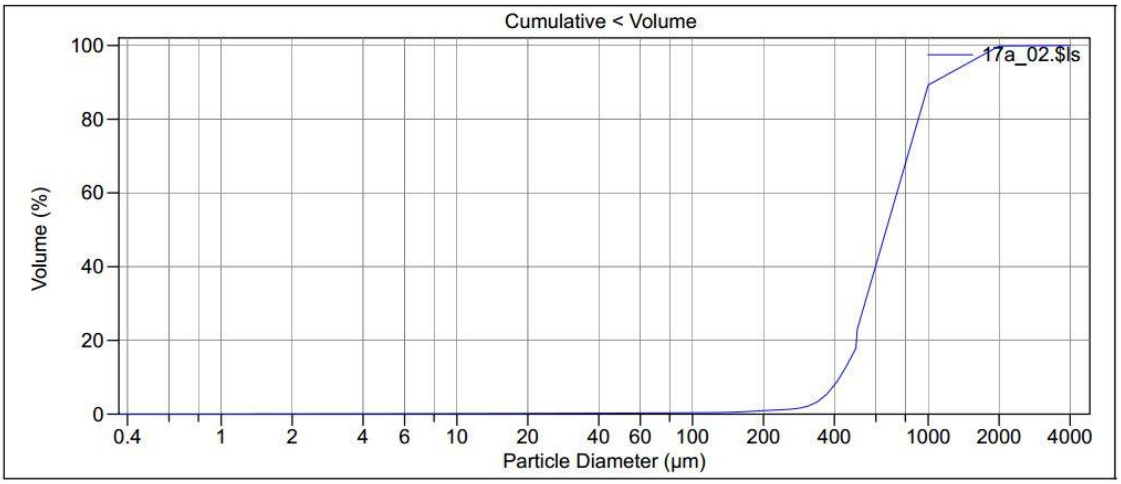

Fig. 142 Grain-size analysis of sample 17 from core NL2 (16-18 cm depth)

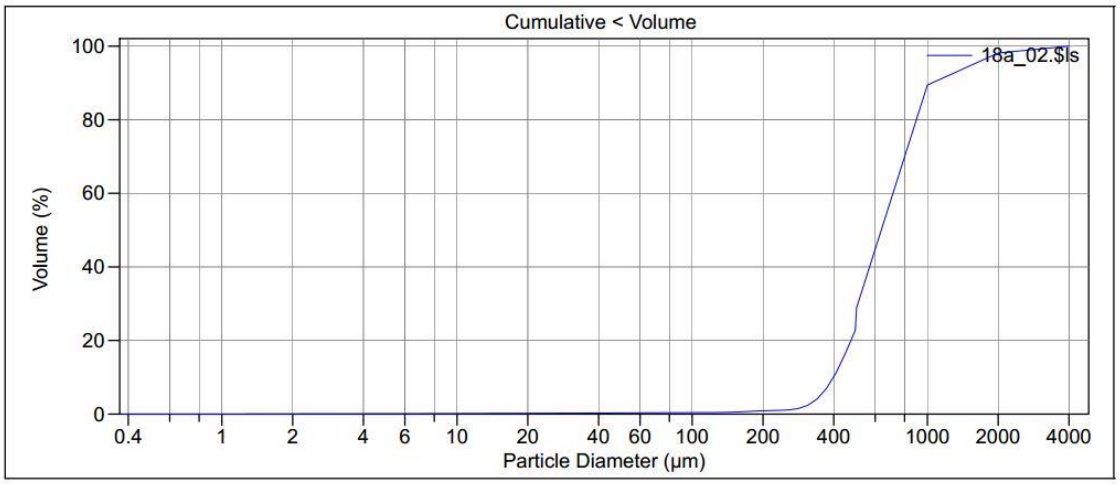

Fig. 143 Grain-size analysis of sample 18 from core NL2 (48-50 cm depth)

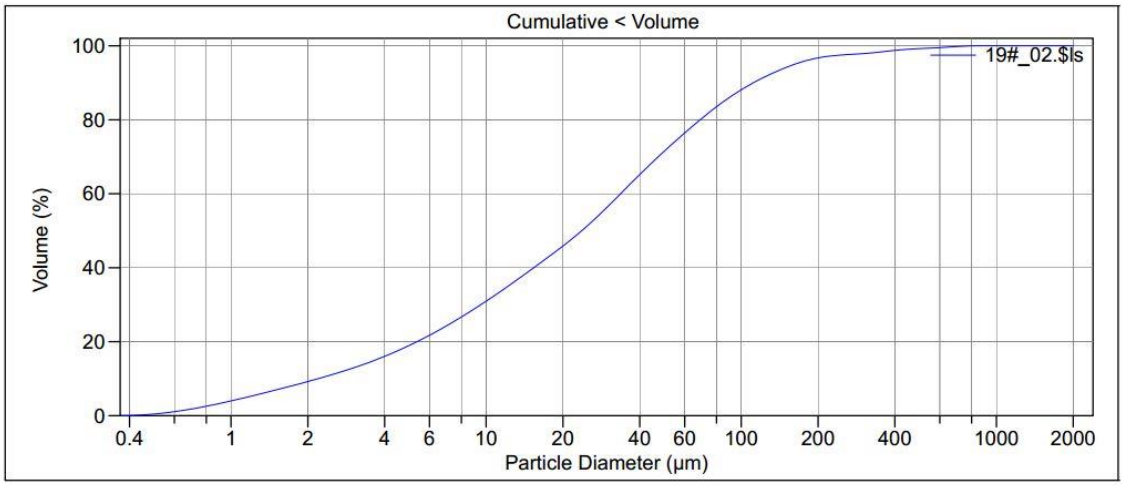

Fig. 144 Grain-size analysis of sample 19 from core NL2 (69-70 cm depth)

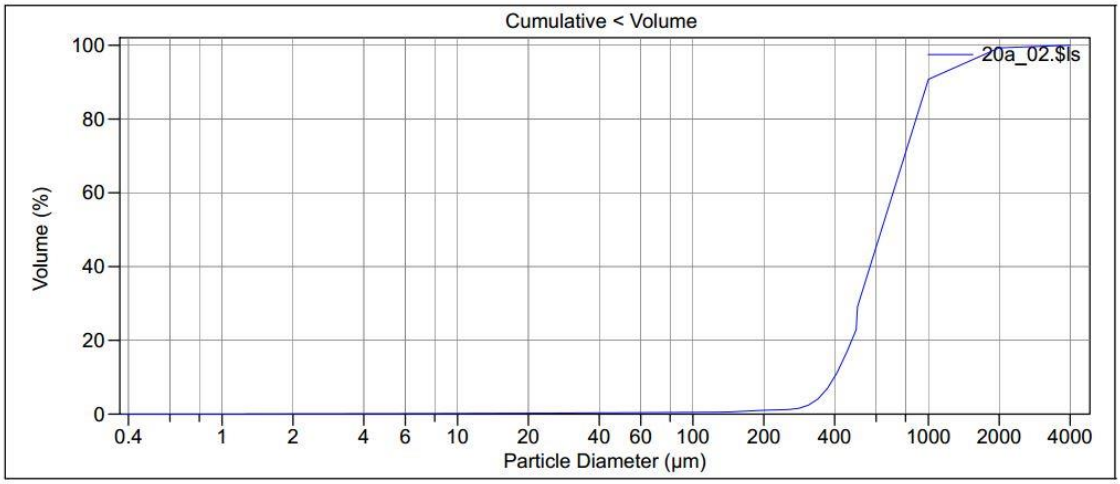

Fig. 145 Grain-size analysis of sample 20 from core NL2 (32-34 cm depth)